3-1982

Skeletal Age Changes in *Saguinus fuscicollis* and *Saguinus oedipus*

David Michael Glassman
University of Tennessee, Knoxville

Recommended Citation

Glassman, David Michael, "Skeletal Age Changes in *Saguinus fuscicollis* and *Saguinus oedipus*. " PhD diss., University of Tennessee, 1982.
https://trace.tennessee.edu/utk_graddiss/4041

To the Graduate Council:

I am submitting herewith a dissertation written by David Michael Glassman entitled "Skeletal Age Changes in *Saguinus fuscicollis* and *Saguinus oedipus*." I have examined the final electronic copy of this dissertation for form and content and recommend that it be accepted in partial fulfillment of the requirements for the degree of Doctor of Philosophy, with a major in Anthropology.

Fred H. Smith, Major Professor

We have read this dissertation and recommend its acceptance:

Richard Jantz, William M. Bass, Gary F. McCracken

Accepted for the Council:
Dixie L. Thompson

Vice Provost and Dean of the Graduate School

(Original signatures are on file with official student records.)

To the Graduate Council:

I am submitting herewith a dissertation written by David Michael Glassman entitled "Skeletal Age Changes in *Saguinus fuscicollis* and *Saguinus oedipus* (Callitrichidae, Primates)." I have examined the final copy of this dissertation for form and content and recommend that it be accepted in partial fulfillment of the requirements for the degree of Doctor of Philosophy, with a major in Anthropology.

Fred H Smith
Fred H. Smith, Major Professor

We have read this dissertation
and recommend its acceptance:

William M. Bass

Gary F. McCracken

Accepted for the Council:

L Evans Roth
Vice Chancellor
Graduate Studies and Research

A

SKELETAL AGE CHANGES IN *SAGUINUS FUSCICOLLIS* AND *SAGUINUS OEDIPUS* (CALLITRICHIDAE, PRIMATES)

A Dissertation
Presented for the
Doctor of Philosophy
Degree
The University of Tennessee, Knoxville

David Michael Glassman
March 1982

In memory of my father, Maurice Lewis Glassman

and

my grandfather, Louis Michaels

ACKNOWLEDGMENTS

This dissertation would not have been made possible without the efforts of a number of advisors, colleagues, and friends to whom I am extremely grateful. First, I would like to thank my committee chairman Dr. Fred H. Smith and committee members, Drs. Richard L. Jantz, William M. Bass, and Gary F. McCracken for their individual encouragement and unwavering attention to this project. I am honored to be accepted as a colleague by this committee. I am particularly grateful to Fred Smith for his support throughout my graduate studies and his special interest in the development and study of the marmoset skeletal collection. Second, I would like to extend special thanks to Dr. Conrad Richter and the Oak Ridge Associated Universities marmoset colony advisory board for recognizing the value of this project and providing the marmoset cadavers used in analysis.

Several individuals unselfishly made available resources essential to the completion of this study. Thanks are given to Dr. Paul Parmalee for use of his zooarcheology laboratory facilities, Drs. Walter Klippel and Jeff MacCabe of The University of Tennessee, Knoxville and Dr. Rhodes Holliman of Virginia Tech for use of their microscopes, and Drs. Donald Ortner and Douglas Ubelaker of the Smithsonian Institute for use of their thin-section equipment during the early stages of this research. In addition, I would like to acknowledge the appreciated services of Kathy Abbott and Patti Moisan in preparing the graphics, Betty Dyer for the drawings of the two tamarins, the staff at the Dark Room, Knoxville for preparing the thin-section photographs, Gayle Slutzky for computer assistance, and Karen Glenney-Smith for editorial assistance of the dissertation manuscript.

Two colleagues were involved in all aspects of this research from the initial maceration of the tamarins to the final analysis. I would like to thank Regena Pittman-Sharma and Dwight Schmidt for their dedication to this project.

Continual support and helpful suggestions were provided by Drs. Gerald Schroedl, Anthony Cavender and Robert Hinton, and Ken Parham, Pat Key, Terry Zobeck, Mark Guagliardo, Pat Willey, William Baden, and Steve Symes. Additional appreciation is extended to the computer centers of The University of Tennessee and the Virginia Polytechnic Institute and State University.

Financial aid for this project was graciously provided by the Office of the Vice Chancellor for Graduate Studies and Research and the Department of Anthropology at The University of Tennessee.

Finally, I would like to extend my deepest appreciation to my mother, Mrs. Harriet Glassman, family, and Ms. Claudette Nadeau for their constant aid and support of my academic pursuits. Only with their love could I have completed this goal.

ABSTRACT

The South American tamarin, genus *Saguinus* is used extensively as a model for interpreting human disease. Recently, techniques for estimating the age from skeletons of wild-caught tamarins have been requested by biomedical researchers. These skeletal aging techniques are subsequently used as an aid in documenting the timing of disease onset and latency periods.

Skeletal age changes are examined in 157 *Saguinus fuscicollis* and 59 *Saguinus oedipus* specimens of known age. The entire approximate 15 year life span of these animals is represented within the sample. The species are treated independently for all analyses. Documentation of the ontogenetic skeletal changes in immature specimens is made for the sequences and timing of dental eruption and epiphyseal union and for the chronology of long bone growth. For adult specimens, the age-related patterns associated with intracortical bone remodeling and mid-diaphyseal cortex size and shape are documented.

Results of this research indicate that the greatest accuracy for estimating age in these species is obtained within the developmental growth stage, from birth to maturity. During this stage, accurate age assignment can be made to within approximately three months. For aging adult specimens, the trends of intracortical bone remodeling and mid-diaphyseal cortex size and shape exhibit extensive intraspecies variation and thus are applicable with limited accuracy.

TABLE OF CONTENTS

CHAPTER PAGE

LIST OF TABLES

LIST OF FIGURES

FIGURE PAGE

CHAPTER I

INTRODUCTION

The South American tamarins and marmosets (Callitrichidae, Primates) are used extensively in many areas of biomedical research (see for example, Ammons et al., 1972; Benirschke and Richart, 1960; Britton et al., 1938; Deinhardt, 1970a; Deinhardt et al., 1967a, 1970, 1972; Dunn, 1961; Gengozian, 1969, 1971; Hampton et al., 1969; Levy, 1963; Levy et al., 1969, 1970; Marczynska et al., 1970; Porter and Young, 1967).

The growing appreciation of their value to this research has prompted a commitment to the conservation and health care of these primates (Bermont and Lindburg, 1975; Bernstein et al., 1976; Cosgrove et al., 1968, 1970; Deinhardt, 1970b; Deinhardt et al., 1967b; Gengozian et al., 1977; Harrison, 1971; Hearn, 1975; Heltne, 1957; Heltne and Thorington, 1975; Mittermeier et al., 1977; Thorington and Heltne, 1975; Tsalickis, 1972). This commitment is evident in both the growing number of governmental and private breeding colonies established in the United States (Cooper, 1964; Epple, 1970a; Fritzgerald, 1935; Gengozian et al., 1977; Hampton, 1964; Hampton et al., 1966; Hampton ahd Hampton, 1967; Kingston, 1977; Levy and Artecona, 1964; Mallinson, 1977; Wolf et al., 1975) and the increase in field studies undertaken by anthropologists and zoologists to identify the behavioral and morphological complexes characteristic of these animals (e.g., Castro and Soini, 1977; Dawson, 1976; Durham, 1974; Garber, 1979; Hershkovitz, 1977; Izawa, 1976; Moynihan, 1970; Neyman, 1977; Thorington, 1968). The endangered status of some species such as *Saguinus oedipus* has expedited much of the recent research (Heltne and Thorington, 1975).

This recent surge in callitrichid study has prompted a major concern for determining the age of wild-caught specimens. One area in which age assessment is useful is in field evaluation of population structure. Heltne and Thorington (1975:118) state:

> Age criteria for field evaluation of population structure are extremely important. It was felt by most at the conference (on "Neotropical Primates: Field Study and Conservation") that more effort should be made to refine our techniques for estimating the age of wild primates.

Furthermore, they continue:

> More data are desirable on the eruption and wear of teeth, on the rates of skeletal maturation, and on the weights of animals of known age.

It was agreed at the conference that the best procedure for obtaining these data is through the examination of primates produced from zoo and institutional breeding programs. In addition to the evaluation of population structure, age prediction techniques have been sought by investigators in biomedical research to aid in determining latency periods and initial onset of various diseases in feral animals.

In May 1978, Dr. Conrad Richter, veterinarian for the Oak Ridge Associated Universities marmoset breeding facility, sought a skeletal morphologist to determine the potential for estimating ages of unknown tamarin specimens. He requested this information to assist him in his research on colonic carcinoma. Of all nonhuman primates, it appears that this form of cancer manifests spontaneously only in *Saguinus oedipus*, thus promoting this species of tamarin as the best model for studying this disease as it relates to humans. To date, all colonic cancer-inflicted specimens in the Oak Ridge colony have been wild-caught animals.

A. Defining the Research Problem

To predict the age of an unknown tamarin from skeletal material, skeletal age changes spanning the life cycle of individuals must initially be documented with samples of known age. The degree of accuracy for age estimation is dependent upon the number of known-aged individuals included in the analysis, their representation of all phases of skeletal development and degeneration, and the inherent degree of intraspecies variation in growth and development. Skeletal age changes may be defined as the natural modification of any skeletal structure as a direct result of the normal biological aging process.

The examination of ontogenetic effects in *Saguinus* skeletons has been hampered in the past by the unavailability of known-aged samples of all age classes. Consequently, there is a general lack of information concerning skeletal growth and development. To this end, Richter was able to provide a small, yet age representative, sample of *S. oedipus oedipus* cadavers collected at the Oak Ridge facility. Additionally, a much larger sample of age-documented *S. fuscicollis* comprised of four subspecies was obtained for the comparison of ontogenetic variation between the two species. Thus we may assess the probability of accurately estimating age in *S. oedipus* from data documented from *S. fuscicollis*. Skeletalization of these two samples began in August 1978. Analysis for documenting specific age-related skeletal changes was initiated in January 1980.

Traditionally, skeletal and dental ontogenetic development have been categorized into two stages. The first stage, developmental, corresponds to all skeletal growth changes that occur from conception to the onset of skeletal maturity—the point of complete epiphyseal union. The second stage, the period of skeletal degeneration and remodeling, continues for the remainder of the life cycle. Different methodological procedures and techniques have been applied to document the specific age changes associated with each stage.

Using techniques similar to those applied by morphologists to human material, the assessment of age-related skeletal trends in nonhuman primates has customarily concentrated on the developmental stage. However, the interest in assigning ages to unknown tamarins of adult status warrants the examination of degenerative changes as well. The specific ontogenetic changes selected for documentation in the present study were chosen on the basis of feasibility, high probability of accurate age-estimating potential, and collective representation of all ages in the tamarin life cycle.

The developmental age changes selected for analysis were eruption of the dentition, growth of the long bones, and union of the epiphyses. Similar skeletal growth studies of human and nonhuman primates have demonstrated that when these changes are observed together, the composite pattern represents a highly reliable assessment of chronological age during the developmental period.

Age-related changes observed in the adult primate skeleton have been less useful in estimating age than developmental changes. This may be due, in part, to greater intraspecies variation that accompanies adult age and/or less refined techniques available to precisely record adult skeletal changes. The traditional methods of estimating age in adult humans are commonly derived from correlations between chronological age and cranial suture closure, changes in the surface of the pubic symphysis, and the magnitude of normal bone destruction observed from osteoarthritis (degenerative joint disease) and vertebral osteophytosis. All have been omitted from the present study on the basis of recent challenges to their credibility for accurate age assessment (Brooks, 1955; McKern and Stewart, 1957; Singer, 1953; Suchey, 1977) and their apparent inapplicability to tamarin material.

In the last decade, investigators interested in the growth processes of adult humans for the purpose of estimating age have begun examining the various systematic changes in the patterns of the histological structures within cortical bone over time. The most common technique has been osteon counting (Kerley, 1965).

In the normal aging process, intracortical bone is subjected to continual remodeling. In accordance with this remodeling, a number of age-related structural patterns manifest themselves systematically and may be observed in microscopic examination of cortical thin sections. Collectively, the observable changes in cortical bone have provided researchers with a powerful set of diagnostic age indicators.

Concurrent with the chronological changes observed within the cortex, additional changes have been reported in the size and shape of the bone cortex and medullary cavity. The majority of changes have been attributed to an overall loss of bone associated with older age, but these changes may also simply reflect a shifting in the cortical thickness of specific dimensions, known as cortical drift. To date, the documentation of systematic changes in the size and shape of the cortex have not been used for the purpose of estimating age. In this study, however, both the examination of cortical microstructure and cortex size and shape were selected as the variables to identify and document systematic age-related changes in adult tamarins.

An additional microscopic technique for estimating adult age has been developed from correlating chronological age to the number of cementum annulae of the dentition (Stott et al., 1981). Although this technique was not incorporated into the present study due to time limitations, a discussion of the methodology and the probability for accurately assigning age in adult tamarins is provided in Appendix A.

In summary, to comply with Richter's request to develop criteria for estimating the chronological age of unknown *Saguinus oedipus*, this project documents the correlation between chronological age and the ontogenetic skeletal changes of dental eruption, long bone growth, epiphyseal union, cortical microstructure, and mid-diaphyseal cortex size and shape in known-aged samples of *S. oedipus* and *S. fuscicollis*. In addition, the extent of intra- and interspecies variation for each age-change feature is identified, thus allowing for the reliability of these age-estimating techniques to be tested.

B. Research Assumptions

Two assumptions regarding the representativeness of the samples have been made for this project. The first is that the parameters examined for tamarins raised in captivity reflect the condition for those existing in their natural habitat. Second, even though the specimens included in the research sample are animals that have died prematurely, they do not significantly diverge from the normal chronological growth pattern characterizing tamarin development.

Two considerations may be raised regarding the validity of the above assumptions. The first is that since biological growth of animals is controlled by the complex interaction of genetic and environmental components, a change in one or both components may be expected to alter normal development. Since the colony-raised tamarins included in the study sample existed within a totally artificial environment wherein the diet, habitat, exposure to seasons, and almost all other behavioral patterns had been modified, a corresponding influence on development may be suspected. However, all attempts were made to provide the best possible environment for normal development of colony-raised animals.

Second, the immature specimens examined were not sacrificed, but died from disease or other natural causes. Since they had health-related problems significant enough to cause death, this may have altered their normal growth rate.

Although the validity of the assumptions can be questioned, the extent of influence in normal growth patterns by the effects of captivity and illness remains unknown. The position taken here is that the general acceptance of the assumptions is justified as long as recognition of their existence and possible implications are acknowledged. Their acceptance is the basis for the age-estimation of unknown tamarins from growth data documented in the laboratory sample.

C. Research Objectives

The objectives of this research are:

1. Development of a basic methodology for documenting age-related changes in cortical and gross bone structure of *Saguinus* primates.
2. The collection, analysis and documentation of data correlating chronological age to the skeletal age changes systematically patterned in dental eruption, long bone growth, epiphyseal union, cortical microstructure, and mid-diaphyseal cortex size and shape from individuals of various documented age in *S. oedipus* and *S. fuscicollis*. Analyses of the species are taken independently.
3. Determination of the extent of inter- and intraspecies variation with respect to the timing of each skeletal age change.
4. Identification of the predictive potential for estimating chronological age in unknown *S. oedipus* adult and subadult individuals from the documented age changes.

CHAPTER II

BACKGROUND AND LITERATURE REVIEW

A. *Saguinus fuscicollis* and *Saguinus oedipus*

A general discussion of various aspects of the distribution, morphology and behavior of *S. fuscicollis* and *S. oedipus* is presented below. Additional and more detailed information concerning the behavior and biology of tamarins may be found in several texts and journal articles (e.g., Dawson, 1976; Hershkovitz, 1977; Kleiman, 1977; Moynihan, 1970; Thorington and Heltne, 1975).

1. Taxonomy

Saguinus fuscicollis and *S. oedipus* are members of the South American primate family, Callitrichidae, which is comprised of four genera: *Callithrix,* the common marmosets; *Cebuella,* the pygmy marmosets; *Saguinus,* the tamarins; and *Leontopithecus,* the lion tamarins. These monkeys are collectively known for their small body size and possession of a variety of so-called "primitive" traits (see below).

Thirteen subspecies of *S. fuscicollis* and two subspecies of *S. oedipus* have been recorded (Hershkovitz, 1977). Subspecies designation reflects a variety of minute intraspecies variation in morphology, ecology and/or behavior.

2. Geographical Distribution

The distribution of *S. fuscicollis* is the "Upper Amazonian region from the west bank of the Rio Madeira south of the Rio Amazonas in Brazil, and the south (right) bank of the Japura'-Rio Caqueta-Caguan north of the Amazonas in Brazil and Columbia, Equador, Peru and Bolivia" (Hershkovitz, 1977:636). The four subspecies of *S. fuscicollis* included in this study, *nigrifrons, illigeri, lagonotus,* and *leucogenys*, occupy the central and western environs of the region.

Saguinus oedipus inhabits the tropical forested areas from southern Costa Rica to northwestern Columbia between the Rio Arato to the west and the Rio Magdalena to the east. A geographical distribution map of the *S. fuscicollis* and *S. oedipus* subspecies relevant to this study is presented in Figure 1.

3. Morphology

Possibly the most distinguishing characteristic of *S. fuscicollis* and *S. oedipus*, as well as the Callitrichidae in general, is the small body size in relation to other anthropoids. *Saguinus* body size approximates that of a small squirrel. The smallest Callitrichid, *Cebuella,* is among the most diminutive of all primates, with a size slightly greater than, or overlapping, *Microcebus,* the mouse lemurs; *Tarsius*; and the smallest species of *Galago, Galago demidovii* (Napier and Napier, 1967). On the average, *S. oedipus* tends to be slightly larger than *S. fuscicollis* in head and body length and in tail length, although intraspecies variation produces extensive size overlap

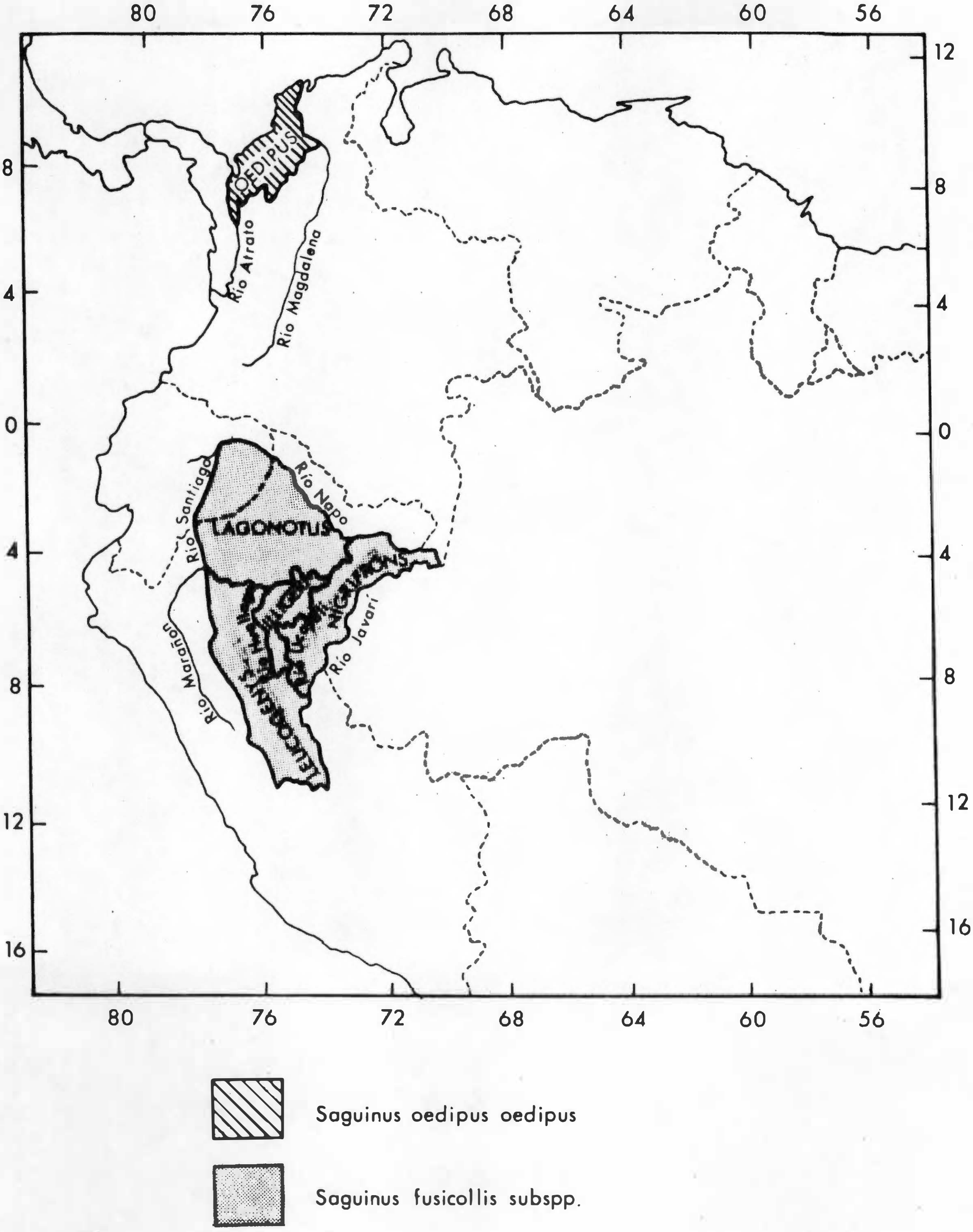

Figure 1. Geographical distribution in South America of the *Saguinus fuscicollis* and *Saguinus oedipus* subspecies included in the analysis.

(Table 1). Sexual dimorphism in linear body measurement for both species is slight.

Table 1. Body Length Measurements of *Saguinus fuscicollis* and *Sagninus oedipus* in Millimeters as Reported by Hershkovitz (1977:945)

	Head and Body			Tail Length		
Species	N	$\bar{X}$	Range	N	$\bar{X}$	Range
Saguinus fuscicollis	96	222	175-270	95	322	250-383
Saguinus oedipus	149	237	200-287	147	368	307-423

Although tamarins have small body size, they possess relatively long tails. The tails are covered with hair, with a variety of color patterns exhibited among different *Saguinus* species and subspecies. They are not prehensile as are the tails of some other groups of Platyrrhine monkeys. On the average, the percent of tail length to body length including the head is 145.0 for *S. fuscicollis* and 155.3 for *S. oedipus* (Table 1).

Tamarins often exhibit diversified color patterns and various species and subspecies possess a variety of diagnostic hairy crests, tufts, and manes. An adult *S. oedipus oedipus* is shown in Figure 2. The face of an adult *S. oedipus oedipus* has little hair, exposing predominately black facial skin. Two characteristic narrow bands of whitish hair are found on the face. The first begins at the sides of the nasal bridge and stretches downward, surrounding the mouth. The second band surrounds the perimeter of the entire face and is most

Figure 2. An adult *Saguinus oedipus oedipus*.

prominent in the brow regions and lateral to the cheeks. The right and left sides of the forehead are hairless, as are the ears. In the middle of the forehead, occasionally starting as a peak, grows a crest of relatively long white hairs which stretch down to the nape of the neck, surrounding the posterior margins of the ears. It is from this diagnostic crest that the common name for *S. oedipus oedipus*, the cotton-top tamarin, has been derived.

The body hair of *S. oedipus oedipus* generally is two distinct shades. The long hair of the chest, abdomen, forelimbs and posterior regions of the hindlimbs is white, which darkens slightly to the pale grey of the paws. The back, shoulders, and anterior areas of the hindlimbs are dark, ranging from black to a reddish-brown, and are covered by hair of similar length to that of the underbelly and chest. The tail is predominantly black although in the proximal area, it often takes on an orangish hue.

None of the subspecies of *S. fuscicollis* have the white hair crest of *S. oedipus oedipus*. They do, however, possess their own diagnostic configurations such as a thick band of white hair surrounding the lips and a saddling effect of coloration on the back. Although there is extensive geographic metachromism in *S. fuscicollis,* the subspecies, *illigeri, lagonotus, leucogenys,* and *nigrifrons* exhibit only minor differences in their color patterns.

Unlike *S. oedipus*, the adult face of *S. fuscicollis* is covered with hair (see Figure 3). White hairs surround the lips and dark brown to black hairs cover the cheeks and forehead. The hair of the

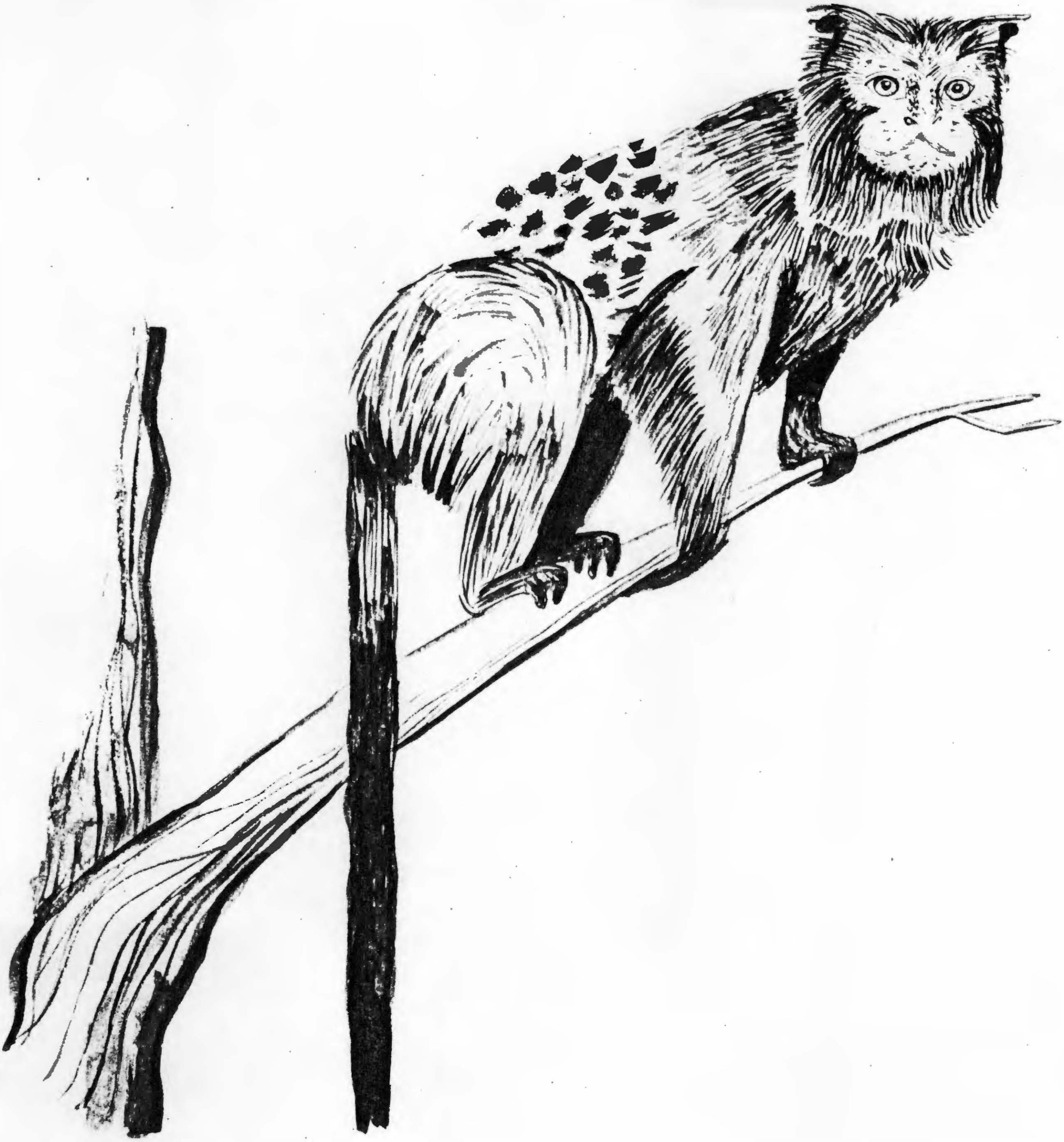

Figure 3. An adult *Saguinus fuscicollis illigeri*.

crown is black to brown which continues to the nape of the neck. Across the shoulders and both pairs of limbs, the coloration varies from brown to a reddish hue. On the backs of the *S. fuscicollis* subspecies, the hair is mottled dark and light, grey and brown, giving a marbled appearance from which comes the common name for this species, the saddle-back tamarin. The tails are black and lighten to a reddish-brown in the proximal area.

The dentition of *S. fuscicollis* and *S. oedipus* is basically similar and both have a dental formula of $\frac{2\text{-}1\text{-}3\text{-}2}{2\text{-}1\text{-}3\text{-}2}$ for the 32 adult teeth and $\frac{2\text{-}1\text{-}3}{2\text{-}1\text{-}3}$ for the 24 deciduous teeth. The *Saguinus* incisors are spatulate and expanded, although I2 is less expanded than I1. All incisors possess a well-developed lingual cingulum. The canines are long, projecting, sharp-pointed, and somewhat triangular in cross-section. A distinctive mesio-lingual groove is present in both the upper and lower canines. The upper premolars are bicuspid, with the paracone dominant in size. Crown height decreases from P^2 to P^4. The lower premolars are more heteromorphic, including a P_2 which is somewhat caniniform. One of the minor dental differences between *S. fuscicollis* and *S. oedipus* occurs in the morphology of P_3, which is more molarized in *S. oedipus*. For both species, height decreases from P_2 to P_4 and molarization increases respectively. The upper molars are generally tritubercular with the absence of a hypocone. A small hypocone has been observed, however, as a rare condition (Swindler, 1976). The occlusal surface is subtriangular in the upper molars and more oblong to square in the mandibulars. The size of the first molar is predominant. In some individuals, it is found to be twice the size of the second molar.

The dentition of *Saguinus*—especially the tritubercular pattern of the maxillary molars—has suggested to some investigators the "primitiveness" of *Saguinus* primates in relation to other anthropoids (Hershkovitz, 1972, 1977; Kinzey, 1973, 1974). Recently, Ford (1980), using a phyletic dwarfism model, has contested the validity of this observation. She presents evidence to suggest that the three-cusp pattern is not necessarily a retention from some ancestral stock, but rather, the result of a recent simplification in molar morphology that previously included the hypocone.

An additional morphological feature of tamarins is their possession of claws on all digits except the hallux, which bears a flattened nail. This condition, which is unique to the callitrichids among anthropoids, has also suggested "primitiveness." Morphologically, there has been much debate as to whether the tamarin claw-like structures are analogous to "true mammalian claws" or deviate radically from this pattern (e.g., Cartmill, 1974; Le Gros Clark, 1936; Garber, 1979; Thorndike, 1968). Ford (1980), in her discussion of dwarfism and the Callitrichidae, cites the findings of Thorndike (1968) and Rosenberger (1977) to suggest that not only do the tamarin claws appear distinct from the typical mammalian pattern, but also may have been the result of phyletic specialization from an ancestral primate with nails. She thus questions the relationship between primitive status and the possession of claws in tamarins.

4. Behavior

Saguinus primates are essentially arboreal and inhabit various levels of the forest canopy. Although there is some indication of interspecies variation in preference of canopy height (Castro and Soini, 1978; Moynihan, 1970), this preference can often be attributed to the season in which they were observed, as there is a general relationship between season, diet, and the canopy area exploited. In captivity, however, where season and diet are controlled factors, it has been noted that *S. fuscicollis* primarily inhabits the lower branches of their enclosures, while *S. oedipus* spends a greater proportion of their time in the higher areas (Richter and Davis, personal communication). This agrees with the scant data collected on these two species in the wild (Izawa, 1976; Moynihan, 1970; Neyman, 1977).

Tamarins are considered omnivorous and incorporate both plant and animal resources into their diet. Their primary protein intake comes from insects and small anthropods captured in the lower areas of the canopy. Moynihan (1976) points out the positive correlation between the small body size of these primates and their ability to forage for and capture insects on the terminal branches. The predation of insects appears not to involve piercing with the claws, but rather, grasping the prey and killing it with a bite to the head. In addition to insects, small fruit, seeds and flowers make up a large proportion of the *Saguinus* diet. They are found in various levels of the canopy and are limited in availability by season.

Recently, investigators have observed gum-feeding behavior in both *S. oedipus* and *S. fuscicollis* (Garber, 1979; Izawa, 1976). Although the extent to which plant exudates contribute to the tamarin diet is unknown, Garber (1979) suggests from his field observations of *S. oedipus* that approximately 14 percent of all food resources were plant exudates. It has been suggested that exudates may provide some essential components not acquired in sufficient form from other resources. In addition, they may be a food supplement during seasons in which little fruit and/or insects are available (Coimbra-Filho and Mittermeier, 1977; Garber, 1979).

Napier and Napier (1967) classify the locomotor behavior of *Saguinus* primates as quadrupedal of the branch-running and walking subtype. They display a propensity towards canopy movement by horizontal and diagonal leaps, as opposed to ascending and descending trunks (Garber, 1979; Castro and Soini, 1977; Moynihan, 1970). Functional analysis of the postcranial skeletons of *S. fuscicollis* and *S. oedipus* suggests possible interspecies variation in locomotor behavior with a greater morphological adaptation in *S. oedipus* for the generation of propulsive power (Glassman, 1981). Although sufficient behavioral data have not been recorded to substantiate this hypothesis, Richter's personal observations of capitve specimens provide support by noting a greater tendency in *S. oedipus* towards climbing and more powerful leaping than observed for *S. fuscicollis*.

Although only few long-term field investigations have been undertaken, the social structures of *S. fuscicollis* and *S. oedipus* appear to differ. Generally, five to ten individuals comprise the group organization of *S. fuscicollis*. Moynihan (1976:113) notes that, "These [groups] appear to be 'extended' families, to consist of a few pairs of adults, probably real mates, with their infants and juveniles." *S. oedipus*, however, tends to structure its groups solely around the small nuclear family comprised of one adult male and female and one to four young (Hershkovitz, 1977; Hampton, 1964). Both species are thought to be generally characterized by a monogamous long-term pair bonding in which the adult males actively participate in rearing the young.

The breeding seasons of tamarins have not been accurately recorded in the wild. However, Hershkovitz (1977) reports that pregnant females and newborn infants have been observed only between January and June. With an estimated gestation period of 140 to 150 days for both species (Hampton and Hampton, 1965; Hershkovitz, 1977; Wolfe et al., 1975), mating most probably occurs between August and January. Preslock et al. (1973) have determined the estrus cycle for both species to be 15.5 ± 1.5 days. Dizygotic twins are the most common birth in tamarins. Although this characteristic has been correlated with "primitiveness" (Hershkovitz, 1977; Schultz, 1948), the association has recently been questioned (Ford, 1980; Leutenegger, 1973). The twins are cared for by both parents until maturity when they are driven from the nuclear family.

Communicative behavior in *S. fuscicollis* and *S. oedipus* includes, to varying degrees, all categories suggested for mammals—olfactory, tactile, visual and vocal. Scent marking by the secretory glands, primarily the circumgenital, but also the suprapubic and sternal, appears to be more prominent in callitrichids than other anthropoid groups. Although the importance and implications of pheromone signals in *Saguinus* are virtually unknown, Epple (1970b, 1971, 1974) has made significant contributions toward understanding their role. In laboratory tests, she has determined that *S. fuscicollis* and *S. oedipus* are able to distinguish the scent marks produced by different sexes, between dominant and submissive males, and between known and foreign individuals of their species (Epple, 1971, 1974). It would therefore appear that the extensive marking of branches comprising the territory and the intragroup markings left on each other could provide an efficient identification mechanism for members within groups and among outsiders.

Tactile communication is predominantly expressed as allogrooming which occurs between all members of the group and occasionally between adults of neighboring groups. Although it commonly occurs in daily activity, grooming behavior tends to intensify in frequency and duration during the mating season.

Tamarins do not possess an elaborate system of facial expression. However, complex visual cues are transmitted from a variety of postures, body and head movements, and pilo-erection, most commonly of the head, distal tail, and back. These display characters, taken individually or in combination, express behavioral patterns of dominance, submission, acknowledgment, familiarity, excitement, aggression and a variety of other communications.

The vast majority of *Saguinus* vocalizations are high-pitched whistling, chirping, trills and rasping calls. Similar to visual cues, they convey a variety of behavioral attitudes and patterns (Epple, 1968; Moynihan, 1970). The vocal repertoire of *S. oedipus* has been extensively described by Epple (1968) and Moynihan (1970).

In summary, tamarins are small South American monkeys, strictly arboreal, and generally give birth to twins. Morphologically they are best known for their colorful and exaggerated fur crests and manes, their possession of claws on all digits except the hallux, and their simple tritubercular molar pattern. Behaviorally, tamarins move through the forest by springing and rapid movement. They form stable pair-bonds and live in small groups often comprised of one adult male and female with one to four offspring. Similar to other primates, their communication system is highly complex. However, callitrichids use pheromone signals to an extent unparalleled by other anthropoids.

B. Examination of Skeletal Age Changes

The vast majority of investigators interested in skeletal age changes in nonhuman primates have concentrated on subadult individuals. The traditional and most reliable developmental changes observed by these researchers for the purposes of estimating age in feral animals have been the timing of dental eruption, chronological growth of the long bones, and timing of the long bone epiphyseal unions. In the present study, all of these age changes have been examined with respect to ontogenetic development in *S. fuscicollis* and *S. oedipus*. Additionally, because of the interest in estimating the age of feral adult tamarins as well as the immature, data documenting the skeletal age changes associated with cortical microstructure and mid-diaphyseal cortex size and shape were also collected.

1. Dental Eruption

The sequence and timing of eruption of the deciduous and permanent dentition represent the most widely used parameters for estimating chronological age in wild-caught primates. The frequent application of these parameters may be attributed to the ease with which the data can be collected and documented from samples comprised of individuals whose ages are known and subsequently applied to unknown individuals. Of greater importance, however, is that the systematic patterning of dental eruption expresses one of the highest correlations with chronological age of all the traditionally observed age changes (Garn et al., 1959; Lewis and Garn, 1960; Voors and Metselaar, 1958). The basis of the high correlation is the apparent extreme degree of genetic influence on dental development (Glasstone, 1963, 1964; Niswander and Sujaku, 1965; Paynter and Granger, 1961, 1962). However, some genetic and environmental factors such as endocrine disturbances, radiation and severe malnutrition may interfere with the normal pattern (Hurme, 1960; Cohen, 1960).

Data for determining primate dental eruption sequence and timing have been taken from both roentgenographic (Bowen and Koch, 1970; Byrd, 1979; Johnston et al., 1970) and gross visual inspections (Gavan, 1967; Nissen and Riesen, 1964; Schultz, 1935). What constitutes an erupted tooth has not been methodologically standardized in the literature—varying from the first appearance of any aspect of a tooth crown penetrating the gingiva (Hurme and Van Wagenen, 1953, 1961; Nissen and Riessen, 1964) to the complete appearance of the entire top of the crown (Schultz, 1935). Therefore, care must be taken to identify how eruption was defined when comparing the results of various investigators and in using published standards to age feral specimens.

The optimal form of study of dental development permits longitudinal observations to be taken on colony-born animals whereby over time, the sequential order of eruption can be identified and standard age ranges calculated for the eruption of each morphological type of tooth. Unfortunately, long-term studies are generally not feasible. More often, the sequences and timing of dental eruption have been inferred from cross-sectioned samples. Furthermore, the chronological ages of the individuals comprising these samples are rarely known, thus allowing for only the sequential pattern of eruption to be suggested with no reference to timing. Procedures for analysis of cross-sectioned data differ slightly from longitudinal but are complementary. For example, in the cross-sectioned analysis of specimens of unknown age, eruption sequences are identified by first examining the relative degree of eruption for each tooth type in each individual, and then combining and comparing the data for the sample as a whole (Byrd, 1979; Schultz, 1935; Wintheiser et al., 1977).

Data collection from cranial material poses a unique problem not encountered in observations of cadaver and living animals—the inability to precisely determine gingival eruption in the absence of gum tissue. This has led some investigators to devise new criteria allowing for standardized measurements to be taken (Byrd, 1970; Kovacs, 1971).

Problems associated with estimating primate age from dental eruption data have been reported. For example, Hurme (1960) cites three variables relating to the success of estimating age. They are the number of observations which may be taken on the unknown-aged primate, the health and normality of the animal, and the availability of an accurate standard from which to infer age. With respect to the latter, Gavan and Hutchinson (1973) point out that the sample used to devise the standard is often the only sample against which the standard has been tested. They caution that the accuracy of a standard for estimating age can only be determined from comparisons with independent sample results. Unfortunately, with the possible exception of *Macaca mulatta*, numerous analyses of the same species do not exist.

To a great extent, the documentation of the sequences and/or timing of dental eruption in nonhuman primates has been restricted to Old World forms (Berkson, 1968; Bowen and Koch, 1970; Clements and Zuckerman, 1953; Krogman, 1930; Nissen and Riesen, 1945, 1964; Ockerse, 1959; Rahlman and Pace, 1969; Wintheiser et al., 1977), with particular attention given to *Macaca mulatta* (Eckstein, 1948; Gavan and Hutchinson, 1973; Haigh and Scott, 1965; Hurme, 1960; Hurme and Van Wagenen, 1953, 1956, 1961). Only a few investigators have attempted to decipher the dental eruption schedules in New World primates, with the least amount of data having been collected on the Callitrichidae.

Schultz (1935) provided the first attempt at documenting the dental eruption sequences for the permanent dentition within Platyrrhini genera. Observations were taken from unknown-aged, immature crania representing

Ateles, Cebus, Alouatta, and *Saimiri*. All analyses were made at the generic level. In addition, observations from three *Saguinus* (listed as *Oedipomidas*) specimens led Schultz to tentatively conclude that, ". . . all M2 appear before any of the premolars and that the canines are the last teeth to erupt completely" (Schultz, 1935:512).

In 1952, Serra expanded the knowledge of dental eruption sequences in New World primates to include all genera except *Cebuella* and *Callimico*. Data were collected from crania representing unknown-aged individuals. Analysis was left at the generic level and restricted to the permanent dentition. For genus *Saguinus*, Serra reports the following eruption sequence applicable to both jaws, although the mandibular eruption was most often observed to precede the maxillary complement: M1→I1→I2→M2→P4→P2→P3→C. Serra additionally provided a partial sequence for the genus *Oedipomidas*, now taxonomically considered *S. oedipus*. It was reported as: M1→I1→M2→__→__→__→__→C, with spaces representing areas of indeterminable sequence. It is interesting to note that it was observed to differ from the *"Saguinus"* pattern.

Following the work of Schultz (1935) and Serra (1952), investigators of New World primates began to examine the sequences and/or timing of eruption in both the deciduous and permanent dentitions, often treating sexes independently and at the species level rather than generic. Most notable for the Cebidae are the eruptive sequence studies by Tappan and Severson (1971) on *Saimiri sciureus* and *Cebus albifrons*, Thorington and Vorek (1976) on *Aotus trivirgatus*, and Long and Cooper (1968) on *Saimiri sciureus*. The former two studies were based on observations from cranial material and detailed only the permanent dentitions. The study by Long and Cooper reported longitudinal data from colony-born specimens for which examination was made of both deciduous and permanent dentitions and age ranges were calculated for the eruption of each morphological type of tooth.

Within the Callitrichidae, Johnston, Dreizen and Levy (1970) observed through radiographic and gross examination the dental development of 40 age-documented *Callithrix jacchus* cadavers. Deciduous and permanent eruption sequences and timing schedules were calculated. In their study, the sexes were treated independently and sexual dimorphism was determined insignificant.

Chase and Cooper (1969) examined the deciduous and permanent dental eruption sequences longitudinally in 16 colony-born *Saguinus nigricollis*, a closely related species to *S. fuscicollis* (Hershkovitz, 1977). Sexes were pooled for analysis. The permanent dentition eruption sequence derived for *S. nigricollis* is similar to, yet slightly different from, Serra's (1952) formula for genus *Saguinus*. Primarily, the differences lie in the mandibular eruption order of P_2 and P_3 (which is probably best explained as sequential variability between these teeth), and in the sequential timing of eruption between the mandibular and maxillary dental complements.

Byrd (1979) has completed an extensive study of dental development and eruption in Platyrrhine primates. Data were collected from roentgenographs of 1483 immature ceboid crania representing 44 species. Analysis was limited to the permanent dentition. From observations of

32 *S. fuscicollis* and 37 *S. oedipus*, Byrd reported the following eruptive sequences with parentheses indicating sequential variability.

For *S. fuscicollis*: $$\frac{\text{M1 I1 I2 M2 P4 (P3 P2) C}}{\text{M1 I1 I2 M2 (P4 P2) P3 C}}$$

For *S. oedipus*: $$\frac{\text{M1 I1 (I2 M2) P4 (P3 P2) C}}{\text{M1 I1 (I2 M2) (P4 P2) P3 C}}$$

The sequences for both *S. fuscicollis* and *S. oedipus* are extremely similar and closely approximate the results of Chase and Cooper (1969) for *S. nigricollis*. A test of significance between the eruption sequences of male and female *S. oedipus* led Byrd to conclude that no significant sexual dimorphism was indicated.

Although the sequence of dental eruption in *S. fuscicollis* and *S. oedipus* appears to have been accurately documented, no previous study has documented the timing of eruption for each morphological type of tooth, deciduous and permanent, for these two tamarin species. It is this documentation that allows for the estimation of chronological age of unknown specimens to be made based on dental eruption criteria.

2. Long Bone Growth

Body and long bone growth have been documented less frequently in nonhuman primates than dental eruption and epiphyseal union. More often, it has been applied to human material for the determination of growth standards which subsequently have been used for identification of variation in age-related growth between the sexes and races (Tanner, 1962, 1978). The use of long bone growth data as a technique for estimating age has also had greatest application in human samples, specifically archeological, where the recovery of subadult dentitions are commonly incomplete or totally absent (Johnston, 1962; Merchant and Ubelaker, 1977; Sundick, 1972). The problems associated with growth data as age-estimation criteria lie in the high degree of inter- and intraracial or species variability (Gavan and Hutchinson, 1973; Ubelaker, 1978) and the high susceptibility to environmental influence (Tanner, 1962, 1978).

Of all nonhuman primates, body and long bone growth data have been collected primarily from the various species of macaques (Gavan and Hutchinson, 1973; Gavan and Swindler, 1966; Haigh and Scott, 1965; Ikeda and Hayama, 1963; Kerr et al., 1972; Rahlmann and Pace, 1969; Watts, 1980). The studies have generally been longitudinal, examining colony-born individuals at periodic intervals by roentgenographic and gross inspections. The research of Kerr et al. (1972) presents an exception to the longitudinal form of study whereby observations were taken from sacrificed animals of known ages between conception and approximately five postnatal months. Collectively, the research on macaques has led to the extensive documentation of chronological growth of the body, head and skeleton within this species.

Only two major studies have been reported documenting chronological body and long bone growth in species of New World monkeys. Lusted et al. (1966) radiographically examined long bone growth of the tibia, femur, humerus and radius in 168 immature *Alouatta caraya*. Additionally, growth data of the 5th metatarsal, L3 and L6 vertebral body heights, and talus length were collected. Because the sample consisted of wild-caught individuals of unknown age, correlations of bone lengths and chronological age were not feasible. Correlations were made, however, using body weight and degree of dental wear as substitutes for chronological age. Males and females were treated independently. The results indicate that although an overall pattern of similarity in long bone growth is characterized by both sexes, females may reach maturity at an earlier age than males.

Chase and Cooper (1969) represent the only attempt to document the correlation of chronological age and linear growth in a *Saguinus* species. Weekly observations were recorded for head-body length and right foot length in 16 *S. nigricollis* from birth to maturity. At each weekly age, the sample range and mean were calculated for both measures. The general pattern of head-body growth appears to fit a smooth single curve reflecting a uniform rate of increasing length from birth until approximately 16 weeks, at which time growth decelerates and plateaus. Adult length is attained at approximately 12 months of age. Although a pubertal growth acceleration period has been observed in some nonhuman primates (van Wagenen and Catchpole, 1956; Watts, 1980; Watts and Gavan, 1979), the *S. nigricollis* growth curves do not support its presence within this species.

It is unfortunate that the documentation of body and long bone growth, a viable aid in predicting the age of individuals, is so poorly represented for most Old World primates, and virtually nonexistent for New World forms. This lack of data may be attributed to the unavailability of known-aged samples necessary to complete this type of research. Furthermore, many of those studies which have been attempted are based upon sample sizes so small they preclude the reliability of the proposed growth curves and thus diminish their predictive potential for assigning ages to feral animals.

3. Epiphyseal Union

The final developmental age change to be reviewed is the sequence and timing of fusion between the epiphyses and their respective diaphyses, culminating the longitudinal growth process of skeletal elements. Growth and development of bones in the mammalian skeleton, with the exception of various cranial bones, occur within cartilagenous preforms. The intracartilagenous ossification of a bone takes place in a variety of individual centers. In the long bones for example, the primary center is the location for growth of the shaft, or diaphysis. The growth and development of the epiphyses, or ends of the bones, and certain specific processes which develop into attachment areas for muscles are represented by secondary centers. The primary and secondary centers are separated from one another by an epiphyseal plate composed of hyaline cartilage. During the growth process, the plate is eventually replaced by bone at which time the epiphyses fuse, or unite, to the diaphysis forming a single adult bone. Further detailed discussions of skeletal ossification and growth may be found in numerous anatomy and histology tests (e.g., Goss, 1976; Ham, 1957).

The basis for the practical use of epiphyseal union data in determining the state of skeletal maturation and as a parameter for estimating age in feral animals is that the unions occur at different times for different bones following a genetically predetermined pattern. Environmental, genetic, and endocrine abnormalities may, however, alter the normal pattern and timing of fusion (Dawson, 1929, 1934; Todd, 1933). Once the sequential pattern has been identified and correlated with chronological age, age prediction can easily be inferred from the developmental state of union observed for various skeletal elements in the unknown individual. Furthermore, the sequence and timing of the epiphyseal union contribute to the extension of the range for estimating age past the point where dental eruption and long bone growth are applicable.

Although the sequences and, less often, timing of epiphyseal union have been documented in a number of nonhuman primates, there has been no standardization of methodology regarding which epiphyseal centers to observe, nor how the various stages of union should be scored and recorded. This has led to the virtual impossibility of making comparisons among studies and necessitates careful consideration when attempting to assign ages from published data.

Similar to the research conducted on dental eruption and long bone growth in nonhuman primates, epiphyseal union data have been collected by radiographic and/or gross examinations. However, determination of the stages of fusion by each of these two techniques may not necessarily be completely compatible (Wintheiser et al., 1977). This further demonstrates the need for caution when making comparisons among research results of different studies.

Traditionally, observations have been made on skeletal samples comprised of individuals whose ages were unknown which allowed for the sequence of union to be determined but not the chronological age associated with their fusion. More recently, with the growing number of private and governmental primate breeding facilities, observations of animals of known age have been taken both longitudinally on living forms and from skeletal samples. These observations have provided the basis for documenting the timing of union. Also, the pioneering studies of epiphyseal union often documented sequences at the generic level, pooling species for analysis. Alternatively, consideration has recently been made at the species level with the sexes treated independently to allow for examination of interspecies variability and sexual dimorphism.

The sequences and timing of epiphyseal union in nonhuman primates have been examined predominantly in Old World forms. Sequences of union based on skeletal samples have been reported for various species within, or at the generic level for, *Gorilla* (Randall, 1943), *Hylobates* (Schultz, 1944), *Pongo* (Schultz, 1941), *Pan* (Schultz, 1940), *Nasalis* (Schultz, 1942), *Papio* (Bramblett, 1969), *Cercopithecus* (Schultz, 1956; Wintheiser et al., 1977), *Cercocebus* (Schultz, 1956; Wintheiser et al., 1977), *Macaca* (Washburn, 1943), and *Presbytis* (Washburn, 1943). Hayama (1965) examined the sequences in *Macaca fuscata* from roentgenographs taken on feral animals. Additionally, the timing of fusion has been suggested from longitudinal observation of colony-born animals for *Macaca mulatta* (van Wagenen and Asling, 1958; Gisler et al., 1960) and *Macaca nemestrina* (Rahlmann and Pace, 1969).

The first attempt to document the sequence of epiphyseal union in New World primates was carried out by Schultz (1956). Fifteen centers of union were observed for analysis from animals representing *Cebus*, *Ateles* and marmosets (genus not specified by Schultz). Sequences for fusion were presented for intraskeletal regionalized centers (e.g., hip, shoulder and elbow) even though slight overlapping in the sequences in different centers was shown to occur. The general pattern of sequence determined for *Ateles* and *Cebus* was: elbow-hip-ankle-knee-shoulder-wrist. This sequence differs slightly from the most common pattern accepted for Old World primates by the inversion of wrist and shoulder order (Shigehara, 1980). The marmoset sequence was found to differ from both patterns and was characterized as: elbow-hip-ankle-wrist-knee-shoulder.

Lusted et al. (1966) examined epiphyseal union in 168 *Alouatta caraya* by roentgenographic observation. Fusion centers of the undocumented-aged sample were scored as early, intermediate, or late union. The results indicated that fusion of hip and elbow precede fusion of the knee, shoulder, and wrist within this species.

From gross examination of skeletal material, Tappan and Severson (1971) identified the sequence of epiphyseal union in *Cebus albifrons*, *Saimiri sciureus*, and *S. nigricollis*. Although the sample was characterized by individuals of unknown age, the investigators were able to assign tentative ages to the youngest individuals of *S. sciureus* and *S. nigricollis* by applying the dental eruption research of Long and Cooper (1968) and Chase and Cooper (1969). Consequently, an estimated chronological age of union for some epiphyses was obtained. Tappan and Severson observed that the overlap in sequences of union of epiphyses in different centers in their sample appeared to be greater than that previously reported for Old World anthropoids. This may be attributed to the relatively shorter maturation period seen in New World forms. The sequences of union in the two cebids were very similar and although oversimplified, generally exhibited a pattern of elbow-hip-ankle-wrist-knee-shoulder. The tamarins diverged from this pattern only in the inversion of wrist and knee. It is interesting to note that Tappan's and Severson's cebid sequence more closely reflects Schultz's (1956) marmoset pattern than his cebid pattern and furthermore, that the sequence for *S. nigricollis* differs from both.

Most recently, the sequence of epiphyseal union in *Aotus trivirgatus* has been added to the list of platyrrhine monkeys by Thorington and Vorek (1976). Their results from gross examination of 95 individuals indicated a similar pattern to that of the cebids observed by Tappan and Severson (1971). An estimated age for the fusion of some epiphyses was provided based on dental sequence data in *Saimiri* (Long and Cooper, 1968; Tappan and Severson, 1971).

To date, the sequence of epiphyseal union in tamarins has been limited to *S. nigricollis* (Tappan and Severson, 1971). The demonstration of different sequences for *Cebus* by Schultz (1956) and Tappan and Severson (1971) indicates the plausibility of interspecies variation within genera and warrants the examination of *S. fuscicollis* and *S. oedipus*. Also, the chronological age associated with fusion, which is the basis for age estimation, has not been sufficiently documented in any New World primate.

4. Cortical Microstructure and Mid-Diaphyseal Cortex Size and Shape

In 1965, Kerley reported a new technique for estimating the age of adult humans. The method, termed osteon counting, is based upon systematic changes in the histological structures associated with intracortical bone remodeling. Although Kerley was the first investigator to use histomorphological components of cortical bone as a parameter to estimate chronological age, earlier research had noted their relationship (Currey, 1964; Frost, 1963; Jowsey, 1960, 1964; Lacroix, 1951). Since its inception, the technique has been increasingly implemented in the anthropological areas of forensic and skeletal biology research (Bouvier and Ubelaker, 1977; Kerley, 1965, 1970; Singh and Gunberg, 1970; Ubelaker, 1974) and has prompted further investigation of the relationship between changes in cortical microstructure and chronological age.

The process of intracortical bone remodeling has been discussed at length in numerous publications (e.g., Enlow, 1963; Frost, 1963; Hancox, 1972; McLean and Urist, 1968) and only a brief description is presented here.

Throughout an individual's life span, intracortical bone is continuously subjected to remodeling. In the earliest stages during ossification, bone is laid down in thin concentric layers known as circumferential lamellae. As the bone grows in thickness by increasing the lamellar layers, it often encapsulates the small blood vessels that surround the growing bone and incorporates them into the cortex morphology. These vascular canals, called non-Haversian canals, are present in greatest number in young and adolescent individuals. At the same time the cortex is expanding to increase thickness, a perpetual bone remodeling process is occurring within the cortex. Osteoclastic activity cuts longitudinal channels through the lamellae. The channels are subsequently filled in with new bone (Haversian lamellae) except for a small central canal, the Haversian canal. The structure formed by the Haversian lamellae and canal is termed an osteon.

Similar to the circumferential lamellae, osteons may be subjected to osteoclastic destruction followed by osteoblastic formation of new osteons. When this occurs, the initial osteon becomes fragmented, losing some portion of its total configuration. With increasing age, the number of osteons and osteon fragments increase and the percentage of circumferential lamellae decreases.

In deriving the osteon counting technique, Kerley (1965) examined midshaft cross sections of the femur, tibia, and fibula of 126 individuals of documented age. Kerley restricted his observations to four 1.62 millimeter diameter (revised value by Kerley and Ubelaker, 1978) circular fields positioned to touch the periosteal border at each of the anterior, posterior, medial and lateral anatomical regions. Four structural components of remodeling were selected for observation and correlation to chronological age. They included for each field: the number of osteons, osteon fragments, non-Haversian canals and the percentage of circumferential lamellar bone. The morphology of the four components has been defined for microscopic identification by Kerley (1965, 1970). Simplified, they may be characterized as follows:

1. Osteon—A central vascular canal surrounded by concentric Haversian lamellae. A dense reversal line at the periphery separates the Haversian lamellae from other structures.
2. Osteon fragments—Fragments of old osteons which have been partially destroyed by osteoclastic action altering their concentric shape.
3. Non-Haversian canal—A vascular canal which, "can be distinguished from normal osteons by the presence of a denser reversal line and usually by the fact that the surrounding circumferential lamellae bend around them whereas osteons cut through the lamellae" (Ubelaker, 1978:65).
4. Circumferential lamellar bone—Thin layers of bony tissue that run parallel to each other around the outer part of the bone cortex.

These four features are schematically illustrated in Figure 4.

Kerley (1965) subjected his data to regression analysis to devise formulae (later revised by Kerley and Ubelaker, 1978) for estimating chronological age. The most accurate formula (with a standard error of estimate of 3.66 years) was derived from fibular osteon fragment data.

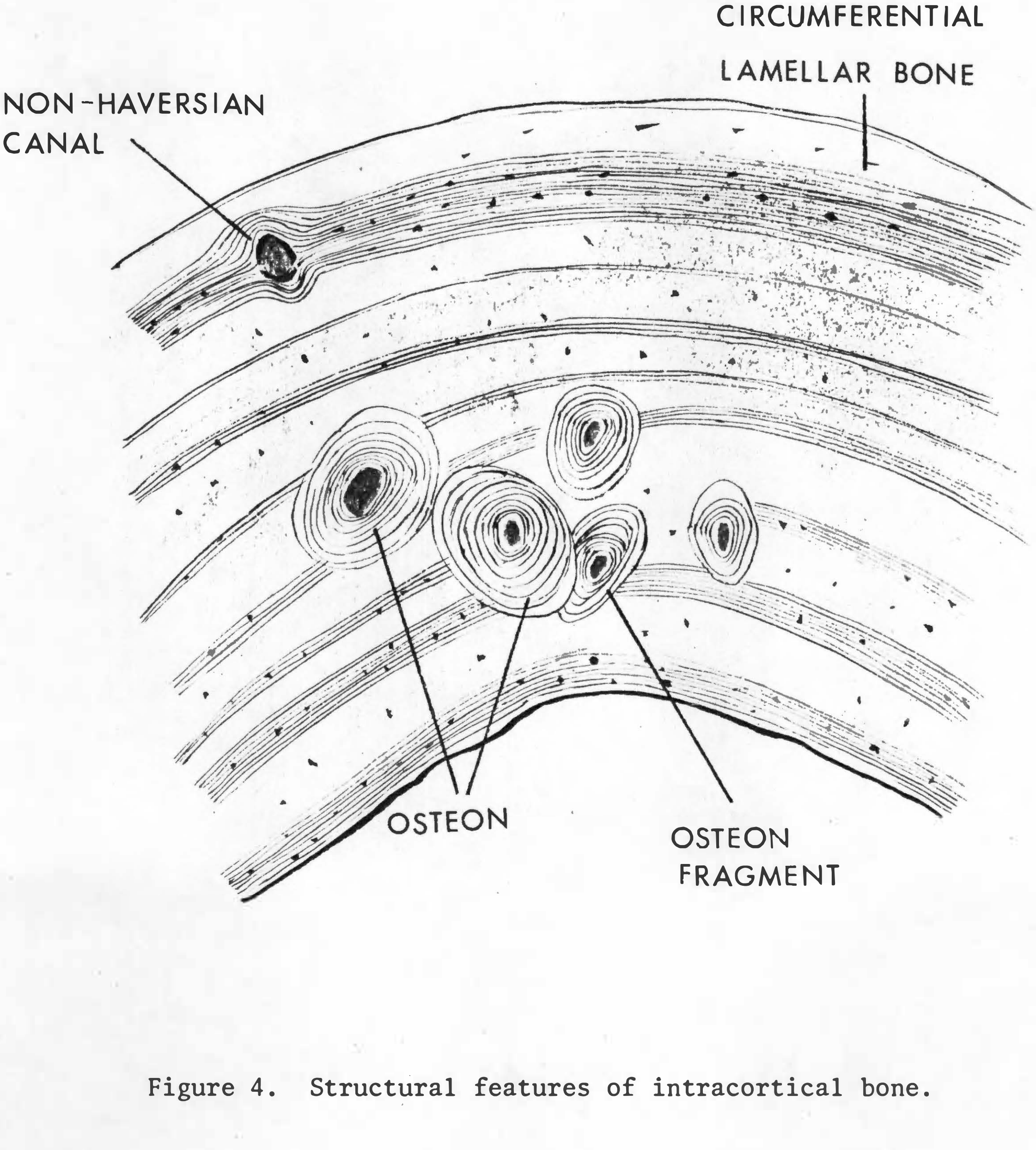

Figure 4. Structural features of intracortical bone.

Since the time that Kerley proposed his osteon counting technique, other investigators have reported similar correlations between advancing age and increasing numbers and density of osteons and osteon fragments (Alqvist and Damsten, 1969; Ortner, 1975; Singh and Gunberg, 1970; Thompson, 1979; Wu et al., 1970). Age changes in additional histomorphological components have been reported for the percent of zonal osteons (Pankovich et al., 1974), osteon diameter size (Kerley, 1965), and Haversian canal diameter size (Epker et al., 1964; Singh and Gunberg, 1970). In response to the continued investigation into using microscopic changes within cortical bone as a parameter for estimating age, alternative methodological procedures to that of Kerley's have been proposed—most notably by Alqvist and Damsten (1969) and Singh and Gunberg (1970).

In the Alqvist and Damsten (1969) modification of the original osteon counting technique, square-shaped fields made up of an ocular 100 square grid (10 squares = 1 millimeter of cortex) were used in place of Kerley's round-shaped fields. They believed that the square shape would alleviate many of the difficulties in observing and quantifying features located near the field borders. Although both methods use four fields for observation, modification was made in field placement by Alqvist and Damsten. They contend that because Kerley's posterior field is located on the linea aspera, remodeling due to muscular stress and unrelated to age may influence the observed condition. Therefore, they positioned their fields adjacent to the periosteal border but at equal distances between Kerley's anatomical sites, thus avoiding the linea aspera.

In quantifying the remodeling features of femoral midshafts, Alqvist and Damsten added together the number of grid squares within each field that were more than half-filled with either osteons or osteon fragments and converted the total into a percentage. A similar procedure was followed for all four fields and averaged. The data were subjected to regression analysis and a standard estimate of error of 6.71 years was computed.

Advantages of the Alqvist and Damsten quantification method include the ease with which features may be counted, the elimination of accurately differentiating between osteons and osteon fragments, and greater precision in determining the extent of nonremodeled bone.

In a comparative analysis of the age estimating abilities of the Kerley (1965) and Alqvist and Damsten (1969) techniques, Bouvier and Ubelaker (1977) suggested that although the Alqvist and Damsten method may be easier to use, the Kerley method provided greater accuracy and was therefore preferable. The poorer results attained from the Alqvist and Damsten formula may, however, be attributed, in part, to the small, uneven age distribution of the sample from which it was derived.

An alternative age estimation technique based on cortical remodeling by Singh and Gunberg (1970) was devised by studying cross sections of the mandible, femur, and tibia from 59 individuals between 39 and 87 years of age. Components of the analysis included the number of osteons, the average number of lamellae per osteon, and the average Haversian canal diameter. Unlike both the Kerley and the Alqvist and Damsten methods, only two observational fields were selected. Their positions within the bone section were chosen randomly but were restricted to the periosteal third. The data were subjected to multiple regression analysis which yielded formulae whose standard estimates of error were smaller than those derived from either of the two previously discussed methods (however, the age range of the sample was more restricted). Approximately 95 percent of their sample was accurately aged to within six years. Also, it was noted that the formulae derived from mandibular observations provided the most accurate estimates of age.

Concurrent with intracortical remodeling, additional remodeling of the bone cortex influenced by the normal aging process is identified in the deposition and resorption of the subperiosteal and endosteal surfaces. Changes in the rates of deposition and resorption produce changes in cortical thickness and shape over time. In general, the pattern for humans is characterized by greater deposition than resorption in developmental growth which is reflected in a rapid increase in cortical thickness. After adulthood has been achieved, there occurs a period of stability in bone thickness wherein the relative rate of formation and resorption remains in a state of equilibrium. This is followed by a period of cortical bone loss with advancing age (Garn, 1970; Silberberg and Silberberg, 1961). The decrease in cortical thickness may be attributed to inadequate formation of new bone, or of increased resorption of old bone, or of a combination of both (Silberberg and Silberberg, 1961:103). Regardless of age, a relationship between cortical bone loss and various metabolic disturbances such as hyperthyroidism, vitamin deficiency, menopause, hyperadrenalism and general malnutrition has been noted (Silberberg and Silberberg, 1950, 1961).

Numerous investigators have examined the age-related patterns of cortex size and shape in human populations (Atkinson and Woodhead, 1973; Dewey et al., 1969; Ericksen, 1976; Jenkins, 1968; Smith and Walker, 1964). Most notable are the works of Garn and his colleagues (Garn, 1970; Garn and Shaw, 1977; Garn et al., 1969) who have confined their examination primarily to cortical thickness in the second metacarpal, the most commonly used skeletal element in documenting the earlier gain and later loss of cortical bone.

Among the results generated from the study of adult cortical bone loss in humans, two general observations concerning its occurrence and variation have been reported. First, evidence suggests that the rates of cortical bone loss vary between specific elements within the skeleton (Barnett and Nordin, 1966; van Gerven, 1973; Ericksen, 1976). Second, significant variation occurs in the timing and degree of bone loss between the sexes (Garn, 1970; Tonna, 1977; Morgan and Newton-Jones, 1969) and between racial groups (Garn and Shaw, 1977; Ericksen, 1979).

The evaluation of cortical bone loss is generally measured by an index value representing the proportion of medullary cavity diameter to the external cortex diameter (Ericksen, 1979). Traditionally, measurements have been taken along the anterior-posterior dimension. Garn (1970) expanded his analysis to include an index value of the total percent of cortical area (PCA). The area measurements were calculated from the diameter of the cortex and medullary cavity based on cylindrical shape. This procedure assumes uniform deposition and resorption rates for all dimensions.

Ericksen (1979) and van Gerven et al. (1969) independently compared the effects of aging on the expansion of the medullary cavity in the anterior-posterior and medial-lateral dimensions of various human long bones. Both investigators arrived at similar conclusions. For humans, increasing expansion caused by endosteal resorption was more highly correlated with age along the anterior-posterior dimension. Therefore, in analyses of age-related cortical bone loss, support was given for the continued use of measurements to be taken along this dimension. Additionally, it demonstrated the need for caution to be taken in using PCA values when calculated from diameter measurements.

From cross-sectional data, the pattern of adult cortical bone loss has been documented most commonly by the plotting of mean values for a sequence of ages and regression analysis (Ericksen, 1979; Garn, 1970). Although many attempts at regressing the cortical loss of bone on age have assumed linearity, Ericksen (1979) has demonstrated that in some cases the relationship is best described as curvilinear.

While the potential for estimating age in nonhuman primates from osteon counting and/or the changes in cortex and medullary cavity diameters appears promising, there has been little attempt to document these age-related changes. Bowden et al. (1979) examined the age-related changes in the cortical thickness in the second metacarpal; the rate of new bone deposition and the density and degree of remodeling of osteons in the femur; and the mineral composition of cortical and trabecular bone in the tibial shaft from 20 *Macaca nemestrina* and 2 *M. fascicularis*. The sample consisted of four-year-olds, ten-year-olds and twenty-year-olds.

With respect to the cortex changes of the second metacarpal, an attempt was made to follow the procedure of Garn's human data so that comparable evaluations could be made. This included the calculations of cortical and medullary cavity areas used in the standard PCA index (Garn, 1970). However, in contrast to Garn, area measures were calculated with the use of a digitizer and microprocessor which provided exact measures to be taken rather than estimates derived from diameter measurements.

Bowden et al. demonstrated that (1) the PCA index value for the second metacarpal significantly differentiated between the three age groups by a continual trend in cortical bone loss with advancing age and (2) the number of femoral osteons as measured by per square centimeter did not vary significantly with age. However, the variation in degree of remodeling did show a significant increase in the older age groups.

In a similar study, Przybeck (1981) investigated the relationship of age and histological variables in 50 *Macaca nemestrina* of known age. His variables included total cross-sectional area, frequency of secondary osteons and osteon fragments, osteon area, and non-Haversian canal size. Data were collected from the sixth rib. Przybeck's results indicated that the age-related changes in *Macaca nemestrina* broadly paralleled those observed in humans. This is in contrast to the findings of Bowden et al. (1979) with regard to the identified correlation between age and the frequency of osteons and osteon fragments.

Previous to this dissertation research, the only study to examine age-related histomorphology in a New World primate was conducted by Glassman and Schmidt (1980). Femoral cross-sections from 22 *S. fuscicollis* and 8 *S. oedipus*, ranging from one day to 15 years of age, were subjected to qualitative observations to document the age-related trends in cortical deposition and resorption, and the frequency of osteons and osteon fragments. The pattern identified in this study is summarized below.

From birth to approximately three months, the cortex incorporates a highly vascular network of non-Haversian canals without exhibiting well-defined periosteal and endosteal borders. By three months, the cortex becomes more structurally organized with rapid deposition of circumferential lamellae, coupled with the endosteal resorption characteristic of primate growth remodeling. Internal or secondary osteon remodeling initially appears at nine months and, soon thereafter, secondary osteon fragments are present. At this age, the internal remodeling is endosteally located and primarily limited to the posterior quadrant of the cortex.

From 9 to approximately 15 months, the rapid cortical expansion continues and an increase in the number of osteons and osteon fragments occur. Between 15 and 24 months, a pronounced anteriorly directed cortical drift begins, with internal remodeling expanding into the medial and lateral quadrants of the cortex. Only after two years are the first individuals with internal remodeling scattered throughout the entire cortex identifiable. From two to five and one-half years, as cortical drift continues, osteon remodeling shifts from the endosteal border to midcortex. Between six and nine years, the degree of variability in the number of osteons and osteon fragments, along with their position in the cortex, is sufficiently great to prohibit isolation of any characteristic trend.[1]

Specimens older than nine years, however, are again distinguished by the expansion of the medullary cavity and the subsequent loss of cortical bone. The extensive endosteal resorption responsible for the cortical bone loss persists to such an extent that in many cases, all evidence of previous internal remodeling is lost. In advanced cases of cortical "thinning" for adults older than 12 years of age, the cortex is approximately one-half to one-third the average thickness for a middle-aged adult.

Except for this dissertation study, no quantitative investigation has been made to determine the potential for estimating adult age in tamarins from the chronological changes manifest in intracortical remodeling and/or the relative degree of adult cortical bone loss. If it can be demonstrated that these changes follow a systematic,

---

[1] A similar degree of increasing variation in the frequency of osteons and osteon fragments with advancing age has been reported for the femur for *Macaca nemestrina* and *M. fascicularis* (Bowden et al., 1979).

age-determined pattern, they may provide a sound basis for the assignment of ages to tamarins of unknown age.

CHAPTER III

METHODS AND MATERIALS

A. ORAU Marmoset Collection: Background and Sample

The sample used in this study is part of a larger collection donated to The University of Tennessee, Knoxville by the Oak Ridge Associated Universities (ORAU). Since the 1960's, the ORAU has been engaged extensively in a marmoset breeding program which has generated numerous studies involving a variety of aspects of behavior, genetics, and anatomy. Dr. Gengozian, the former senior scientist of the breeding facility, began preserving by freezing all of the skulls of the deceased marmosets. He then expanded the frozen collection to include the entire autopsied, eviscerated cadavers. Records were retained detailing cause of death, parentage, age, sex, and other demographic features.

As pointed out in the introduction, it was Dr. Richter, veterinarian for the ORAU marmoset breeding facility, who first suggested that the stored cadaver collection be used for the problem of documenting skeletal age changes. Although only those marmosets that were colony born, hence, of known age, were to be used in this capacity, the ORAU advisory committee recognized that the entire collection, including those cadavers representing captive specimens should be skeletonized and reposited together to maximize future scientific investigation of marmoset skeletal anatomy.

The frozen cadavers were brought to The University of Tennessee for maceration of the soft tissue. Since 1978, approximately 1,200 marmosets have been processed. A summary of the sample size of the overall collection by subspecies is presented in Table 2.

Prior to maceration, each cadaver was x-rayed, a scalp fur sample collected, and the dermal surfaces of the fore- and hindlimbs removed and "fixed" in a formaline solution (Glassman and Webb, n.d.). The maceration technique began by first skinning the primates and removing the majority of soft tissue adhering to the skeleton. Each animal was then disarticulated at the neck, shoulder, pelvic, and two caudal joints to facilitate the space requirements of the maceration jars and to decrease the time needed for skeletonization. The disarticulated skeletal material was then placed in 10 ounce, glass jars and filled with enough water to cover the entire specimen. The jars were sealed and placed within boxes in the zooarcheology lab of the anthropology department.

Using this technique, approximately two months were necessary for complete skeletonization. This time period, however, varied depending on the outside and room temperature and the degree to which the specimen had been dehydrated from the freezing-storing process. The more dehydrated specimens required the longest time to macerate.

The maceration jars were periodically examined and when the bacterial action was determined complete, the water was poured off through a two-inch diameter strainer used to collect the bones and teeth. The recovered skeletal material was left to dry overnight and

Table 2. Overall ORAU Collection Sample Size by Species and Completeness

	Newborn Skeletons (0-14 days)		Infant and Adult Skeletons (>15 days)		Skulls Only (all ages)		
Species	Known Age	Unknown Age	Known Age	Unknown Age	Known Age	Unknown Age	Species Total
Callimico goeldii	1	-	-	-	2	-	3
Callithrix jacchus jacchus	10	-	30	21	4	10	75
Cebuella pygmaea	2	-	1	-	-	1	4
Saguinus fuscicollis illigeri	96	-	81	72	180	50	479
Saguinus fuscicollis lagonotus	3	-	6	18	22	13	62
Saguinus fuscicollis leukogenys	3	-	2	8	1	6	20
Saguinus fuscicollis nigrifrons	16	-	6	28	13	25	88
Saguinus mystax	4	-	-	4	5	5	18
Saguinus nigricollis	2	-	7	7	6	13	35
Saguinus oedipus oedipus	85	-	36	65	35	50	271
Hybrids	51	-	38	1	74	1	165

then labeled, numbered and catalogued into the collection. Skeletal elements of each specimen have been retained in individual cardboard boxes for curation.

Different sample sizes of *S. oedipus* and *S. fuscicollis* were used to document the age trends associated with dental eruption, long bone growth, epiphyseal union, intracortical remodeling, and mid-diaphyseal cortex size and shape. Specimens were chosen for their applicability based on age and skeletal completeness for the specific trend under analysis. *S. oedipus* specimens were all of the *oedipus* subspecies while the *S. fuscicollis* sample was composed of individuals from the *illigeri, nigrifrons, lagonotus,* and *leucogenys* subspecies. In addition, subspecies hybrids of the species *fuscicollis* were included.

Within each species, sexes were pooled for all analyses.[1] This was done to maximize sample size and enhance the extent to which the sample covered the entire approximate 15-year life span of these tamarins. The two species were treated independently for all analyses. A description of the methods employed and the sample sizes used for each age change are presented below.

B. Dental Eruption

The first developmental age change to be documented was the general sequence and timing of dental eruption. Data for dental eruption were

---

[1] *Saguinus oedipus* and *S. fuscicollis* are characterized by the virtual lack of sexual dimorphism in body linear measurements (Hershkovitz, 1977:783 for *S. oedipus* and page 674 for *S. fuscicollis*).

collected from 27 known-aged specimens of *S. oedipus* and 62 specimens of *S. fuscicollis*. For *S. fuscicollis*, the specimens collectively represent all phases of eruption. The limited sample size of *S. oedipus* specimens available for analysis provides for only a tenuous documentation of dental eruption for this species. Dental eruption sample sizes by one-week age intervals for *S. fuscicollis* and *S. oedipus* are presented in Table 3.

All observations for dental eruption analysis were made prior to maceration. The soft lip tissue of the maxilla and mandible were removed by scalpel and the jaws partially disarticulated at the temporomandibular joint to facilitate examination of the alveolus and dentition.

To record the degree of dental eruption, a data form was constructed listing the deciduous (I1, I2, C, P2, P3, P4) and permanent (I1, I2, C, P2, P3, P4, M1, M2) teeth. Maxillary and mandibular dentitions were recorded separately and a value of 1 or 2 was scored for each dental variety. Value designations were:

1. Unerupted: Tooth not visible above gingiva.
2. Erupted: Entire tooth crown visible above the gingiva but not necessarily in full occlusion.

For cases of asymmetrical eruption, where one tooth had erupted while the homologous tooth had not, the dental variety was scored a value of 1, or not erupted. Therefore, a specimen exhibiting a complete set of 24 deciduous teeth was given a value of 2 for each of the maxillary and mandibular deciduous dental varieties and a score of 1 for each of the permanent teeth.

Table 3. Sample Size of Specimens Included in Dental Eruption Analysis by Species in One Week Intervals

Age	*S. fuscicollis*	*S. oedipus*	Age	*S. fuscicollis*	*S. oedipus*
0-1	15	12	26-27	-	-
1-2	6	5	27-28	-	-
2-3	1	1	28-29	-	-
3-4	-	-	29-30	1	-
4-5	1	-	30-31	1	-
5-6	2	-	31-32	1	1
6-7	3	-	32-33	1	-
7-8	2	-	33-34	1	1
8-9	1	-	34-35	-	-
9-10	2	-	35-36	-	-
10-11	-	-	36-37	-	-
11-12	2	-	37-38	1	-
12-13	-	-	38-39	1	-
13-14	1	3	39-40	1	-
14-15	1	-	40-41	-	-
15-16	2	-	41-42	-	-
16-17	1	2	42-43	-	1
17-18	1	-	43-44	-	-
18-19	1	-	44-45	1	-
19-20	2	-	45-46	-	-
20-21	4	1	46-47	-	-
21-22	1	-	47-48	1	-
22-23	1	-	48-49	-	-
23-24	1	-	49-50	-	-
24-25	-	-	50-51	1	-
25-26	-	-	51-52	-	-
				62	27

The recorded data were initially examined to document the sequencing of deciduous and permanent dental eruption. For each species, sequence determination was made independently for the maxillary and mandibular dentitions and was initiated by positioning the recording forms in ascending order according to age, and sequentially comparing which teeth had erupted relative to those that had not. Variation between the maxillary and mandibular sequence for dental eruption was recorded.

To document the timing of dental eruption, examination was first made of the deciduous dentition. Again, species were treated separately and within each species the maxillary and mandibular components were taken independently. Eruption age ranges were calculated for each deciduous dental variety in both the maxilla and mandible. Calculations were based on the age of the youngest specimen to have the particular tooth erupted to the earliest age where all older individuals show an erupted condition. The permanent dentition was subjected to similar procedures.

Following the determination of age of eruption of the deciduous and permanent teeth, comparisons were made of overall interspecies variation and intraspecies variation of the maxillary and mandibular conditions.

C. Long Bone Growth

The second skeletal age-related trend of developmental aged *S. fuscicollis* and *S. oedipus* tamarins involved the documentation of the rates of long bone growth. Data for analysis were collected from 59 known-aged specimens of *S. fuscicollis* and 33 known-aged specimens of *S. oedipus* ranging from one day to 24 months. The entire sample was limited to specimens from which complete sets of data were obtainable.[2] The sample sizes for the two species by two-week age intervals are presented in Table 4.

Long bone data from the humerus, radius, ulna, femur and tibia were recorded for each specimen. In addition, a measure of the maximum length of the ilium was taken. Left bones were used whenever possible, but in cases where the left was broken or missing, the right was substituted.

Measurements were taken for the maximum length of each skeletal element as defined by Bass (1971) and were not restricted to the diaphysis, but also included any united epiphysis. All measurements were taken with a Vernier sliding caliper graduated to one-twentieth millimeter. Recorded data were then punched on standard 80 column computer cards and checked twice against the original measurements to minimize error.

Individual growth plots within each species were constructed to document the relationship between chronological age and the maximum length of each long bone and the ilium for the subadults of *S. fuscicollis* and *S. oedipus*. A curvilinear regression line was fitted to each growth plot using the General Linear Models procedure of the SAS package

---

[2] Exceptions include ten specimens of *S. fuscicollis* missing femoral data, one *S. fuscicollis* missing all hindlimb data, and one *S. oedipus* missing femoral data.

Table 4. Sample Size of Specimens Included in Long Bone Growth Analysis by Species in Two Week Intervals

Age	*S. fuscicollis*	*S. oedipus*	Age	*S. fuscicollis*	*S. oedipus*
0-2	10	10	56-58	-	-
2-4	2	2	58-60	-	1
4-6	1	-	60-62	-	-
6-8	1	-	62-64	1	-
8-10	4	-	64-66	-	2
10-12	2	1	66-68	-	1
12-14	2	-	68-70	1	-
14-16	4	-	70-72	1	-
16-18	5	-	72-74	-	-
18-20	6	2	74-76	-	-
20-22	-	-	76-78	-	-
22-24	2	-	78-80	-	-
24-26	3	-	80-82	1	-
26-28	1	-	82-84	1	-
28-30	2	1	84-86	-	-
30-32	1	2	86-88	-	-
32-34	1	-	88-90	-	-
34-36	1	-	90-92	1	-
36-38	-	1	92-94	1	-
38-40	1	1	94-96	-	-
40-42	-	-	96-98	2	-
42-44	1	-	98-100	-	-
44-46	-	2	100-102	-	1
46-48	-	-	102-104	-	1
48-50	-	-	104-106	-	2
50-52	-	-	106-108	-	-
52-54	-	-	108-110	-	2
54-56	-	-		59	33

(SAS Institute, 1979). The model selected to represent the chronology of long bone growth was the Jenss-Bayley curve (Jenss and Bayley, 1937), which takes the form of the equation

$$y = a + b_1 t + b_2 \log t$$

where

y = the length of the long bone, and

t = age.

This model has been successfully used to represent the relationship between age and human stature growth for the period up to nine or ten years (Deming, 1957; Jenss and Bayley, 1937).

To identify whether significant interspecies variability exists with respect to growth rates, the tamarin long bone data were subjected to an analysis of covariance, (ANACOVA) (SAS Institute, 1979). Here, the interaction of the linear and curvilinear components were tested against the model with species as the treatment and age and the common logarithm of age as covariates. This procedure allows for the determination of species differences in both the slope of the linear and curvilinear components and in the mean age for a given height.

For the prediction of chronological age from long bone lengths, regression formulae were devised using age as the dependent variable. The model selected to generate the formulae was

$$\text{Age} = a + b_1 x + b_2 (x)^2$$

where

x = long bone length.

The model was applied to all categories of long bones and the ilium thus yielding seven age-prediction equations for each species.

D. Epiphyseal Union

Twenty-one areas of epiphyseal union and one area of synchrondrosis closure (Table 5) were examined in 84 *S. fuscicollis* and 36 *S. oedipus*. Only specimens which would allow for complete data sets to be taken were used. Left bones were used whenever possible and the right substituted when necessary. All observations were made directly from the skeletal material and not from the roentgenographs taken of the specimens. The sample sizes of the two species by one-month age intervals are provided in Table 6.

Each epiphyseal union area was scored, and a value of one, two, or three was recorded, similar to the method proposed by Tappan and Severson (1971). Value designations referred to are:

1. Not united: Epiphysis completely separate.
2. Uniting: Includes the formation of the first specules of connection between bones to a state where the line of demarcation remains visable.
3. United: No visible opening between bones. Line of demarcation absent.

These stages are schematically represented in Figure 5.

The general sequence of epiphyseal union was identified by examining the order in which the epiphyseal centers became united with advancing age. Ranges of fusion were calculated to document the

Table 5. Areas of Epiphyseal Union by Skeletal Element Observed for Age Change Analysis

INNOMINATE:

1. Ischium-pubic ramus
2. Ischium-pubis: ilium
3. Ischium-pubis
4. Iliac crest

SCAPULA:

5. Coracoid process

HUMERUS:

6. Medial epicondyle
7. Proximal epiphysis
8. Distal epiphysis

ULNA:

9. Proximal epiphysis
10. Distal epiphysis

RADIUS:

11. Proximal epiphysis
12. Distal epiphysis

FEMUR:

13. Head
14. Greater trochanter
15. Lesser trochanter
16. Distal epiphysis

TIBIA:

17. Proximal epiphysis
18. Distal epiphysis

FIBULA:

19. Proximal epiphysis
20. Distal epiphysis

CRANIUM:

21. Spheno-occipital synchondrosis

Table 6. Sample Size of Specimens Included in Epiphyseal Union Analysis by Species in One Month Intervals[a]

Age	*S. fuscicollis*	*S. oedipus*
0-1	12	12
1-2	3	1
2-3	5	1
3-4	10	-
4-5	8	2
5-6	5	-
6-7	4	1
7-8	2	2
8-9	2	2
9-10	1	-
10-11	-	2
11-12	-	-
12-13	-	-
13-14	-	1
14-15	1	-
15-16	-	3
16-17	2	-
17-18	-	-
18-19	-	1
19-20	3	-
20-21	-	-
21-22	2	-
22-23	2	1
23-24	-	1
24-25	1	3
25-26	1	2
Total	64	35

[a] An additional 23 *S. fuscicollis* and 1 *S. oedipus* each greater than 26 months were examined to document the unions of the ischial epiphysis, iliac crest and spheno-occipital synchondrosis.

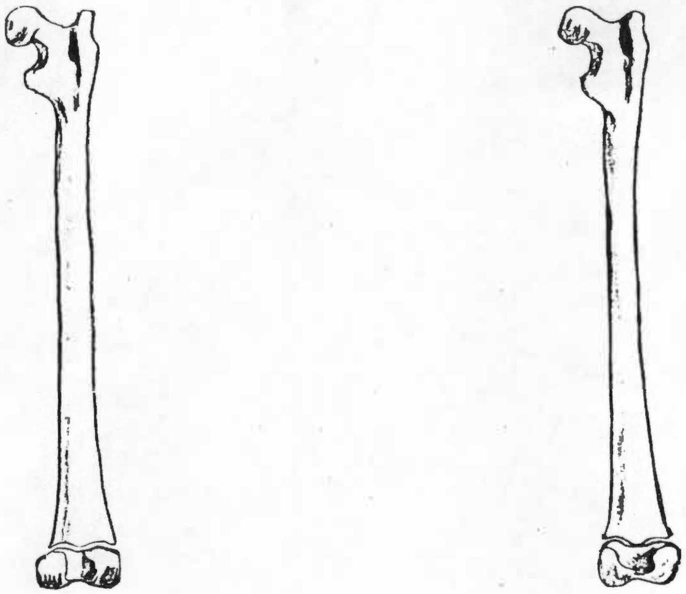

VALUE 1: not united

VALUE 2: uniting

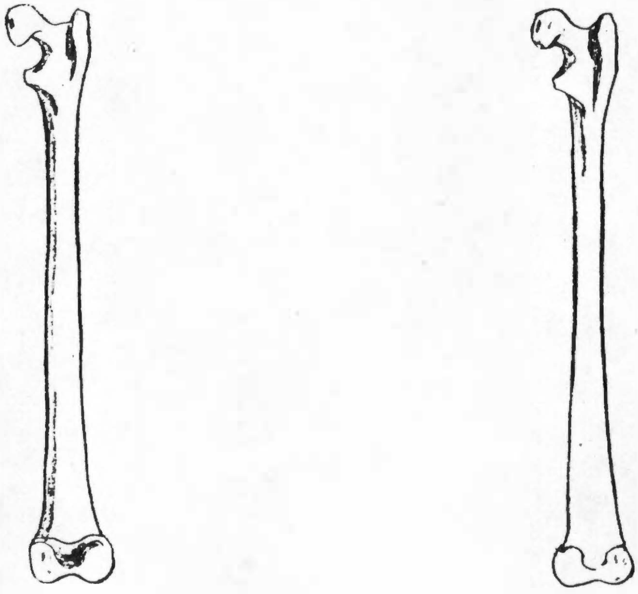

VALUE 2: uniting

VALUE 3: united

Figure 5. Scoring criteria for epiphyseal union (note distal epiphysis).

age of union for each epiphyseal center. The ranges were calculated as the age of the youngest specimen to possess a uniting (value 2) epiphysis to the youngest age where all older individuals exhibited a condition of complete union (value 3). The first occurrence of complete union within the fusion range was also recorded. Comparisons were made to determine the existence of interspecies variation in the general order of epiphyseal union and in the timing of fusion.

E. Cortical Microstructure and Mid-Diaphyseal Cortex Size and Shape

Documentation of age changes in degenerating or adult tamarins was limited to trends which occur within cortical microstructure and in mid-diaphyseal cortex size and shape.

Thin sections of the humerus, ulna and tibia were observed for specimens ranging between one and fifteen years of age. Sample sizes varied by bone for each species are presented in one-half year intervals in Table 7. Left bones were used when available. Femora were not included in this study, but are being analyzed separately by Dwight Schmidt of The University of Tennessee. Unfortunately, that research has not been completed, rendering comparison of age prediction ability between the femur and the skeletal elements under study impossible at this time.

Before sectioning, the bones were color-coded according to anterior, posterior, medial and lateral quadrants. Next, they were placed in a small open glass jar filled with 10 percent formalin

Table 7. Sample Size of Specimens Included in Cortical Microstructure and Cortex Size and Shape Analyses by Species in Years

	S. fuscicollis			*S. oedipus*		
Age	Humerus	Tibia	Ulna	Humerus	Tibia	Ulna
1.0-1.5	2	2	1	4	4	4
1.5-2.0	6	5	5	3	3	4
2.0-2.5	2	-	3	3	2	3
2.5-3.0	1	1	1	1	1	1
3.0-3.5	3	3	3	-	-	-
3.5-4.0	-	-	-	-	-	-
4.0-4.5	2	2	2	-	-	-
4.5-5.0	1	1	1	1	1	1
5.0-5.5	4	4	3	-	-	-
5.5-6.0	5	5	4	-	-	-
6.0-6.5	3	3	3	-	-	-
6.5-7.0	1	1	1	-	-	-
7.0-7.5	1	1	2	-	-	-
7.5-8.0	4	4	3	-	-	-
8.0-8.5	1	-	1	-	-	-
8.5-9.0	1	1	-	-	-	-
9.0-9.5	1	2	2	1*	1*	1*
9.5-10.0	1	1	1	-	-	-
10.0-10.5	1, 1*	1	1	-	-	-
10.5-11.0	1*	1*	1*	-	-	-
11.0-11.5	1	2, 1*	1	-	-	-
11.5-12.0	2*	1*	1*	-	-	-
12.0-12.5	-	-	-	-	-	-
12.5-13.0	1	1	2	-	-	-
13.0-13.5	-	-	-	-	-	-
13.5-14.0	-	1*	-	-	-	-
14.0-14.5	-	-	-	-	-	-
14.5-15.0	1*	1*	-	-	-	-
	47	45	42	13	12	14

*Individuals of unknown age, known to be greater than 10 years old who were selected for inclusion into the sample to increase size for older adults.

solution and placed in a water-operated vacuum chamber. The vacuum was operated at 25 Hg for 25 to 30 minutes. The bones were then sealed in the formalin jar to await sectioning which occurred within three days.

All sections were removed from the midshaft with a Buehler Isomet low speed saw. A slower speed setting was desired (four on a scale of ten) to minimize the hinging effect on the periosteum when the saw completed its cut. Placing slight tension on the bone during the final stages of cutting also acted to reduce the size of the hinge. Cutting time was approximately three minutes. Two sections were taken from each bone and hand-ground on Buehler 600 grit Carbimet paper discs affixed to a 5 × 7 inch flat glass plate to a thickness of 80 to 90 microns. Measurement was taken using a Starrett micrometer caliper. Once the desired thickness was achieved, the sections were hand-polished using a Buehler six micron Metadi diamond polishing compound on a polishing cloth for approximately five minutes per side. The polished sections were placed in a small beaker containing xylene and partially submersed in an ultrasonic cleaner to remove all polishing paste and dirt particles. Both sections were mounted on the same 1 × 3 inch clear glass slide, labeled, and cover-slipped using Permount as a mounting medium.

Once the sections were mounted, they were subjected to photomicroscopy using a Nikon 35 millimeter camera affixed to a Wise binocular dissecting scope under approximately forty power. A dark field background was found to be superior in enhancing the contrasts of the intracortical microstructure. Photographs were taken with

Kodak Panatomic X black and white film with an exposure of two seconds at a maximum light setting. Two to four photographs were required to represent the entire section. Composites were made by cutting and taping the photographs at areas where distinct features were located in order to minimize error.

At the beginning and end of each roll of film, a photograph was taken of a hemacytometer grid scale. The photographed scales were subsequently used to determine the possible presence of variation in the photographic printing procedures and additionally provided a constant from which actual cortex size could be determined.

The variables used to document the chronology of intracortical remodeling were the combined number of osteons and osteon fragments and the number of non-Haversian canals. Standardization for the effects of cortical size difference was achieved by dividing the respective counts by the cortex area in square millimeters. Counts were taken from the humerus, tibia, and ulna of all individuals and were made without knowing the actual ages of the animals.

To determine the cortex area, the composite photographs were digitized using The University of Tennessee IBM 360 computer and entered into the computer for area calculations. The program, TENTAB.FOR, by which the interactive graphics tablet allowed the data to be digitized, was taken from Slutzky (1981).

The formula used to calculate area was based on arc segments and taken from Chasen (1978:190). It may be represented as the equation:

$$\text{Area} = 1/2[(X_1Y_2 + X_2Y_3 + \ldots + X_{N-1}Y_N + X_NY_1) - (X_2Y_1 + X_3Y_2 + \ldots + X_NY_{N-1} + X_1Y_N)]$$

Two computer-generated area measurements were taken from each photograph. The first measured the area inside the perimeter of the periosteum providing a measure of the total section area (TSA). The second area calculated represented the medullary cavity taken as the area inside the perimeter of the endosteal border (MCA). Therefore, the area of cortical bone could be determined as

$$\text{Cortical Area} = \text{TSA} - \text{MCA}.$$

Values were provided in square millimeters and divided by the constant derived from the photographed grid scales to document the actual cortex area. It was determined that one millimeter of bone was equivalent to 41.3 millimeters of photographed bone. To test for the overall reliability of digitization and area computation, a designated square millimeter of the photographed hemacytometer grid scale for each roll of film was subjected to digitization and area calculation. For the 14 scales tested, the mean calculated area was .99 square millimeters with a standard deviation of .01 square millimeter. Therefore, the procedures used to determine cortical area were considered acceptable.

Osteon, osteon fragment and non-Haversian canal counts were taken using a binocular Olympus microscope under 100 power magnification. Polarized light was used to enhance the histomorphologic features, thus allowing for greater precision in counting. As mid-diaphyseal diameter does not exceed five millimeters and the average cortical thickness of the larger bones, the humerus and tibia, is less than 0.5 millimeters, the entire cortex was examined.

A possible obstacle to the accurate compilation of osteons and osteon fragments was identified in the irregular shapes of the borders of many of these features. The irregular shapes gave the impression of extensive remodeling.[3] To ensure consistency, each section was counted twice, in reverse order of its original counting. That is, the section counted first during the primary examination was counted last in the final. After the two counts were completed, they were compared. The average difference was approximately plus-or-minus three features.

The initial procedure for documenting the chronology of intracortical remodeling was to subject the standardized data along with the variable, age, to a Pearson product-moment correlation analysis (SAS Institute, 1979). This analysis provides a matrix of the correlation coefficients between all variables and a test of the null hypothesis that $p = 0$. *A priori* expectations based on analyses of human material include a positive correlation between the number of osteons and osteon fragments and advancing age, and a negative correlation between the number of non-Haversian canals and advancing age (Kerley, 1965).

---

[3] A similar condition has been reported from femoral thin-sections for various macaque species (Bowden et al., 1979).

For each skeletal element, the variables found to be significantly correlated with chronological age were plotted with the variable count on the vertical axis and age on the horizontal. Using regression analysis (SAS Institute, 1979), a series of linear and curvilinear models were tested to further document the significant relationships. The model which generated the greatest R^2-value with all components significantly contributing was considered to best reflect the particular relationship. The "best" fit model was found to be dependent upon the age-correlation examined (i.e., osteon counts or non-Haversian canal counts) and the skeletal element from which it was taken (i.e., humerus, tibia or ulna). Once a model was selected as best representing a relationship, it was used to fit a regression line to its respective developmental plot.

To document the adult changes observed in the size and shape of the mid-diaphyseal cortex, eight variables reflecting both thickness and diameter of various dimensions were taken. Measurements were taken from the photographic sections of all individuals for each skeletal element using a vernier sliding caliper graduated to one-twentieth millimeter. The measurements were then converted by the hemacytometer constant to actual size, to the nearest .001 millimeter. Similar to the osteon counting procedure, the age of the specimens was not known at the time measurements were taken.

Prior to measuring, the photographic sections were color-coded to represent the anatomical positions of anterior, posterior, medial, and lateral. Following this, bisecting lines were drawn connecting anterior to posterior and medial to lateral. These perpendicular lines form the axes on which all measurements were taken.

The variables used in the analysis of cortex size and shape are provided in Figure 6. All cortex thickness variables were measured as the distance between the periosteal and endosteal borders of their respective dimension.[4] The diameter variables, selected to reflect the overall section size and the size of the medullary cavity in two dimensions, were taken as the distance between opposing periosteal and endosteal borders.[5]

The first analytical procedure in documenting the age changes in cortex size and shape was to develop a standardization technique whereby the overall effect of general tamarin body size variation could be eliminated. It was felt that dividing all variables by the square root of total cortex area would serve to satisfy this criterion. However, to justify using the square root of cortical area as a standardization parameter, it was necessary to assume that no significant loss or gain of cortical bone was associated with advancing age but rather, the changes in cortex size and shape reflect a "shifting" in the rates of deposition and resorption for specific dimensions.

To test the relationship between cortical area and chronological age, data from the humerus, tibia, and ulna were subjected independently

---

[4] For the ulnar photographic sections, modification was made in the positioning of the endosteal anterior and posterior landmark points to compensate for irregular cavity shape. Landmark points were located on the designated axis at a level representing the furthest extension of the cavity.

[5] Ibid.

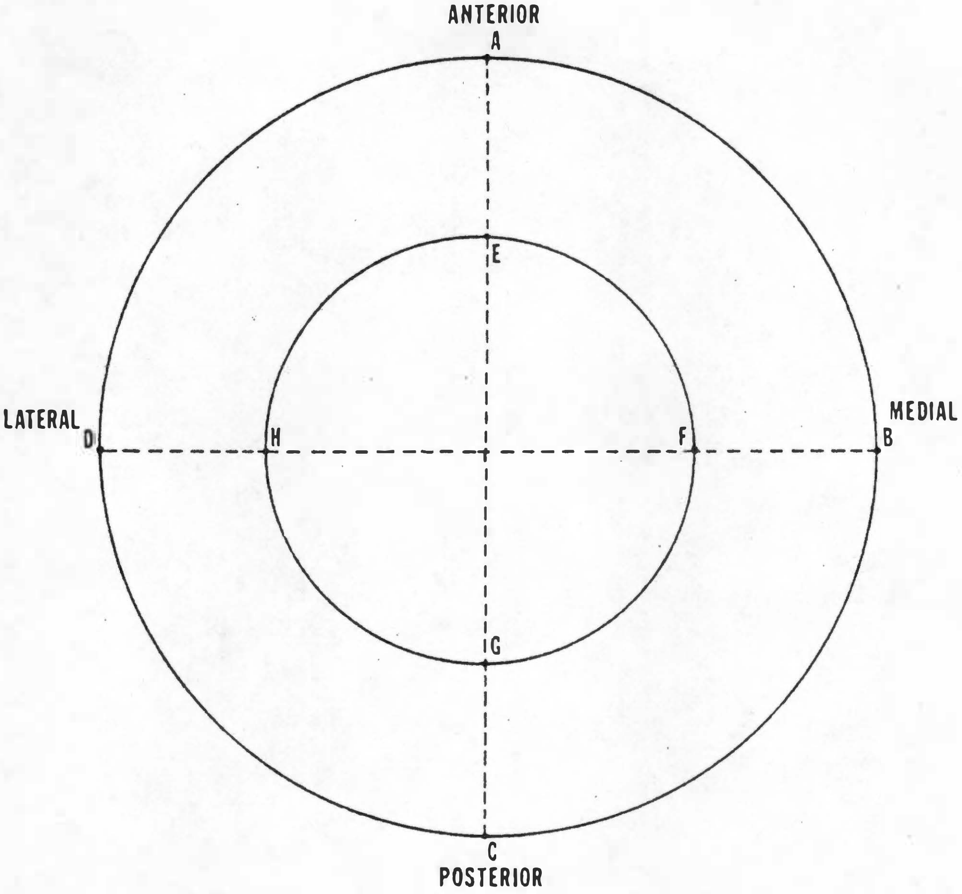

THICKNESS VARIABLES

1. Anterior Cortex Thickness (ANT). From A to E.
2. Posterior Cortex Thickness (POS). From C to G.
3. Medial Cortex Thickness (MED). From B to F.
4. Lateral Cortex Thickness (LAT). From D to H.

DIAMETER VARIABLES

1. External Anterior–Posterior Diameter (EAP). From A to C.
2. External Medial–Lateral Diameter (EML). From B to D.
3. Anterior–Posterior Cavity Diameter (IAP). From E to G.
4. Medial–Lateral Cavity Diameter (IML). From F to H.

Figure 6. Cortex size and shape variables.

to a Pearson product-moment correlation analysis (SAS Institute, 1979). If it was determined that the age/area correlation was not significant, the square root of cortical area was considered acceptable for use in standardizing the variables. However, if the correlation was found significant, an alternative standardization was considered necessary.

Once the variables were standardized in an acceptable manner, the complete data sets for each bone were again subjected to a Pearson correlation analysis. From the correlation matrix, an examination was made to identify significant relationships between the various thickness and diameter variables and chronological age. Age-correlations for each bone exhibiting the highest degree of significance were selected for representation by developmental plots. The plots were used to document the general pattern of the specific changes in cortex size and shape associated with advancing age.

Using regression analysis (SAS Institute, 1979), the relationships were further explored. Due to variation in the plots, a series of linear and curvilinear models were tested for goodness of fit. In all cases, the model which generated the greatest R^2-value with all components significantly contributing was the linear model

$$y = a + b(x)$$

where

y = the cortex variable, and

x = age.

This model was subsequently used to generate regression lines fitted to the developmental plots.

To determine the potential for predicting tamarin chronological age from osteon counting or mid-diaphyseal measurements, regression formulae were devised using age as the dependent variable. Lineal and polynomial models up to cubic terms were tested for their age-predictive accuracy. In addition, separate multiple regressions using intracortical remodeling variables and mid-diaphyseal cortex variables were run.

CHAPTER IV

RESULTS AND DISCUSSION

A. Dental Eruption

The data taken to determine the sequence and timing of dental eruption is presented for both species in Appendix B. The specimens are arranged by age in days from the youngest to oldest. Species are presented separately. Although the sexes were pooled for analysis, the sex of each individual is provided when possible. The morphological dental types are arranged in sequential order of eruption with three exceptions.[1]

Due to the small sample size of *S. oedipus*, determination of standards for the sequence and timing of dental eruption was restricted to *S. fuscicollis*. However, comparisons are made to detect the extent to which individual *S. oedipus* specimens adhere to or diverge from the *S. fuscicollis* pattern.

For the deciduous dentition, the sequence of dental eruption for *S. fuscicollis* proceeds directly from anterior to posterior in both jaws. The mandibular P2 and P4 erupt prior to their maxillary counterparts suggesting the following eruption sequence:

$$\begin{array}{cccccccc} \mathrm{I1} & \mathrm{I2} & \mathrm{C} & & \mathrm{P2} & \mathrm{P3} & & \mathrm{P4} \\ \hline \mathrm{I1} & \mathrm{I2} & \mathrm{C} & \mathrm{P2} & & \mathrm{P3} & \mathrm{P4} & \end{array} .$$

---

[1] One specimen of *S. fuscicollis*, a female of 224 days and two *S. oedipus*, a male and a female, both one day old, deviate slightly from this pattern.

This pattern is consistent with the deciduous sequence determined for *S. nigricollis* by Chase and Cooper (1969) and may reflect a generalized pattern of tamarin dental development. This is supported, in part, by examination of the *S. oedipus* data (see Appendix B). Within this limited sample, eruption of the incisors and canines follow the anterior to posterior pattern. Exceptions occur in two cases: an I_2 erupted previous to I^1 in one case and a P^2 previous to C_1 in the other. No information is available to ascertain the eruption sequence of premolars in this sample.

The age of eruption of the deciduous teeth for *S. fuscicollis* is provided in Table 8. Dental eruption is well underway at birth with all incisors and canines having pierced the gingiva by this time. All deciduous teeth are erupted by 12 weeks of age. Only slight variation is noted in the timing of eruption for the various dental types. The greatest range occurs in the maxillary P^4 where six weeks separate the youngest specimen to have this tooth erupt and the age where all specimens have erupted P^4. From comparisons with the *S. oedipus* sample (see Appendix B), interspecies variability in the timing of the deciduous dental eruption is apparent. Unlike *S. fuscicollis*, the *S. oedipus* individuals appear to exhibit no erupted teeth at birth, although the incisors may be observed "cutting" through the gingiva during the first days of postnatal development. The deciduous canines of *S. oedipus* appear to erupt between the first and second weeks. The only evidence observed for the timing of eruption for the premolars in *S. oedipus* suggests that the maxillary and mandibular P2 erupt between

Table 8. Age of Eruption of Deciduous Teeth in *Saguinus fuscicollis* in Weeks

	Dental Type					
	I1	I2	C	P2	P3	P4
Maxillary	Birth	Birth	Birth	2	2-5	6-12
Mandibular	Birth	Birth	Birth	Birth-2	2-5	5-8

one day and two and one-half weeks. This closely approaches the *S. fuscicollis* pattern.

The sequence of eruption for the permanent dentition in *S. fuscicollis* has been determined as[2]

$$\begin{array}{ccccccccccc} & \text{M1} & \text{I1} & \text{I2} & & \text{(M2} & \text{P4)} & \text{P2} & & \text{P3} & \text{C} \\ \hline \text{M1} & & \text{I1} & \text{I2} & \text{M2} & \text{P4} & & \text{P2} & \text{P3} & & \text{C} \end{array} .$$

The observed pattern differs to a small degree from that noted by Byrd (1979) from the skulls of 32 immature *S. fuscicollis* specimens. For example, Byrd indicates that in all cases, the eruption of the mandibular teeth precede their maxillary counterparts. Although this trend is reflected in many of the dental types in the present study, the homologous I1, I2, P2 and canines suggest an alternative pattern whereby the maxillary and mandibular counterparts erupt concurrently. Both studies, however, support the contention of Chase and Cooper (1969) that a generally earlier eruption of the manidbular counterparts is characteristic of tamarin dental development.

An additional difference between the Byrd (1979) dental sequence and the one presently proposed involves the number and specific types of teeth which share sequential similarity within individual jaws. Byrd indicates that the maxillary P3 and P2 share similar eruption times as does the mandibular P4 and P2. Neither condition is supported by the present data which suggests that the maxillary P2 precedes P3

---

[2] Parentheses indicate sequential similarity between the enclosed teeth.

and the mandibular P4 precedes P2 in eruption. The only dental types observed to share sequential similarity are the maxillary M2 and P4. This observation is not noted by Byrd.

Although minor differences have been noted in the sequences proposed by Byrd and this study, caution must be taken in suggesting real diversity between the two samples. Factors such as small sample size in both studies, inconsistencies in methodology between scoring eruption from alveolar criteria (Byrd) and gingival penetration (present study), and the lack of known-aged data (Byrd) may be responsible for the observed differences.

Virtually no information was obtainable for determining the permanent dental eruption sequence for *S. oedipus*. Only five subadult specimens undergoing development of the permanent dentition were available for observation (see Appendix B). In all cases, however, the observed condition is consistent with the sequencial pattern reported for *S. fuscicollis*. This basically agrees with Byrd's (1979) results.

The age of eruption of the permanent dentition for *S. fuscicollis* is provided in Table 9. As indicated from the eruption sequence, the initial permanent teeth to erupt are the mandibular and maxillary M1 appearing at approximately 16 and 18 weeks, respectively. Eruption takes place behind the deciduous fourth premolars with no replacement or loss of deciduous elements. Beginning with the eruption of the permanent central incisors at approximately 21 weeks, the deciduous teeth undergo replacement by their permanent counterparts. The canines

Table 9. Age of Eruption of Permanent Teeth in *Saguinus fuscicollis* in Weeks

	Dental Type							
	I1	I2	C	P2	P3	P4	M1	M2
Maxillary	21-23	23-29	39-45	32-39	38-39	29-39	18-23	29-39
Mandibular	21-23	23-29	39-45	32-39	37-39	29-39	16-23	29-31

are the final teeth to erupt, thus completing the permanent dentition at approximately 45 weeks.

The age ranges of eruption for specific teeth vary considerably from a one-week interval for the maxillary P3 to ten-week intervals for the maxillary and mandibular P2 and the maxillary second molar. The disproportionate age ranges may be a result of sample size rather than reflecting any real developmental pattern.

The proposed timing schedule for the eruption of the permanent dentition in *S. fuscicollis* resembles that suggested for *S. nigricollis* from longitudinal observations by Chase and Cooper (1969). However, it is observed that for virtually every dental type, *S. fuscicollis* exhibits a later eruption age, both at the onset of earliest eruption and at the maximum value of the given age range. Greatest diversity occurs between the maxillary P2 with an age range for *S. nigricollis* of 28 to 34 weeks and 32 to 39 weeks for *S. fuscicollis*, and between the maxillary second molars with an age range of 27 to 29 weeks for *S. nigricollis* and 29 to 39 weeks for *S. fuscicollis*.

The magnitude of the age ranges for *S. nigricollis* (Chase and Cooper, 1969) are generally smaller than those determined for *S. fuscicollis*, thus reflecting either greater homogeneity in eruption for *S. nigricollis* or an extraneous artifact generated by greater precision in the longitudinal research model. Nevertheless, it appears that relative to *S. nigricollis*, *S. fuscicollis* exhibits a slower dental development with final completion, based on canine eruption, approximately one month behind.

Six specimens of *S. oedipus* undergoing various phases of permanent dental eruption were examined to provide data on the timing of eruption in this species (see Appendix B). The data suggest that the first molars may erupt as early as 16 weeks but not necessarily by 20 weeks. Additionally, the central incisors and the mandibular lateral incisors may erupt by 31 weeks; the maxillary lateral incisor by 33 weeks; and the second molars, fourth and second premolars, and maxillary third premolar by 42 weeks. Unfortunately, it is not possible to determine strict age ranges for any of the dental types nor an age for eruption of the mandibular P3 and canines for this species. Comparison of the *S. oedipus* and *S. fuscicollis* dental data indicate an overall similarity in the timing of dental eruption. However, the *S. oedipus* mandibular M1 may erupt earlier and the maxillary I2 and mandibular P3 may erupt later than the normal pattern suggested for *S. fuscicollis.*

1. Estimating Chronological Age from Dental Eruption

The use of dental eruption data appears to be an accurate and valuable criterion for estimating chronological age in feral *S. fuscicollis* specimens as indicated by the diversity in age for the eruption of various dental types and the limited sizes of the age ranges associated with these types. A generalized schedule of eruption may be proposed as follows:

At birth—Deciduous incisors and canines erupted.
12th week—All deciduous teeth erupted.
16-23rd week—Eruption of first permanent teeth (M1).
20-30th week—Eruption of permanent incisors.
30-40th week—Eruption of permanent premolars and M2.
40-45th week—Eruption of permanent canine.
45 weeks—Permanent dentition fully erupted.

With respect to *S. oedipus*, the available data suggest that the schedule of eruption proposed for *S. fuscicollis* may be tentatively acceptable for use in predicting chronological age of *S. oedipus* individuals. Although some deviation from the *S. fuscicollis* pattern was identified, the deviations remain small (generally extending beyond the *S. fuscicollis* range by less than four weeks) and the overall pattern appears similar. Validation of this assertion awaits further study of *S. oedipus* dental development.

The greatest limitation of dental development as a predictor of chronological age in tamarins lies in the limited age span to which it may be applicable. Because all teeth are erupted by 45 weeks in *S. fuscicollis* and possibly a bit later in *S. oedipus*, this criterion is useful only for individuals within the earliest phases of ontogenetic development.

B. Long Bone Growth

Individual generalized growth curves documenting the relationship between chronological age and the maximum length of each long bone and the ilium are provided for *S. fuscicollis* and *S. oedipus* in Appendix C. A curvilinear regression line is fitted to each curve. The regression model from which these lines are derived will be considered below.

As discussed in Chapter III, the model fitted to the age-length data was the Jenss-Bayley curve (Jenss and Bayley, 1937) which takes the form of the equation:

$$y = a + b_1 t + b_2 \mathit{log}\, t$$

where

y = the length of the long bone

t = age.

No further attempt was made to investigate additional models as the goodness of fit reflected by the R^2-value for each curve was considered acceptable. Summary statistics of the regression model of the long bone lengths on age and the common logarithm of age are presented for *S. fuscicollis* and *S. oedipus* in Tables 10 and 11.

The R^2-value may be calculated as the ratio of the sum of squares for the model divided by the sum of squares for the corrected total. From the available data,[3]

Model SS = SSAge + SS log10(Age)

and

Corrected Total SS = Model SS + MS Error (Error d.f.).

For *S. fuscicollis*, the amount of variation in the individual long bones which can be accounted for by the model is 93 percent for the humerus and ilium and 94 percent for the radius, ulna, femur, tibia and fibula. An equivalent goodness of fit is identified for the *S. oedipus* growth curves with R^2-values slightly higher in all cases ranging from 95 percent for the humerus and ilium, to 97 percent for the femur.

---

[3] In this case, with one degree of freedom, the sums of squares for age and the log of age are equal to the mean squares for the two components.

Table 10. Regression Statistics of Long Bone Lengths on Age and the Common Logarithm of Age for *Saguinus fuscicollis*[a]

		Age			Log 10 (Age)				Error
Bone	N	Mean Sq.	Slope	F	Mean Sq.	Slope	F	Intercept	Mean Sq.
Humerus	59	5965.95	0.03	640.22*	931.76	8.27	99.99*	10.09	9.32
Radius	59	4924.48	0.03	845.57*	499.07	6.05	85.70*	10.91	5.82
Ulna	59	6377.12	0.03	798.55*	735.82	7.35	92.14*	11.78	7.99
Femur	48	9036.93	0.04	663.47*	1327.52	10.40	97.46*	9.21	13.62
Tibia	58	10112.38	0.04	709.67*	1395.79	10.19	97.95*	10.22	14.25
Fibula	58	9012.69	0.04	710.24*	1077.77	8.96	84.93*	10.40	12.69
Ilium	59	2013.35	0.02	638.06*	278.91	4.53	88.39*	3.68	3.16

[a] Degrees of freedom for model = 2, for error = N-3.

*P > 0.0001

Table 11. Regression Statistics of Long Bone Lengths on Age and the Common Logarithm of Age for *Saguinus oedipus*[a]

		Age			Log 10 (Age)				Error
Bone	N	Mean Sq.	Slope	F	Mean Sq.	Slope	F	Intercept	Mean Sq.
Humerus	33	4955.15	0.01	572.97*	1100.45	10.51	105.04*	10.07	10.48
Radius	33	3931.29	0.02	604.62*	616.18	7.86	94.77*	9.88	6.50
Ulna	33	5499.80	0.02	594.48*	893.50	9.47	96.58*	10.51	9.25
Femur	32	9790.38	0.03	734.99*	1548.64	12.68	116.26*	9.60	13.32
Tibia	33	9947.75	0.03	605.45*	1512.61	12.32	92.06*	10.14	16.43
Fibula	33	8766.69	0.02	583.13*	1371.13	11.73	91.20*	9.75	15.03
Ilium	33	1971.13	0.01	511.67*	317.10	5.64	82.31*	4.28	3.85

[a] Degrees of freedom for model = 2, for error = N-3.

*P > 0.0001

The F-values expressed in Tables 10 and 11 indicate the relative significance of the individual components (age and the common logarithm of age) to the overall model. Thus, for both species, the linear and curvilinear components of each long bone regression are found to be significant at the .0001 level.

Regression growth curves of the individual long bones are given in Figures 7 and 8 for *S. fuscicollis* and *S. oedipus*, respectively. In general, growth of all long bones for both species follows a similar pattern. Initial growth is rapid followed by a period of marked deceleration and then continues in a virtually linear fashion until maturity is achieved. This is reflected in the single curve of the regression line. No subpubertal or pubertal spurt is indicated for either species in any long bone.

The period of marked deceleration in the growth curves for both species occurs between 25 and 100 days of postnatal development. The growth curves of the hindlimb elements indicate greater initial growth and less severe deceleration than those for the forelimb. In one instance, the growth curves of two elements, the humerus and radius, intersect at a point beyond the initial period of rapid growth. This pattern is common to both species with the intersection occurring at approximately 175 days for *S. fuscicollis* and 425 days for *S. oedipus*. It suggests that relative to the ulna, the humerus experiences a greater initial growth and subsequently greater deceleration during the period represented by the curve in the growth line.

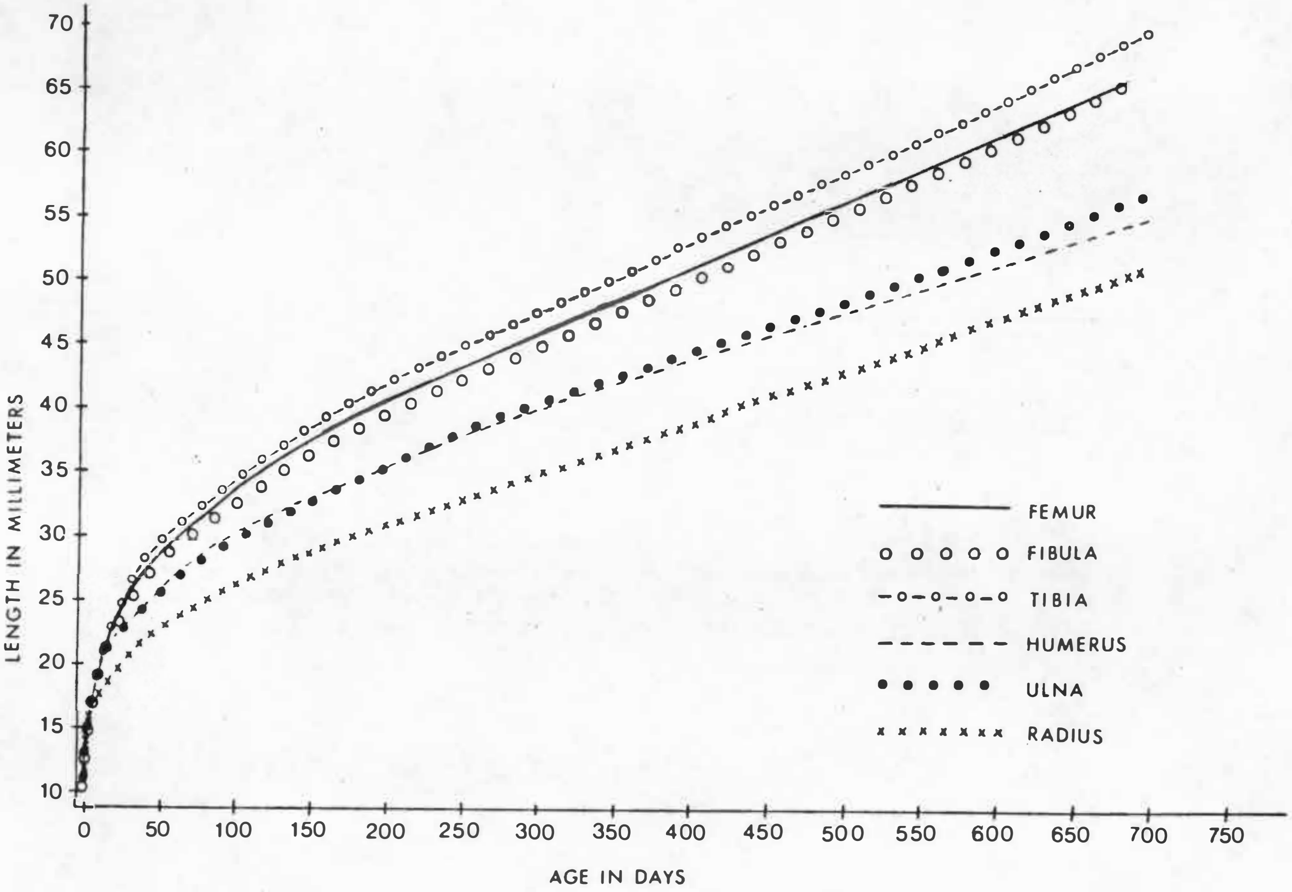

Figure 7. Regression growth lines for *Saguinus fuscicollis*.

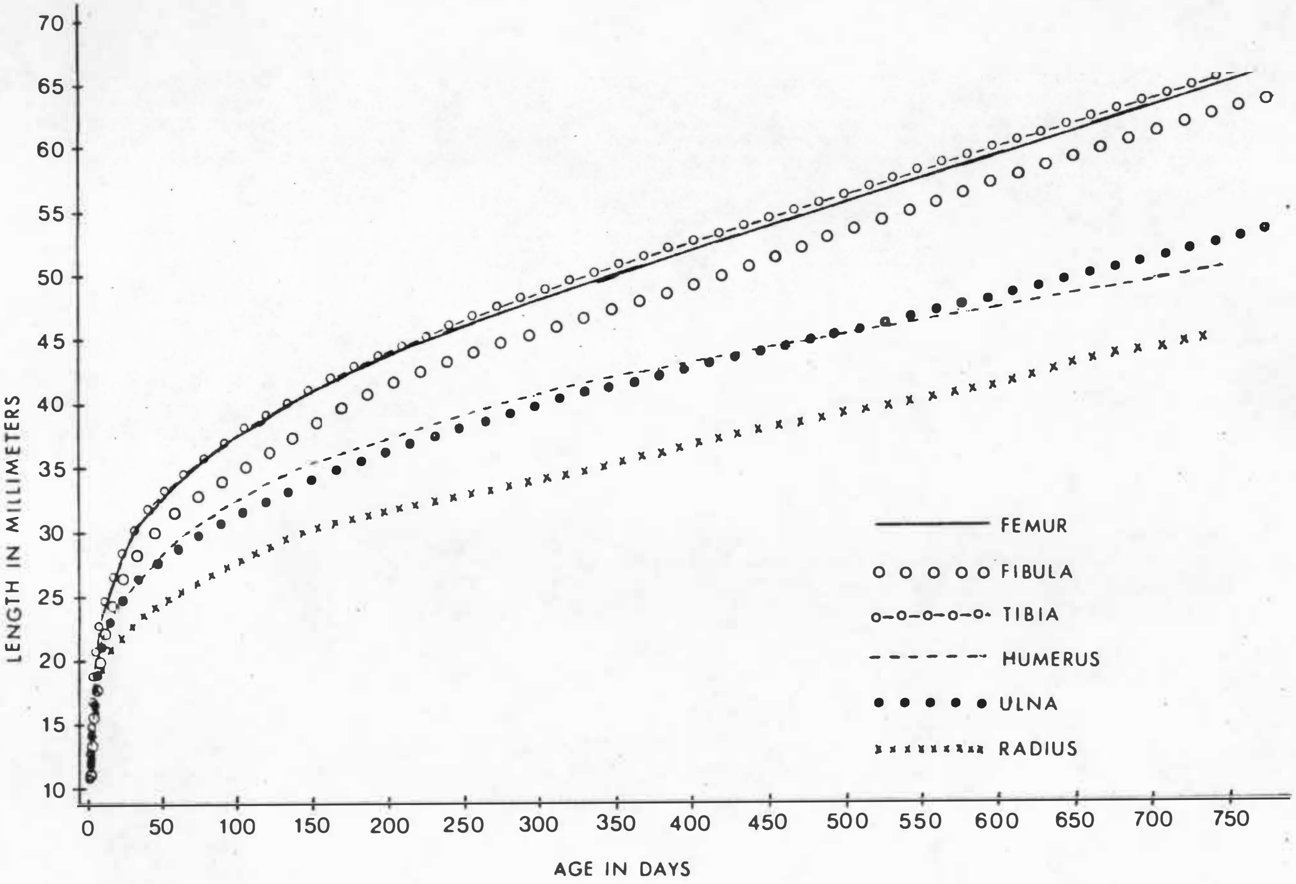

Figure 8. Regression growth lines for *Saguinus oedipus*.

In comparing the long bone growth curves between the two species for all elements, *S. oedipus* exhibits an expected length that is greater at every age up to some point between 250 and 350 days, depending upon the specific element involved. At this time, the growth curves of *S. fuscicollis* and *S. oedipus* intersect and reverse the pattern. That is, at any age beyond approximately 350 days, the expected long bone length is greater for *S. fuscicollis*. It should be noted that in reality, however, substantial overlap occurs between the lengths of specific long bones at every age between the two species. This is evident in the growth plots presented in Appendix C. Nevertheless, the observed pattern of initially more rapid growth in *S. oedipus* followed by an increased deceleration rate for this species is contrary to expectation. The contradiction is based on two factors. First, it was suggested earlier in this chapter from observation of dental eruption data that *S. oedipus* appears to exhibit relatively slower initial development. Second, published standards of tamarin body length indicate slightly greater average body size in adult *S. oedipus*.

To test whether the differences in the slopes of the growth curves between *S. fuscicollis* and *S. oedipus* are statistically significant, an analysis of covariance (ANACOVA, SAS Institute, 1979) was performed on the long bone growth data. A summary of the ANACOVA results is provided in Table 12. The individual bones were taken as the dependent variables with species as the treatment and age and the common logarithm of age as covariates. The F-value is the ratio produced by dividing MS

Table 12. Summary of the ANACOVA Results Testing for Slope Differences in Long Bone Growth between *Saguinus fuscicollis* and *Saguinus oedipus*

Bone	Source	Sum of Squares	Degrees of Freedom	Mean Square	F
Humerus	Between B's	133.29	2	66.65	6.86**
	Within B's	836.14	86	9.72	
Radius	Between B's	115.67	2	57.83	9.54**
	Within B's	521.20	86	6.06	
Ulna	Between B's	113.75	2	56.87	6.75**
	Within B's	724.76	86	8.43	
Femur	Between B's	95.65	2	47.82	3.54*
	Within B's	999.23	74	13.50	
Tibia	Between B's	130.48	2	65.24	4.34*
	Within B's	1276.63	85	15.02	
Fibula	Between B's	143.52	2	71.76	5.31**
	Within B's	1148.94	85	13.52	
Ilium	Between B's	19.27	2	9.64	2.84
	Within B's	292.27	86	3.40	

*P > .05 **P > .01

(between coefficients of species) by MS (within coefficients of species). If the F-value is significant, which is observed in all cases, the slopes are considered to differ and no further ANACOVA tests are warranted.

1. Estimating Chronological Age from Long Bone Growth

To predict the chronological age of feral tamarins from long bone growth data, additional regression analyses are necessary. For prediction, age becomes the dependent variable and the attempt is made to ascertain how much of age variation can be explained by bone length. In the above discussion concerning the ANACOVA results, it was determined that the growth slopes significantly differ between the two species. This demonstrates the inappropriateness of either pooling the species or assigning ages to *S. oedipus* individuals based on *S. fuscicollis* growth standards. Therefore, it is necessary to calculate age-predicting regression equations for each species independently.

The relationship between age and bone length has been demonstrated to be curvilinear. This necessitates the inclusion of a quadradic variable into the regression model. To this end, the model employed to generate age-prediction equations was

$$\text{Age} = a + b_1x + b_2(x)^2$$

where

x = long bone length.

The model was applied to all categories of long bones and the ilium thus yielding seven age-prediction equations for each species.

A summary of the regression results is provided for *S. fuscicollis* and *S. oedipus* in Tables 13 and 14.[4] The provided F-value is a test of the overall model and is highly significant for each long bone regression for both species. The goodness of fit of the regression line to the dependent variable (age) is measured by the R^2-statistic that ranges between .92 and .94 for *S. fuscicollis* and between .89 and .95 for *S. oedipus*. Due to the high R^2-values, the model was considered acceptable and no other models were tested. Further substantiation of the model is indicated from the Type I sums of squares which were found to be significant at the .0001 level for both the linear and quadradic components in all regressions.

The degree of predictive accuracy for assigning ages from the regression equations is identifiable from the standard deviations of estimates measured in days (Tables 13 and 14). For *S. fuscicollis,* the estimate standard deviations vary between 47.95 and 55.19 days and indicate the femur to be the best long bone from which chronological age may be predicted using this criteria. Therefore,

$$\text{Age} = 64.64 - 7.56\ (\text{femur length}) + .25\ (\text{femur length})^2$$
$$\pm\ 47.95\ \text{days}$$

represents the most accurate equation for this species.

---

[4] The regression equations and subsequent age-predictive potential for immature *S. oedipus* individuals must remain tentative until larger samples may be observed.

Table 13. Regression Statistics for Predicting Age in *Saguinus fuscicollis* from Long Bone Lengths

			Slope				
Bone	N	Intercept	Bone	$(\text{Bone})^2$	Model F	R^2	Std. Dev. of Est. (in days)
Humerus	59	110.38	-13.15	0.44	314.33*	0.92	55.19
Radius	59	50.40	-9.53	0.45	422.49*	0.94	48.11
Ulna	59	62.61	-9.25	0.36	388.32*	0.93	50.05
Femur	48	64.64	-7.56	0.25	360.86*	0.94	47.95
Tibia	58	52.15	-6.29	0.22	360.75*	0.93	49.07
Fibula	58	42.03	-5.89	0.24	371.38*	0.93	48.41
Ilium	59	86.27	-19.75	1.41	396.64*	0.93	49.55

*P > 0.0001

Table 14. Regression Statistics for Predicting Age in *Saguinus oedipus* from Long Bone Lengths

			Slope				
Bone	N	Intercept	Bone	$(\text{Bone})^2$	Model F	R^2	Std. Dev. of Est. (in days)
Humerus	33	304.44	-31.36	0.78	119.04*	0.89	94.50
Radius	33	251.31	-30.42	0.92	208.68*	0.93	73.15
Ulna	33	256.23	-26.87	0.69	212.29*	0.93	72.57
Femur	32	191.80	-18.22	0.41	306.01*	0.95	60.58
Tibia	33	186.21	-17.26	0.39	254.26*	0.94	66.68
Fibula	33	196.02	-19.00	0.45	240.46*	0.94	68.45
Ilium	33	200.77	-41.29	2.06	201.62*	0.93	74.34

*P > 0.0001

For *S. oedipus,* estimated standard deviations range between 60.58 and 94.50 days. Similar to *S. fuscicollis,* femur length is identified as the best predictor of chronological age. The regression formula for predicting age from the femur is

$$\text{Age} = 191.80 - 18.22\ (\text{femur length}) + .41\ (\text{femur length})^2 \pm 60.58\ \text{days.}$$

Overall, the chronology of long bone growth exemplified via regression analysis is considered to be a valuable parameter for predicting age in the two species. In the range of applicability, from birth to approximately 700 days, the regression results indicate accurate age assignment for *S. fuscicollis* to within approximately three months and for *S. oedipus* to within four.[5] Small sample size of *S. oedipus* may account for the relatively greater standard deviations of estimates observed for this species.

C. Epiphyseal Union

The data taken on epiphyseal development for *S. fuscicollis* and *S. oedipus* are provided in Appendix D. The species are presented independently and sex designation is provided for each individual when possible. Individuals are listed in chronological order by age in days and are provided with a value of 1, 2 or 3 in the manner described previously for each of 21 areas of epiphyseal union and the

---

[5] Based on one standard deviation.

spheno-occipital synchondrosis. Epiphyseal unions are listed in a generally sequential order from earliest fusion to most recent, although variability exists between specific individuals. Epiphyseal sequences differ between *S. fuscicollis* and *S. oedipus* and are reflected in their respective tables.

The generalized sequence of epiphyseal union, age range of fusion, initial occurrence of complete unions, and associated anatomical joint or element of each epiphyseal area are provided for *S. fuscicollis* in Table 15. The sequence of eruption is determined as the chronology of earliest fusion for each epiphyseal union (e.g., .26 years for distal humerus, .30 years for ischium-pubic ramus, .33 years for the unions between the ischium-pubis and the ilium, and so on). In cases where the initial occurrence is similar between two or more unions, sequence order is defined by the shorter associated age range being given initial sequential preference. Therefore, the proximal ulna with an age range of .67 years to 1.32 is positioned earlier in sequence than the distal radius with an associated age range of .67 years to 1.85, and so on. In cases where the entire age ranges are similar for two or more unions, the sequential order is chosen randomly.

In *S. fuscicollis*, a distinct pattern in the fusion of elements comprising regionalized centers is obscured by two factors. First, within regionalized centers, corresponding unions are not always close in sequence (such as within the wrist and shoulder). Second, there is a substantial overlap in the sequence of various regions (e.g., the ankle, knee, and elements of the wrist and shoulder all begin to fuse

Table 15. Sequence and Timing in Percent of Year of Epiphyseal Union for *Saguinus fuscicollis*

Epiphysis	Range of Fusion	Initial Complete Union	Associated Joint or Element
Distal Humerus	0.26-0.81	0.31	Elbow
Ischium-Pubic Ramus	0.30-0.67	0.30	Innominate
Ischium-Pubis to Ilium	0.33-0.81	0.43	Innominate
Ischium to Pubis	0.33-1.21	0.43	Innominate
Medial Epicondyle	0.33-1.21	1.21	Elbow
Coracoid Process	0.43-1.21	1.21	Shoulder
Lesser Trochanter	0.48-1.32	1.32	Hip
Proximal Ulna	0.67-1.32	1.32	Elbow
Distal Radius	0.67-1.85	1.75	Wrist
Greater Trochanter	0.81-1.32	1.32	Hip
Head of Femur	0.81-1.32	1.32	Hip
Proximal Radius	1.21-1.32	1.32	Elbow
Distal Tibia	1.32-1.63	1.32	Ankle
Distal Fibula	1.32-1.63	1.32	Ankle
Distal Ulna	1.32-1.85	1.75	Wrist
Proximal Tibia	1.32-1.98	1.98	Knee
Proximal Fibula	1.32-2.24	1.98	Knee
Proximal Humerus	1.32-2.24	1.75	Shoulder
Distal Femur	1.32-2.24	2.24	Knee
Ischial Epiphysis	1.63-4.05	2.24	Innominate
Spheno-Occipital Syn.	1.75-2.24	1.75	Cranium
Iliac Crest	2.24-6.30	2.24	Innominate

at approximately 1.3 years). Similar observations of regional overlap and temporal variation in epiphyseal unions within joints have been reported for other New World primates (Tappan and Severson, 1971). Nevertheless, a trend does emerge from the *S. fuscicollis* data for the succession of anatomical joint development in the form of

Elbow → Hip → Ankle → Wrist → Knee → Shoulder .

The relative positioning of the shoulder as the last anatomical joint to unite is suggested by the greater contribution on the part of the proximal humerus to the formation of this joint than the coracoid process which exhibits an early union.[6] This sequence is compatible to that defined for marmosets (Schultz, 1956) and a variety of cebids (Tappan and Severson, 1971; Thorington and Vorek, 1976). Surprisingly, it differs from the sequence suggested by Tappan's and Severson's (1971) data for a closely related species, *S. nigricollis*, but only in the inversion of wrist and knee.

Fusion of the long bone epiphyses in *S. fuscicollis* begins in the third month of postnatal development with the union of the distal humerus and continues until approximately two and one-quarter years. Epiphyses for two muscle attachment areas of the innominate, the ischial epiphysis and the iliac crest, fuse as late as 4.05 years and 6.30 years, respectively.

---

[6] Epiphyses of the innominate and cranial union were not included in the derivation of this sequence so that comparisons with previous investigations could be made.

For a further interpretation of the epiphyseal development of *S. fuscicollis*, it is useful to define the various fusion centers as representing either early or late unions. Designation was determined from whether the initial fusion of the center occurred prior to, or later than, one year of age (selected as approximating one-half of the period of epiphyseal union development). Therefore, early union is characteristic of the primary elements of the innominate, all elements of the hip and distal humerus, the coracoid process of the scapula, proximal ulna, and distal radius. Alternatively, all elements of the ankle and knee, proximal radius, distal ulna, proximal humerus, ischial epiphysis and iliac crest are characteristic of late union.

For *S. fuscicollis*, the time in which fusion of an epiphysis occurs, as measured by fusion age ranges, varies substantially between specific centers. This variation may be attributed, in part, to small sample size and/or the disproportionate representation of ages by the specimens included in the sample. For example, no individuals are represented between the ages of 296 and 441 days.

Age ranges vary in magnitude from .11 years for the epiphysis of the proximal radius to 4.06 years for the iliac crest. However, all but three centers exhibit completed union for the sample within one year of initial fusion. Furthermore, the data suggest that the magnitude of the age ranges are not dependent upon whether the center represents an early or late union.

The initial complete union for a center represents the age of the youngest individual to be scored "united" (score value of 3) for the epiphysis of a particular center. In the *S. fuscicollis* data, ten centers exhibit initial complete union within the first half of their designated age range of fusion while twelve exhibit this union within the second half. The data suggest a trend in the relationship between the centralized regions or joints and the occurrence of first- or second-half initial complete union. First-half initial complete union is observed for all elements or epiphyses comprising the innominate and ankle, and second-half for all comprising the hip, wrist and knee. The various epiphyses of the elbow and shoulder differ between first- and second-half unions. The implications of first- or second-half initial complete union for a center or multiple centers associated with an anatomical joint is not determined. However, the possibility that this trend reflects small sample size or the lack of longitudinal data rather than "real" developmental patterning must be acknowledged.

The sequence of epiphyseal union, age ranges of fusion, age of earliest completed union and associated anatomical joint or structure for the epiphyseal centers of *S. oedipus* are provided in Table 16. Sequence order is determined from similar criteria described for *S. fuscicollis*. Due to the limited number of *S. oedipus* available for analysis, the following discussion and interpretation of epiphyseal development for this species must be considered tentative.

Similar to *S. fuscicollis*, the *S. oedipus* data suggest a considerable overlap in the timing of epiphyseal unions comprising specific anatomical joints as well as marked diversity in the position of some epiphyses

Table 16. Sequence and Timing in Percent of Year of Epiphyseal Union for *Saguinus oedipus*

Epiphysis	Range of Fusion	Initial Complete Union	Associated Joint or Element
Distal Humerus	0.38-0.70	0.38	Elbow
Coracoid Process	0.38-1.53	0.87	Shoulder
Ischium-Pubic Ramus	0.57-0.70	0.57	Innominate
Ischium to Pubis	0.57-0.87	0.70	Innominate
Ischium-Pubis to Ilium	0.57-1.53	1.12	Innominate
Lesser Trochanter	0.57-1.53	1.12	Hip
Medial Epicondyle	0.70-1.53	1.12	Elbow
Greater Trochanter	0.87-1.53	1.12	Hip
Proximal Radius	1.12-1.53	1.12	Elbow
Proximal Ulna	1.12-1.53	1.53	Elbow
Head of Femur	1.12-1.53	1.53	Hip
Distal Tibia	1.25-1.84	1.84	Ankle
Distal Fibula	1.53-1.84	1.84	Ankle
Distal Radius	1.53-2.00	1.84	Wrist
Distal Femur	1.53-2.00	1.84	Knee
Proximal Humerus	1.53-2.07	1.84	Shoulder
Distal Ulna	1.84-2.00	1.84	Wrist
Proximal Tibia	1.84-2.07	1.84	Knee
Proximal Fibula	1.84-2.07	1.84	Knee
Ischial Epiphysis	1.84-4.93	4.93	Innominate
Spheno-Occipital Syn.	1.98-4.93	4.93	Cranium
Iliac Crest	2.07-	-	Innominate

contributing to the same joint (e.g., the epiphyses of the shoulder and elbow). Due to the extent of overlap, a generalized sequence of unions for anatomical joints is not identified for this species. However, the data suggest that the elbow and hip respectively unite prior to the ankle, wrist, shoulder and knee.

The span of epiphyseal union development for *S. oedipus* is approximately from four and one-half months with the initial fusion of the distal humerus and coracoid process to two years, at which time the major epiphyses of all long bones have completed union. The span is extended to over five years by the inclusion of the ischial epiphysis, spheno-occipital synchondrosis, and iliac crest. No individual within the *S. oedipus* sample exhibited a united iliac crest.

Although the small *S. oedipus* sample allows for little more than tentative interpretations, the sequence, age ranges of fusion, and initial complete unions for the epiphyseal centers are compared with the pattern exhibited by *S. fuscicollis* in Figure 9. For each epiphyseal center, the horizontal lines correspond to the age range of fusion with the top line reflecting the pattern of *S. fuscicollis* and the lower, *S. oedipus*. The marked asterisk on each line represents the initial complete union for that center.

Although the species differ in the absolute sequential order of epiphyseal unions, a similarity in the pattern of sequence is observed. The greatest differences occur in the relative positioning of the distal radius and coracoid process. General similarity in the sequence

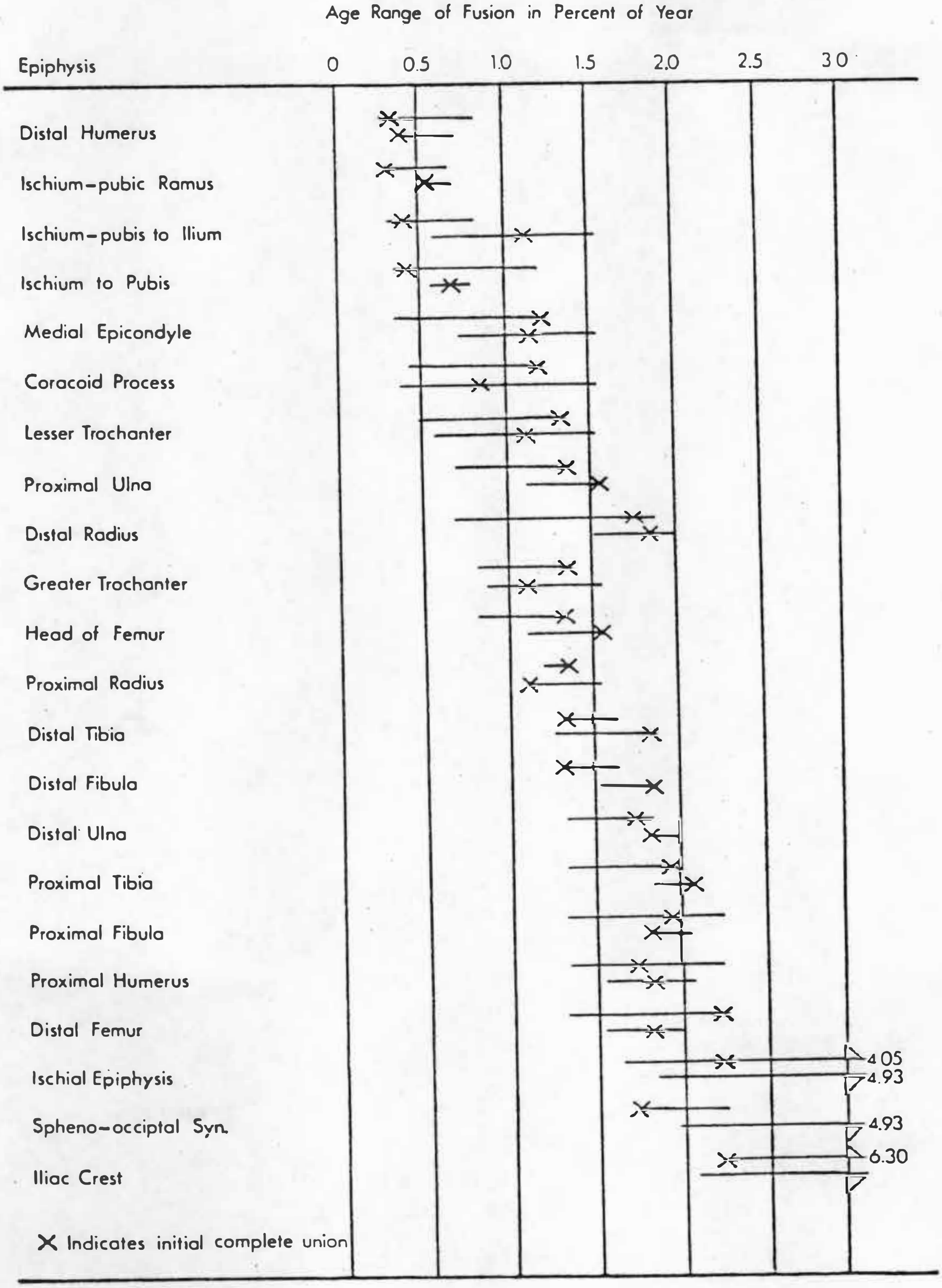

Figure 9. Sequence, age ranges of fusion, and initial complete unions for the epiphyseal centers of *Saguinus fuscicollis* (top lines) and *Saguinus oedipus* (bottom lines).

is supported by the observed overlap in the age ranges of fusion for all centers. However, in eighteen of the twenty-two epiphyseal and synchondrosis centers, the initial onset of fusion (minimum value of age range) occurs earlier in *S. fuscicollis* and, conversly, in the termination of union development (maximum value of age range), *S. oedipus* exceed *S. fuscicollis* in sixteen centers. This suggests that relative to *S. oedipus, S. fuscicollis* exhibits an increased rate in epiphyseal union development. The magnitude of this increased rate appears to be small, as the majority of age range initial onset and termination values vary less than one-half year between the species.

No pattern of species differentiation is observed in the general length of fusion age ranges. *S. fuscicollis* exhibits greater range in twelve centers and *S. oedipus*, eight. The distal fibula exhibits an age range of .31 years for both species. Additionally, no consistent trend is identified in the timing of the initial complete union between the species for individual centers.

1. Estimating Chronological Age from Epiphyseal Union

For *S. fuscicollis*, estimating chronological age based on the sequence and timing of epiphyseal unions appears promising. The gradual increase in the onset of fusion for the centers in conjunction with fusion age ranges averaging one-half year in duration suggests the possibility for substantial predictive accuracy for individuals between four months and two and one-quarter years. With the inclusion of observation of the ischial epiphysis, the predictive range may be extended to include individuals up to four years in age.[7]

The similarities in the pattern of epiphyseal union between *S. fuscicollis* and *S. oedipus* suggest the possible tentative use of the *S. fuscicollis* standard as a model for predicting chronological age in feral *S. oedipus* specimens. To test this hypothesis, four known-aged *S. oedipus* specimens ranging from four and one-half months to approximately two years were randomly selected and "aged" according to the *S. fuscicollis* standard. Three of the four test cases were assigned ages deviating from their actual age by less than three months. The fourth, a male of approximately 22 months had a predicted age of greater than 27 months. These results are interpreted as providing support for the use of epiphyseal union data as a means to predict chronological age in tamarin specimens. Furthermore, they support the tentative use of predicting age in *S. oedipus* specimens from patterns documented for *S. fuscicollis*.

D. Cortical Microstructure and Mid-Diaphyseal Cortex Size and Shape

Results of the Pearson product-moment correlations between the variables age, standardized osteon counts,[8] and standardized non-Haversian

---

[7] The individuals included by this extension are assigned the limited age range of being between 2.24 and 4.05 years without further refinement.

[8] Osteons or osteon counts refer to the combined number of osteons and osteon fragments.

canal counts are provided for the humerus, tibia, and ulna in Table 17. Analysis was restricted to *S. fuscicollis* because it was the only species of the two samples with adequate sample size. Standardization of the osteon and non-Haversian canal counts was achieved by dividing the respective counts by the total area of the bone cortex in square millimeters. With one exception, the direction of the correlations as indicated by their sign (positive or negative) is consistent with *a priori* expectations generated from similar analyses of human material (i.e., an increase in the number of osteons per square millimeter of cortex with advancing age, a decrease in the number of non-Haversian canals per square millimeter of cortex with advancing age, and an inverse relationship between osteons and non-Haversian canals). The single exception to this pattern is observed for the tibial correlation between osteons and non-Haversian canals which indicate a positive, although not significant, relationship.

Correlations which yield the greatest levels of significance include: age and humeral osteons, age and ulnar osteons, and age and humeral non-Haversian canals. The data indicate no significant relationship between the number of tibial osteons and chronological age for this species. This may partially reflect the subsequent destruction of existing osteons and osteon fragments by extensive cortical bone loss identified in some but not all *S. fuscicollis* tibiae of individuals older than approximately nine years of age.[9] Adult cortical bone loss

---

[9] A similar pattern of decreasing osteons with advancing age in older *S. fuscicollis* has been suggested from qualitative observations for the femur (Glassman and Schmidt, 1980).

Table 17. Correlation Coefficients of the Variables Age, Standardized Osteon Counts, and Standardized Non-Haversian Canal Counts for *Saguinus fuscicollis*

	Correlation with Age		
Bone	Osteons	Non-Haversian	Osteons vs. Non-Haversian
Humerus	0.50***	-0.43**	-0.34*
Tibia	0.02	-0.37*	0.20
Ulna	0.51***	-0.34*	-0.23

*P > .05 **P > .01 ***P > .001

in the long bones of *S. fuscicollis* will be taken up later in this section.

Plots of age on the cortical microstructure variables determined to be significantly correlated with age are provided in Figures 10 through 14. Age is represented in days, and osteons and non-Haversian canals in number per square millimeter. Osteon/age plots of the humerus and ulna (Figures 10 and 11) suggest a general linear relationship although substantial variation is observed within this pattern.

The non-Haversian canal/age plots present a more difficult pattern to identify from initial observation. Similar to the osteon/age plots, a linear relationship is suggested. However, a curvilinear pattern whereby an initial decrease followed by a gradual deceleration of the decrease is also probable. This is especially true in the case of the humerus (Figure 12). The identification of the best fit between the number of non-Haversian canals and age was subsequently determined by regression analysis of a series of linear and curvilinear models. The model which generated the greatest R^2-value with all components significantly contributing was considered to best reflect the relationship.

The regression statistics of standardized osteon counts on age for the humerus and ulna and of standardized non-Haversian canal counts on age for the humerus, tibia and ulna are provided in Table 18. Tibial osteon counts were not subjected to regression analysis on age due to the lack of correlation between these variables (Table 17). The linear model used to regress osteon counts on age for the humerus and ulna was

$$\text{Osteons} = a + b\ (\text{age}) \quad .$$

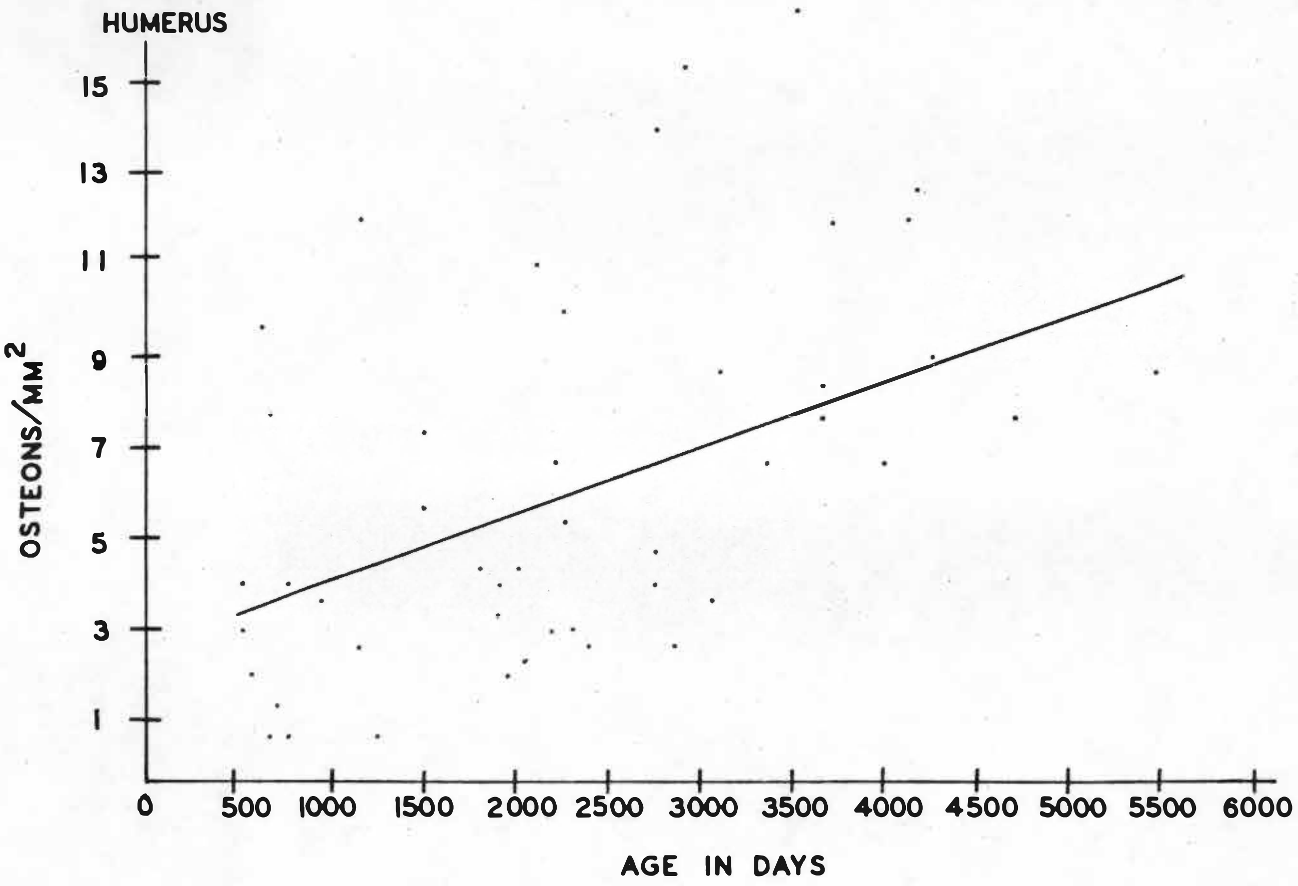

Figure 10. Plot of osteons on age for the humerus of *Saguinus fuscicollis*.

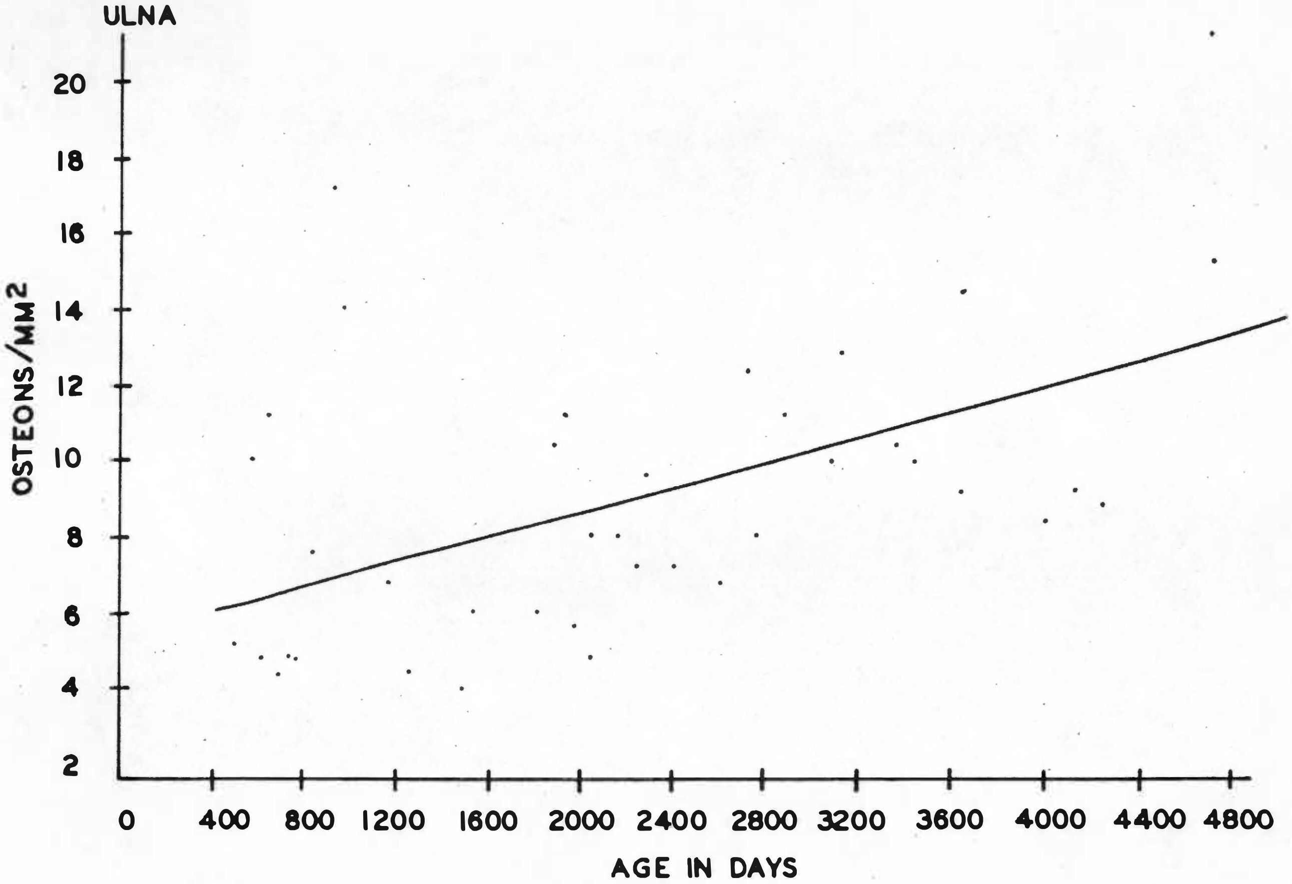

Figure 11. Plot of osteons on age for the ulna of *Saguinus fuscicollis*.

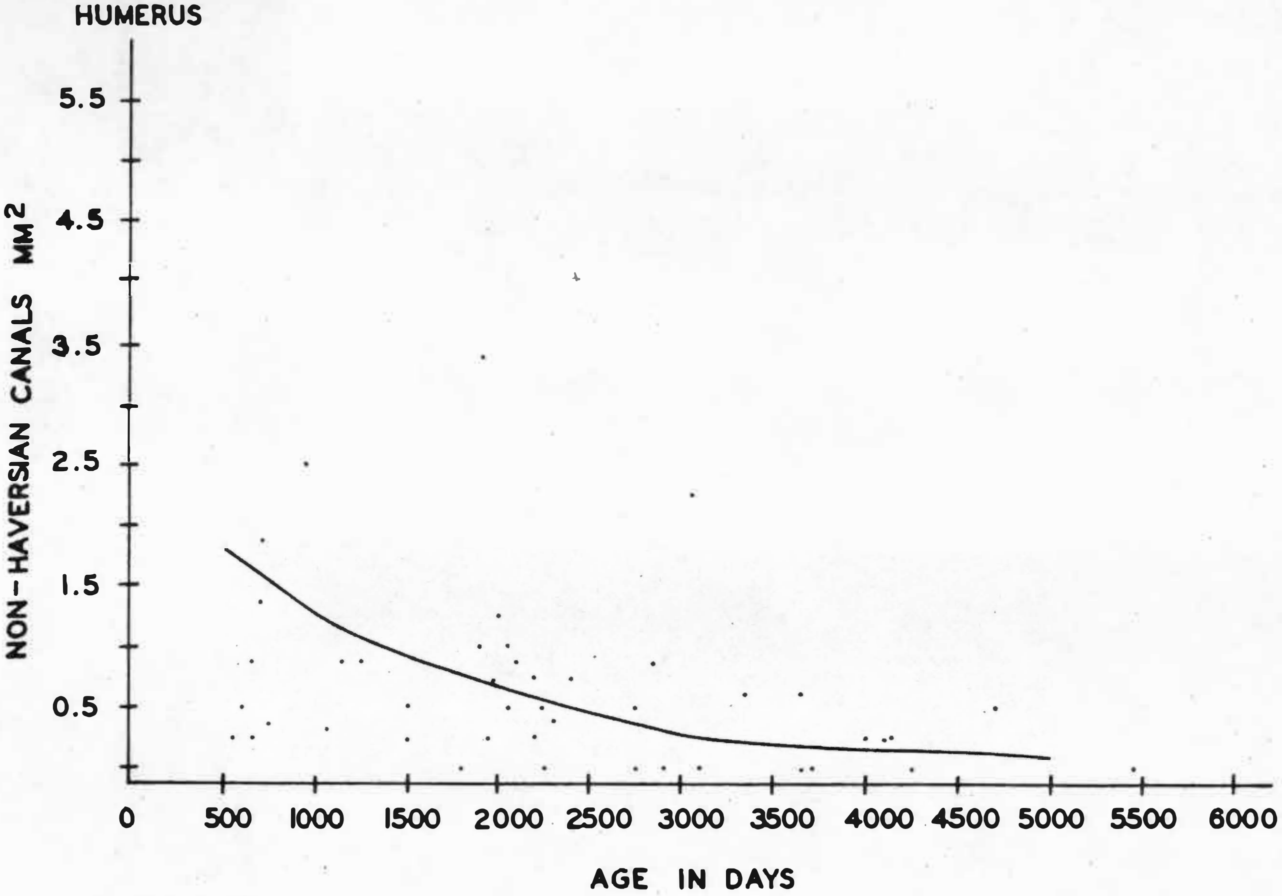

Figure 12. Plot of non-Haversian canals on age for the humerus of *Saguinus fuscicollis*.

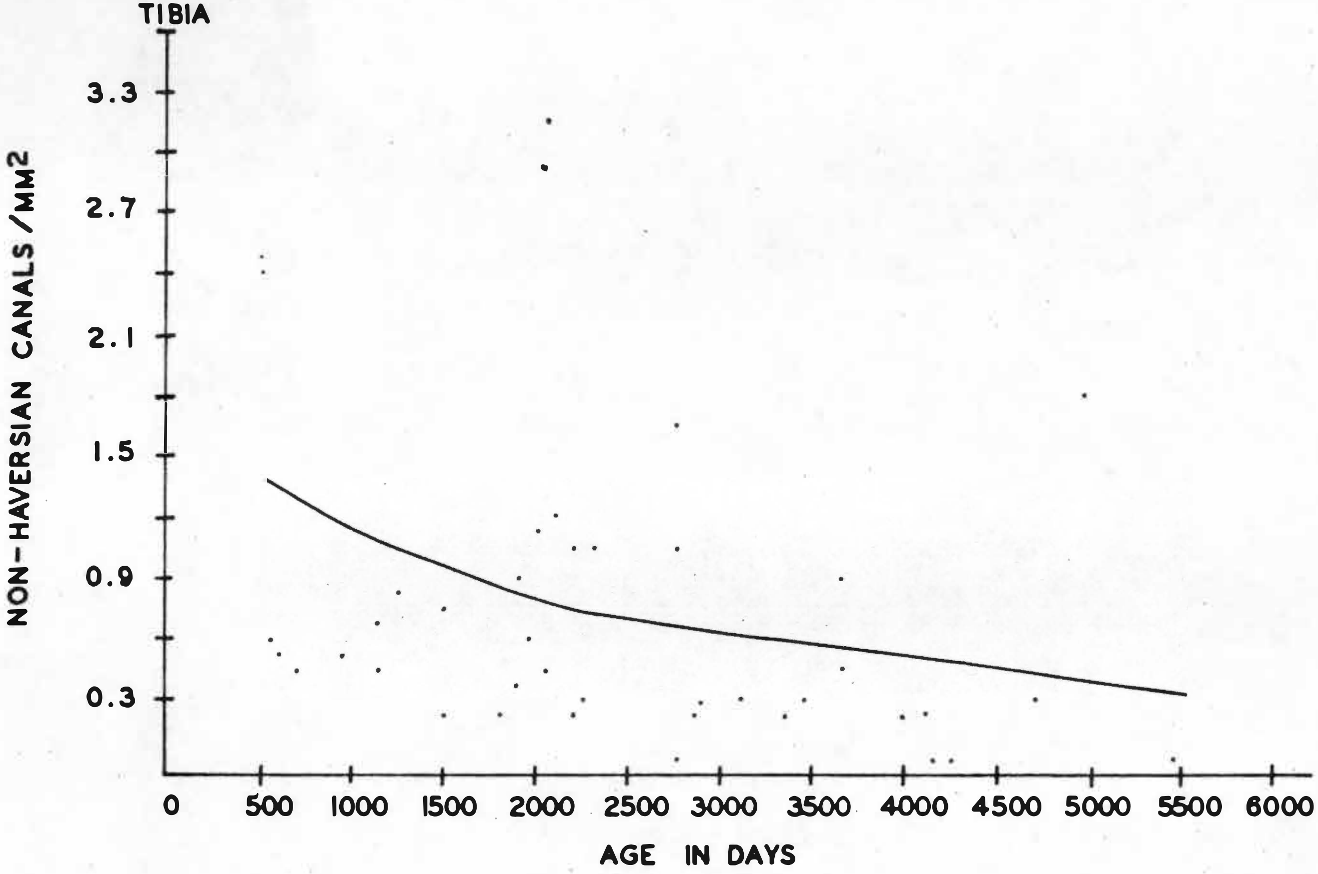

Figure 13. Plot of non-Haversian canals on age for the tibia of *Saguinus fuscicollis*.

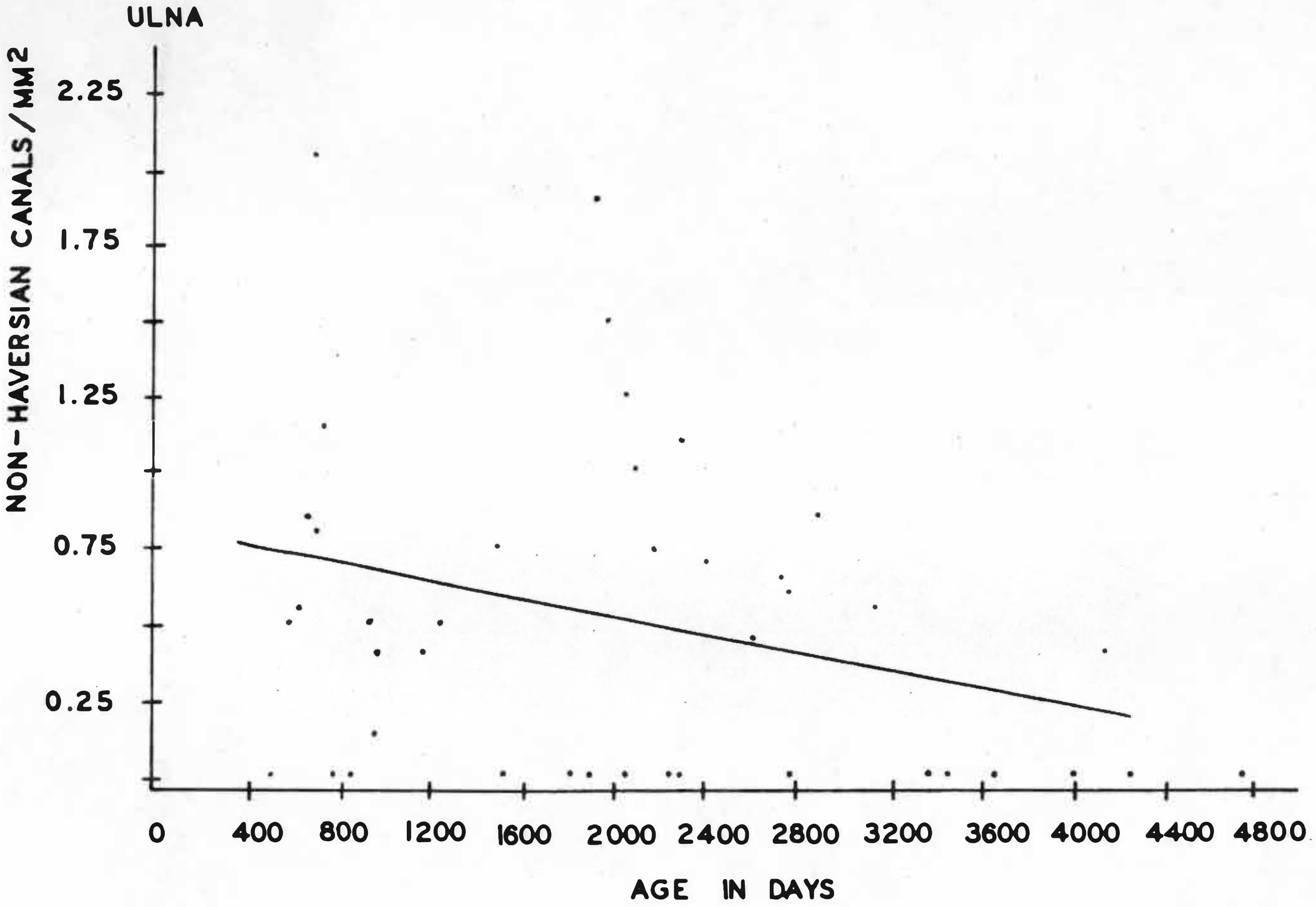

Figure 14. Plot of non-Haversian canals on age for the ulna of *Saguinus fuscicollis*.

Table 18. Regression Statistics of Standardized Osteon Counts on Age and of Standardized Non-Haversian Canal Counts on Age for *Saguinus fuscicollis*[a]

Dependent Variable	Bone	N	Age Mean Sq.	Log[b] Mean Sq.	Error Mean Sq.	Intercept	Slope	F-Value	R^2
Osteon	Humerus	47	164.49		11.03	2.65	0.001	14.91***	0.25
	Ulna	42	142.19		10.71	5.60	0.002	13.28***	0.25
Non-Haversian	Humerus	47		13.02	0.92	6.74	-1.813	14.12***	0.24
	Tibia	45		4.04	0.52	4.26	-1.049	7.80**	0.15
	Ulna	42	1.41		0.27	0.81	-0.0002	5.19*	0.12

[a] See text for standardization procedure.

[b] Log = the common logarithm of age

*P > .05 **P > .01 ***P > .001

The regression lines indicated in Figures 10 and 11 (pages 109 and 110) were generated from the regression results of this model for the two bones. The osteon count model for both bones is found to be significant at the .001 level of probability. The goodness of fit of the model reflected by the R^2-statistic is similar in both the humeral and ulnar regressions and indicate that approximately 25 percent of the variation in osteon counts can be accounted for by variation in age.

A series of linear and curvilinear models was used to test the relationship between the number of non-Haversian canals and age. The models were tested for each bone independently and are given as:

1. N-H canals = a + b (age)
2. N-H canals = a + b_1 (age) + b_2 $(\text{age})^2$
3. N-H canals = a + b_1 (age) + b_2 (common logarithm of age)
4. N-H canals = a + b (common logarithm of age).

In Table 18, the provided regression statistics for non-Haversian canal counts reflect the model which generated the greatest R^2-value with all components contributing significantly. The curvilinear model 4 gave the best fit for the humeral and tibial data which suggests that the relationship between non-Haversian canals and age is best explained logarithmically. The regression lines fitted to Figures 12 and 13 depict this model. In both cases, the relationship documents an initial decrease in the number of non-Haversian canals per square millimeter with advancing age during young adulthood. This decrease gradually decelerates through middle age and beginning at approximately 4000 days, culminates in a linear pattern. The linear model 1 was found to best explain the relationship for the ulna and provided the basis for the regression line fitted to Figure 14.

Examination of the R^2-values of the regressions of osteon counts on age and of non-Haversian canal counts on age for *S. fuscicollis* indicate that a substantial amount of the identified variation in the number of osteons and non-Haversian canals is independent of the variation in age. Given that the sample represents a group in a controlled environment, the probable existence of non-age-related genetic components or genotype/environment interaction contributing to the number of osteons and non-Haversian canals is suggested.

In order to document the chronological changes in the midshaft dimensions of long bones, a procedure for standardizing general size variation was warranted. Standardization was accomplished by dividing the dimension variables by the square root of total cortex area (Chapter III). This procedure was considered acceptable if it was shown that the square root of area was not significantly correlated with age as indicated from Pearson product-moment correlations. Non-significant correlations would imply that an overall increase or loss in cortical bone over time was not the contributing factor for changes in midshaft dimensions. Alternatively, the observed chronological changes are best explained as a result of cortical drift.

Of the three bones subjected to mid-diaphyseal cortex size and shape analysis—the humerus, tibia, and ulna—only the tibia exhibited a significant correlation between age and the square root of cortex area, indicating an overall reduction in cortical bone with advancing age for this skeletal element. Subsequently, an alternative standardization procedure was generated for the tibia using non-age-correlated parameters. This procedure followed the form:

Cortex variable ÷ (EAP + EML ÷ 2)

where

EAP = the external anterior-posterior diameter of the cortex, and

EML = the external medial-lateral diameter of the cortex.

Tables 19, 20 and 21 provide the Pearson product-moment correlation matrices of age and the standardized midshaft dimension variables for the humerus, tibia, and ulna respectively. Due to sample size limitations, *S. oedipus* was excluded from this analysis. In each of the matrices, an additional variable, medial-lateral cavity diameter 1 (IML1) was included. This variable does not follow the respective standardization procedures of the other variables but represents the proportion between the IML and EML dimensions calculated from the raw data. Its inclusion into this study was based on two factors. First, because it follows closely the traditional standardization procedures for study of cortical bone loss in human long bones (Ericksen, 1979), it allows for comparison to be made between the results generated by the traditional standardization techniques for this dimension. Second, because it does not depend on an area measurement for its calculation (which is often difficult to obtain), the variable increases the potential for future comparison with other nonhuman primate data.

Table 19. Correlation Matrix of Standardized Humeral Cortex Size and Shape Variables for *Saguinus fuscicollis* (N = 47)[a]

	Age	ANT	POS	MED	LAT	EAP	EML	IAP	IML(1)[b]	IML
Age	1.00	-0.25	-0.05	-0.27	-0.14	0.06	0.15	0.14	0.26	0.23
ANT		1.00	-0.15	0.07	0.34*	-0.41**	-0.43**	-0.59***	-0.36*	-0.42**
POS			1.00	0.18	0.34*	-0.36*	-0.43**	-0.46**	-0.41**	-0.46**
MED				1.00	0.28	-0.45**	-0.15	-0.39**	-0.71***	-0.49***
LAT					1.00	-0.70***	-0.55***	-0.70***	-0.79***	-0.74***
EAP						1.00	0.63***	0.95***	0.78***	0.77***
EML							1.00	0.71***	0.70***	0.91***
IAP								1.00	0.79***	0.81***
IML(1)									1.00	0.93***
IML										1.00

[a] See text for standardization procedure.

[b] Represents the index of the unstandardized variables: IML/EML.

*P > .05 **P > .01 ***P > .001

Table 20. Correlation Matrix of Standardized Tibial Cortex Size and Shape Variables for *Saguinus fuscicollis* (N = 45)[a]

	Age	ANT	POS	MED	LAT	IAP	IML(1)[b]	IML
Age	1.00	-0.35*	-0.51***	-0.48***	-0.29*	0.43**	0.48***	0.48***
ANT		1.00	0.65***	0.52***	0.68***	-0.83***	-0.72***	-0.73***
POS			1.00	0.62***	0.50***	-0.90***	-0.66***	-0.64***
MED				1.00	0.51***	-0.65***	-0.88***	-0.76***
LAT					1.00	-0.61***	-0.83***	-0.77***
IAP						1.00	0.71***	0.60***
IML(1)							1.00	0.94***
IML								1.00

[a] See text for standardization procedure.

[b] Represents the index of the unstandardized variables: IML/EML.

*P > .05 **P > .01 ***P > .001

Table 21. Correlation Matrix of Standardized Ulnar Cortex Size and Shape Variables for *Saguinus fuscicollis* (N = 42)[a]

	Age	ANT	POS	MED	LAT	EAP	EML	IAP	IML(1)[b]	IML
Age	1.00	0.19	0.25	-0.60***	-0.55***	0.42**	-0.14	0.11	0.62***	0.41**
ANT		1.00	-0.21	-0.22	0.01	0.05	-0.42**	-0.49***	-0.09	-0.30
POS			1.00	0.35*	-0.00	-0.35*	0.11	-0.44**	-0.11	-0.06
MED				1.00	0.60***	-0.64***	0.45**	-0.44**	-0.69***	-0.33*
LAT					1.00	-0.50***	0.25	-0.37*	-0.83***	-0.52***
EAP						1.00	-0.11	0.80***	0.60***	0.43**
EML							1.00	0.13	0.14	0.63***
IAP								1.00	0.52***	0.51***
IML(1)									1.00	0.85***
IML										1.00

[a] See text for standardization procedure.

[b] Represents the index of the unstandardized variables: IML/EML.

*P > .05 **P > .01 ***P > .001

Examination of the correlation matrix for the humerus (Table 19) indicates the total absence of significant correlation between any standardized dimension with chronological age. The directions of the correlations do, however, suggest a consistent trend towards the expected pattern of adult cortical bone loss. That is, cortex thickness in all dimensions—anterior, posterior, medial, and lateral—exhibits an inverse relationship with age. Subsequently, the medullary cavity is found to expand with increasing age in both the anterior-posterior and medial-lateral dimensions. The fact that no significant correlations were identified has led to the elimination of the humerus from further analysis.

The correlation matrix for the tibia (Table 20) exhibits a similar pattern of cortical bone loss between the midshaft dimensions and chronological age as identified for the humerus. That is, a chronological decrease in the cortex thickness and subsequent increase in the medullary cavity dimensions. For the tibia, however, all relationships are found to be significant. Two external cortex diameters, the anterior-posterior and medial-lateral, were eliminated from the tibial correlation matrix because of their role in the formation of the standardization factor. The dimensions which exhibit the most significant correlations with age include the posterior and medial cortex thicknesses and the medial-lateral cavity diameter. Both IML and IML(1) indicate significant correlations of .48 with chronological age. Their great similarity may be attributed to the inclusion of the external medial-lateral diameter in both standardization procedures.

The ulnar correlations provided in Table 21 indicate a departure from the pattern identified for the humerus and tibia. Of the four areas of cortex thickness, only the medial and lateral exhibit significant inverse relationships with age. Conversely, the anterior and posterior, although not significantly correlated with age, exhibit positive correlations suggesting a trend towards greater cortical thickness in these areas. This is further reflected in the significantly positive correlation between chronological age and the external anterior-posterior diameter. Therefore, the emerging pattern is characterized by a chronological increase in the cortex along the anterior-posterior dimension and a chronological decrease along the medial-lateral.

Both of the medial-lateral cavity diameter measurements, IML and IML (1), reflect similar significant positive correlations with chronological age. A difference is observed, however, in the magnitude of the correlations with IML (1) exhibiting a higher value.

To further document the relationships between midshaft dimensional changes and chronological age, plots of the standardized diameter variables found to be significantly correlated with age are provided for the tibia and ulna in Figures 15 through 19. Diameter variables were chosen on the basis of which ones best represented the overall dimensional changes. Regression lines were fitted to each plot based on the regression results discussed below.

For the tibia, two diameter dimensions, IML and IAP, were found to be significantly correlated with age. Their plots are represented in Figures 15 and 16, respectively. Due to the equivalent correlation

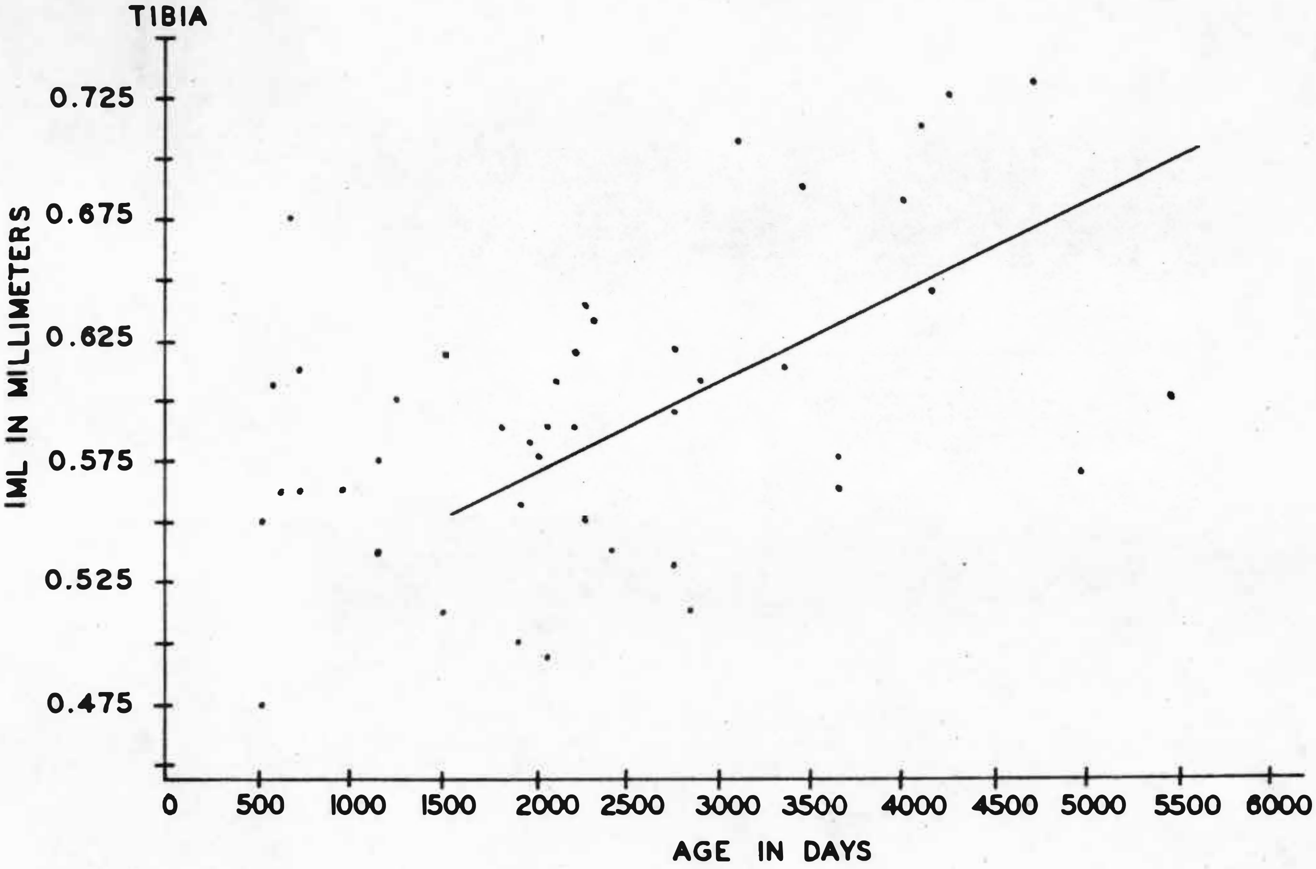

Figure 15. Plot of medial-lateral cavity diameter on age for the tibia of *Saguinus fuscicollis*.

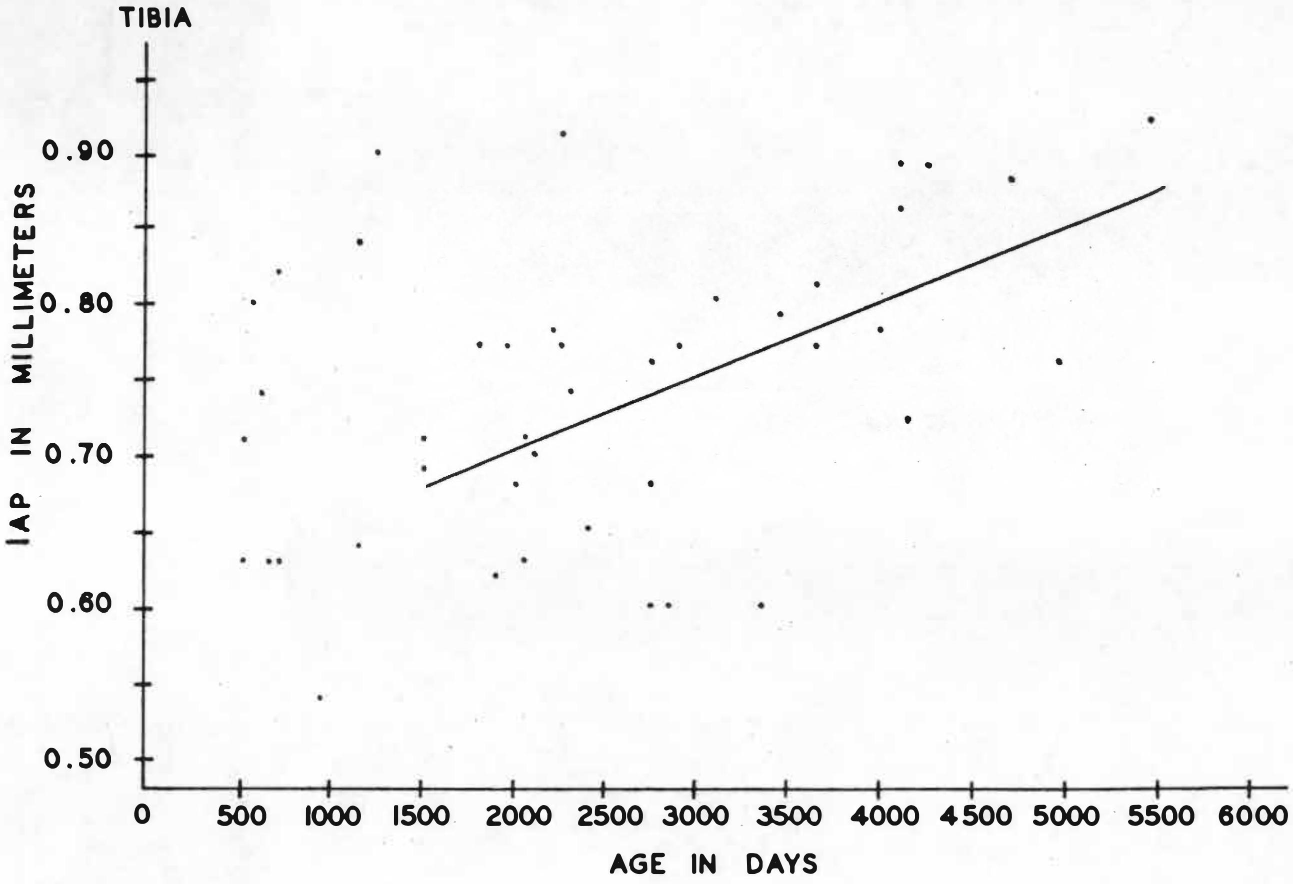

Figure 16. Plot of anterior-posterior cavity diameter on age for the tibia of *Saguinus fuscicollis*.

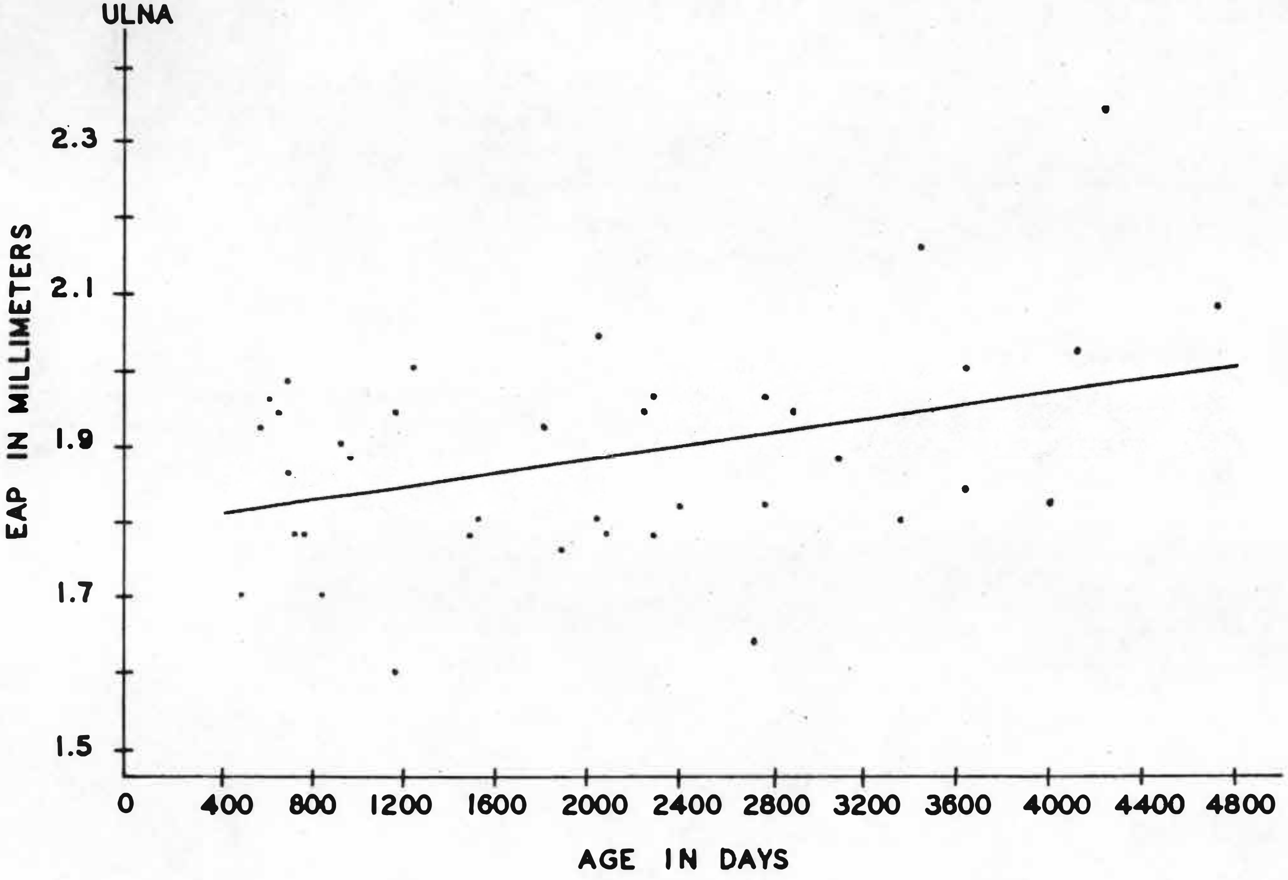

Figure 17. Plot of external anterior-posterior diameter on age for the ulna of *Saguinus fuscicollis*.

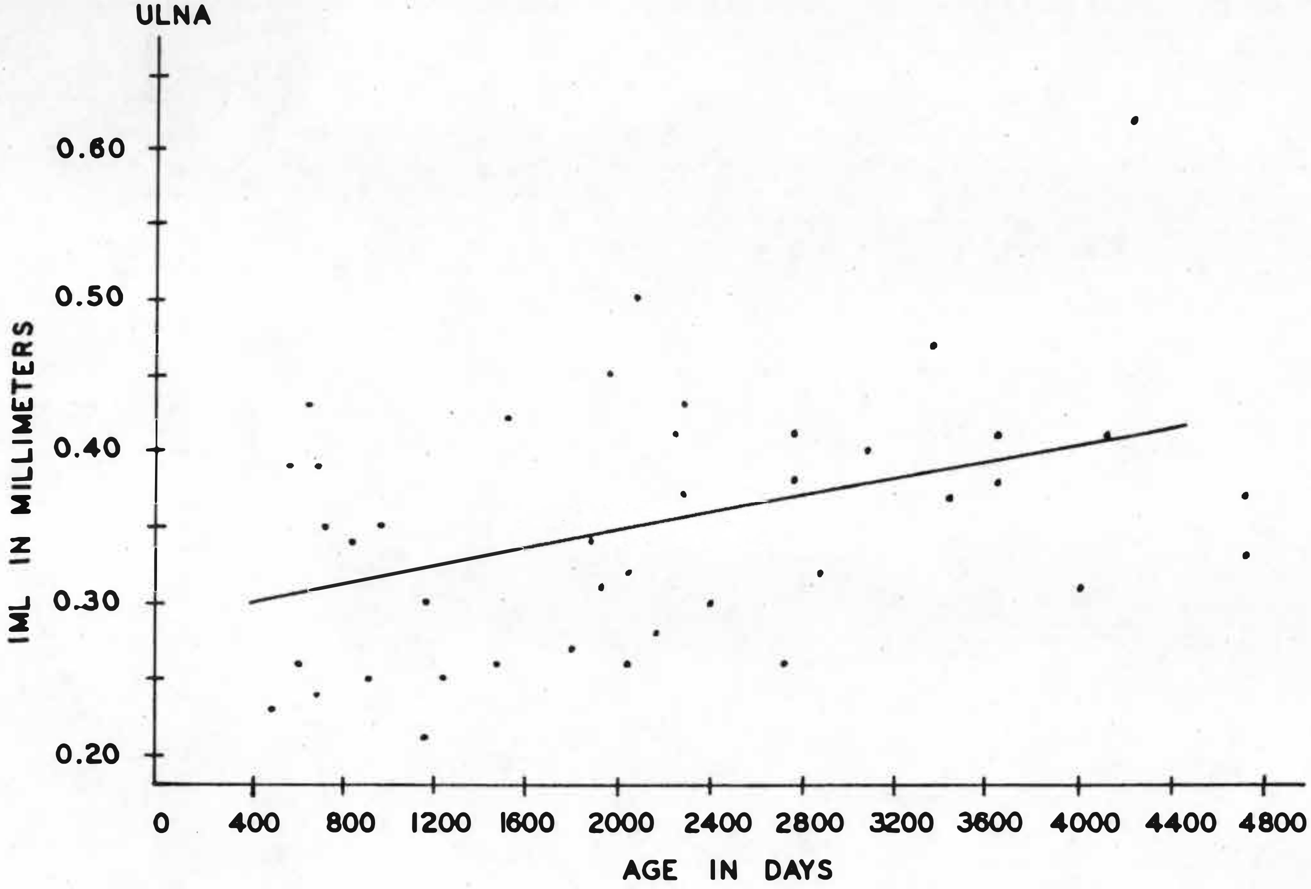

Figure 18. Plot of medial-lateral cavity diameter on age for the ulna of *Saguinus fuscicollis*.

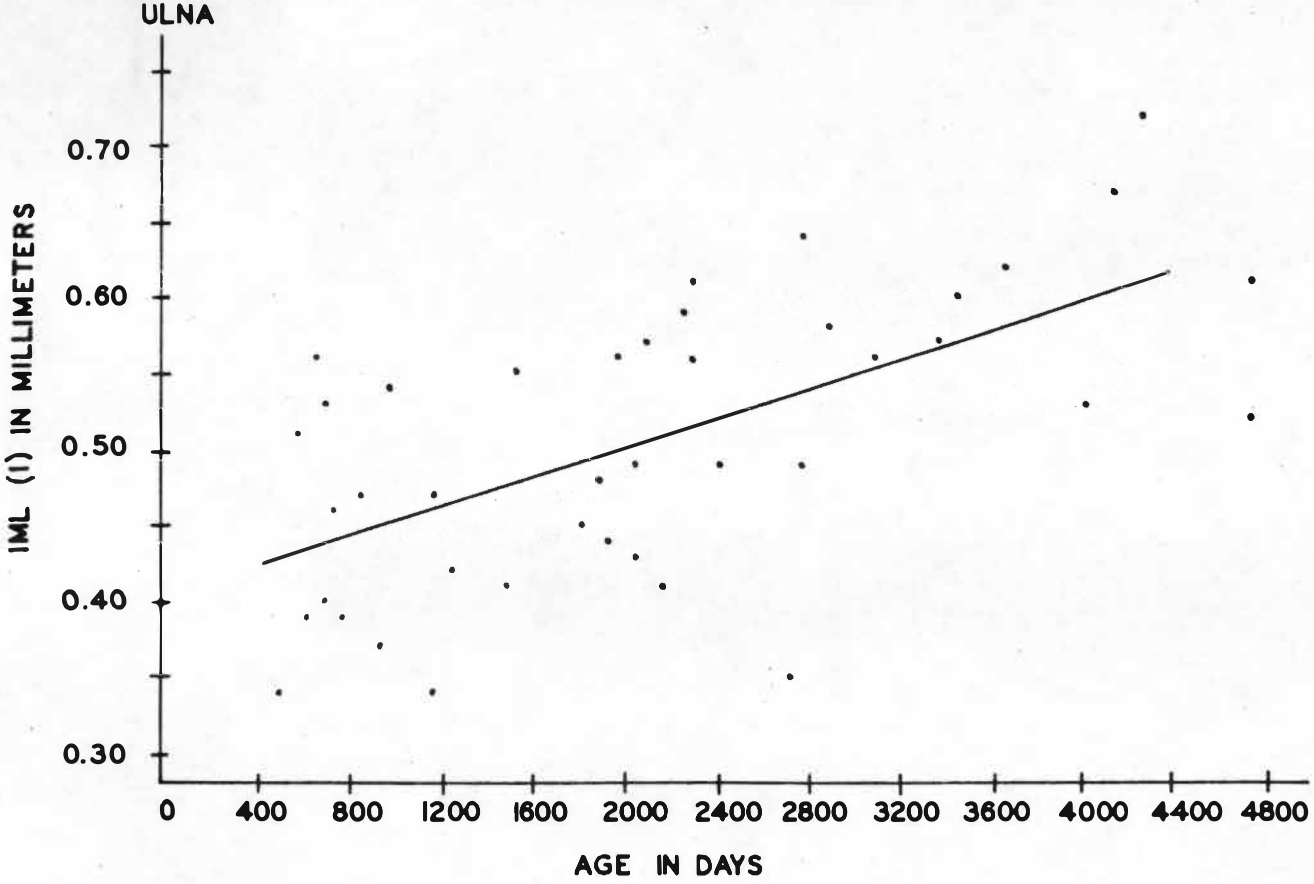

Figure 19. Plot of medial-lateral cavity diameter (l) on age for the ulna of *Saguinus fuscicollis*.

values of the two medial-lateral cavity diameter measures, only one, IML, was selected for presentation. Examination of the plots indicate a similar pattern in their relationship with age. From approximately 500 to 1500 days, both dimensions appear to remain relatively stable or possibly decreasing in size. A decrease would indicate a continuing trend towards expanding cortical thickness during this period. Beginning at approximately 1500 days, a linear relationship is identified whereby medullary cavity diameter increases in both dimensions with advancing age. This period is taken to indicate the onset and continuation of adult cortical bone loss in this element. Variability does exist with respect to this pattern. For example, in the IML dimensional plot, two individuals of ages greater than twelve years exhibit relatively small medullary cavity diameters.

Two diameter variables were also found to be significantly correlated with age in the ulna. The plot of EAP on age (Figure 17) indicates a linear increase in this dimension over time. Because the anterior and posterior cortex thickness variables are positively correlated with age, although not at a significant level (Table 21, page 120), it is assumed that the increasing EAP diameter is a result of increasing cortical thickness rather than a parallel expansion of both the cortex and the cavity.

The medial-lateral cavity diameter represents the second significantly correlated variable with age for the ulna. Due to the substantial difference in correlation values identified from the two standardization procedures for this variable, both have been selected for presentation. The plot of IML on age is provided in Figure 18 and IML (1) in Figure 19. The observed relationship with age in both IML plots is similar and characterized by a linear increase with advancing age. The major difference lies in the magnitude of the slope of the relationships, with IML (1) exhibiting the greater value.

The regression statistics of standardized cortex diameters on age for the tibia and ulna are provided in Table 22. All regressions follow the model

$$\text{Diameter} = a + b\ (\text{age}) \quad .$$

For the tibia, only individuals older than 1500 days (representing the suggested initial appearance of adult cortical bone loss) were included in the regression analysis. The regression model for both diameter dimensions was found to be significant at the .001 level of probability. The results indicate that approximately 30 percent of the size variation in the tibial anterior-posterior and medial-lateral cavity diameters can be accounted for by variation in chronological age.

The regression model was also found to be significant for the three ulnar variables. However, only the IML (1) regression exceeded the .001 level of probability. The relatively small R^2-values of the EAP and IML regressions, .18 and .17 respectively, indicate that a large percent of size variation along these dimensions is independent of age. Interestingly, when the medial-lateral cavity diameter is standardized by the cortex diameter [represented by IML (1)], a substantially greater amount of size variation can be accounted for by variation in age. This

Table 22. Regression Statistics of Standardized Cortex Diameters on Age for the Tibia and Ulna of *Saguinus fuscicollis*[a]

Bone	Dependent Variable	N	Age Mean Sq.	Error Mean Sq.	Intercept	Slope	F-Value	R^2
Tibia[b]	IAP	33	0.080	0.006	0.606	0.000048	13.55***	0.30
	IML	33	0.043	0.003	0.499	0.000035	13.51***	0.30
Ulna	EAP	42	0.133	0.015	1.789	0.000046	8.67**	0.18
	IML	42	0.046	0.006	0.290	0.000027	7.91**	0.17
	IML(1)	42	0.139	0.006	0.406	0.000047	25.07***	0.39

[a] See text for standardization procedure.

[b] Based on individuals greater than 1500 days.

*P > .05 **P > .01 ***P > .001

suggests that standardization on the basis of the dimensional axis, rather than by total cortex area, may be more sensitive to the changes occurring along that axis.

Since there occurs metabolic changes in association with pregnancy, it was necessary to test for possible sexual differences in the pattern of cortical microstructure and mid-diaphyseal cortex size and shape. In order to test this, the residuals of the regressions were individually grouped by sex and subjected to Student's T-test analyses. In all cases with the exceptions of the tests for equal variance in the humeral non-Haversian canals and ulnar EAP diameter regressions, the results indicated that no significant difference exists between the sexes at the .05 level of probability.

1. Estimating Chronological Age from Osteon Counting and Mid-Diaphyseal Cortex Measurements

To develop an equation which would estimate the age of feral tamarins from the number of non-Haversian canals and/or the sum of osteons and osteon fragments, the data were subjected to regression analysis using age as the dependent variable. Lineal and polynomial models up to cubic terms were tested for goodness of fit. The statistical results of the models which provided the best fits are given for the humerus and ulna in Table 23.

In each case, the linear model was identified as yielding the greatest R^2-value, with all source components contributing significantly. For both the humerus and ulna, osteon counts are determined to be a

Table 23. Regression Statistics for Predicting Age in *Saguinus fuscicollis* from Standardized Osteon Counts and Standardized Non-Haversian Canal Counts[a]

Bone	N	Intercept	Slope: Osteon	Slope: Non-Haversian	Model F	R^2	Std. Dev. of Est. (in days)
Humerus	47	1226.11	166.81		14.91***	0.25	1110.28
	47	2634.58		-496.35	10.00**	0.18	1158.78
	47	1704.08	133.91	-338.81	10.54***	0.32	1065.24
Ulna	42	677.27	166.37		13.28***	0.25	1080.44
	42	2524.20		-770.28	5.19*	0.12	1175.13
	42	1095.50	147.81	-530.60	8.40**	0.31	1055.29

[a] See text for standardization procedure.

*P > .05 **P > .01 ***P > .001

better predictor of age than non-Haversian canals and the multiple regression using both variables is shown to be a better predictor than either one taken independently. Both skeletal elements provide a similar degree of predictive accuracy and allow ages to be assigned to within approximately six years. For a species whose members possess approximately a 15-year life span, this degree of accuracy is considered only marginally valuable. It reflects the magnitude of independence between the variation in cortical remodeling and chronological age suggested for *S. fuscicollis* earlier in this section.

Cortical remodeling data taken from four specimens of known-age *S. oedipus* ranging between 463 and 1798 days and one specimen of age greater than 3396 days were standardized and subjected to the multiple regression formulae in Table 23. The actual and predicted ages and their residuals for this sample are provided in Table 24. The residuals in five cases yield values less than the standard deviation of estimate associated with their respective regression equations. The remaining three exceed the standard deviation, although to a minor extent. The margin of error between the predicted and actual ages range from approximately one month to three and one-half years, with five of the estimates over or under aging by less than eight and one-half months. Neither the humerus nor the ulna was identified as being a more consistent predictor of accurate age than the other. Overall, the test sample data suggest that the relationship of cortical remodeling and chronological age in *S. oedipus* follows a similar pattern to that documented for *S. fuscicollis*. Subsequently, the tentative assignment of age based on *S. fusciollis*-derived formulae is considered acceptable.

Table 24. Actual and Predicted Ages in Days for Five *Saguinus oedipus* from Multiple Regression Formulae Derived from *Saguinus fuscicollis* Cortical Remodeling Data[a]

Actual Age	Predicted Age		Residual	
	Humerus	Ulna	Humerus	Ulna
463	718.1	1655.5	255.1	1192.5
712	2015.4	1846.9	1303.4	1134.9
1037	822.2	1071.4	-207.8	34.4
1798	1926.4	1761.4	128.4	-36.6
>3396	2594.0	2375.5		

[a] See Table 23 (page 132) for regression coefficients.

Similar procedures for predicting age from cortical remodeling data were used to evaluate the potential for estimating chronological age from midshaft diameter measurements. Tables 25 and 26 provide the regression results of the models yielding the best fit for selected diameters of the tibia and ulna respectively.[10] The linear model was found to best represent the relationship in all cases. In none of the multiple regressions did both diameter components contribute significantly to the overall model. These regressions were eliminated from presentation here.

For the tibia, the model for both diameter regressions is significant at the .001 level of probability. R^2-values and the standard deviation of estimate is also equivalent for the regressions. The results indicate that the age of middle and older adult *S. fuscicollis* may be accurately assigned to within approximately five years.

The ulnar regressions exhibit greater variability in their individual potential for accurate age prediction. The best predictor of chronological age is the IML (1) model which exhibits an R^2-value more than two times greater than the other models. Interestingly, the differing standardization procedures for the IML dimension account for the considerable differences in age predictability by this dimension. Using the IML (1) model, accurate assignment of age for this sample can be made to within approximately five and one-half years. Because the ulnar models extend the range of applicability to include young

---

[10] Selected diameters represent the dimensions most highly correlated with age in *S. fuscicollis*.

Table 25. Regression Statistics for Predicting Age in *Saguinus fuscicollis* from Tibial Standardized Cortex Diameters[a]

			Slope				
Bone	N	Intercept	IAP	IML	Model F	R^2	Std. Dev. of Est. (in days)
Tibia	33	-1771.95	6328.74		13.55***	0.30	884.37
	33	-2233.22		8609.21	13.51***	0.30	884.73

[a] See text for standardization procedure. ***P > .001

Table 26. Regression Statistics for Predicting Age in *Saguinus fuscicollis* from Ulnar Standardized Cortex Diameters.[a]

			Slope					
Bone	N	Intercept	EAP	IML	IML(1)	Model F	R^2	Std. Dev. of Est. (in days)
Ulna	42	-5123.38	3843.57			8.67**	0.18	1128.71
	42	28.95		6035.68		7.91**	0.17	1137.64
	42	-1989.56			8136.15	25.07***	0.39	976.22

[a] See text for standardization procedure. *P > .05 **P > .01 ***P > .001

adults between one and four years, the IML (1) model is considered to be the best overall parameter for estimating adult age in *S. fuscicollis* from midshaft diameter data.

To test the appropriateness of estimating age in adult *S. oedipus* from regression formulae devised from *S. fuscicollis* cortex diameter data, standardized ulnar data from five *S. oedipus* were subjected to the IML (1) regression formula presented in Table 26. The sample represents the same individuals used to test the cortical remodeling formulae. The actual and predicted ages and their residual differences are given in Table 27.

Only one individual exhibits a residual which exceeds the standard deviation of estimate for this regression. However, a pattern is identified in the residual differences whereby the three youngest individuals exhibit positive error of decreasing magnitude followed by the next individual exhibiting a negative difference. Although this trend possibly suggests diversity in the pattern of the relationship between chronological age and the medial-lateral cavity diameter for the two species, small sample size precludes any positive conclusion.

The ulna represents the only skeletal element from which age prediction multiple regressions may be calculated using combinations of cortical remodeling and cortex diameter data. All combinations of the three variables, IML (1), osteons, and non-Haversian canals, were tested for age prediction potential. The regression formula which provides the greatest accuracy is

$$\text{Age} = -.2391.50 + 6888.32\ (\text{IML}(1)) + 115.89\ (\text{Osteon}) \quad .$$

Table 27. Actual and Predicted Ages in Days for Five *Saguinus oedipus* from the IML(1) Regression Formula Derived from *Saguinus fuscicollis* Diameter Data[a]

Actual Age	Predicted Age	Residual
463	1720.5	1257.5
712	1622.9	910.9
1037	1159.1	122.1
1798	1419.5	-378.5
>3396	3608.1	

[a] See Table 26 (page 136) for regression coefficients.

The model is significant with probability exceeding the .001 level and yields an R^2-value of 0.49. The standard deviation of the regression estimate, 905.25 days, indicates accurate age assignment to within approximately five years.

The overall results from this section indicate that prediction of adult age in *S. fuscicollis* by either cortical remodeling or dimensional changes in the cortex can be made at a similar level of accuracy. Unfortunately, this level, accurate to within approximately five or six years, is not substantially better than that achieved from qualitative data from the femur (Glassman and Schmidt, 1980). This suggests the further need to investigate additional parameters such as the chronology of cementum annulae to improve the ability to assign ages to adult feral tamarins.

CHAPTER V

CONCLUSIONS

This dissertation has attempted to document the pattern, timing, and variation of several skeletal changes associated with the normal, biological aging process for two species of tamarins, *S. fuscicollis* and *S. oedipus*. For the changes that occur during the subadult growth phase, examination was made of the dental eruption, long bone growth, and epiphyseal union. Intracortical bone remodeling and mid-diaphyseal cortex size and shape for the humerus, tibia, and ulna were selected to represent skeletal changes associated with adult aging. All conclusions presented below reflect the results of this study.

Deciduous dental eruption proceeds directly from anterior to posterior in both jaws for both species. For *S. fuscicollis*, eruption is well underway at birth, with all incisors and canines having pierced the gingiva. For *S. oedipus*, however, eruption of the incisors occurs during the first week of postnatal development and the canines between the first and second weeks. All deciduous teeth are erupted by the twelfth week for *S. fuscicollis*.[1]

The sequence of eruption for the permanent teeth in *S. fuscicollis* follows the pattern M1 → I1 → I2 → M2 → P4 → P2 → P3 → C. Mandibular eruption of the M1, M2, P4, and P3 occurs prior to their maxillary

---

[1] The age range of deciduous dental eruption in *S. oedipus* was not determined due to insufficient data.

counterparts. Permanent dental eruption begins at approximately the sixteenth week and continues until approximately forty-five weeks at which time the canines are erupted. The age ranges for the eruption of specific morphological dental types vary from one to ten weeks. Although the small sample size of *S. oedipus* allows for only limited interpretation to be made concerning dental eruption in this species, comparison with *S. fuscicollis* data indicates an overall similarity in sequence and in timing.

Examination of the chronology of long bone growth suggests that in general, growth for both *S. fuscicollis* and *S. oedipus* follows a similar pattern. Growth initiates at a rapid rate followed by a period of marked deceleration, and then continues in a virtually linear fashion until maturity is achieved. The period of marked deceleration for both species occurs between 25 and 100 days of postnatal development. Although a general pattern in growth appears to be shared, an analysis of covariance indicates that the slopes of the growth curves for each long bone differ significantly between the two species.

Although the sequence and timing of epiphyseal union differs slightly between *S. fuscicollis* and *S. oedipus*, general conclusions applicable to both species can be drawn. Fusion of the long bone epiphyses begins approximately in the third month of postnatal development with the union of the distal humerus and continues until approximately two and one-quarter years of age. Additional non-long bone epiphyses such as the ischial epiphysis and iliac crest extend the period of union to more than six years. For both species, the epiphyses associated with the elbow, hip and ankle unite respectively, prior to those for the wrist, shoulder and knee. In 18 of the 22 unions observed for analysis, *S. oedipus* began fusion later than *S. fuscicollis*, although the difference in most cases does not exceed six months.

For both species, the time in which fusion of an epiphysis occurs, as measured by fusion age ranges, varies substantially between specific epiphyseal centers. Age ranges vary in size from approximately one month to more than four years (as for the iliac crest). However, the age ranges for long bone epiphyses average one-half year.

The documented patterns of dental eruption, long bone growth, and epiphyseal union provide accurate parameters for estimating chronological age in subadult *S. fuscicollis* and *S. oedipus* individuals. Dental eruption standards are only applicable for aging individuals between birth and ten months. Long bone growth and epiphyseal union criteria extend this range up to maturity.[2]

For the determination of age in *S. oedipus* subadults, tentative support is given to the use of dental eruption and epiphyseal union standards derived for *S. fuscicollis*. Prediction from long bone growth data, however, is restricted to the regression formulae devised for this species. The research results indicate that when all three

---

[2] Maturity is achieved at approximately two years of age for both species.

parameters are used in conjunction with one another, chronological age may be accurately estimated to within four months.[3]

With respect to the adult skeletal age change of intracortical bone remodeling, *S. fuscicollis* exhibits a significant increase in the number of osteons and osteon fragments and a significant decrease in the number of non-Haversian canals with advancing age for the humerus and ulna.[4] No significant correlation exists between the number of osteons and age for the tibia.

The pattern of increase in the number of osteons with advancing age for the humerus and ulna most closely follows a linear model. A linear relationship also reflects the chronological decrease in the number of non-Haversian canals in the ulna. For the humerus, however, the relationship between non-Haversian canals and age is best explained as curvilinear, whereby an initial rapid decrease during young adulthood is followed by a gradual slowing down of the decrease during middle age. In all of the intracortical remodeling relationships, substantial variation occurs with respect to the suggested patterns.

Significant adult age changes in the size and shape of the mid-diaphyseal cortex are identified for the tibia and ulna. For the tibia, the general pattern beginning at approximately 1500 days is one of decreasing thickness in all anatomical areas—anterior, posterior, medial, and lateral. Subsequently, the medullary cavity is found to

---

[3] This estimate is based on the individuals included in the research sample from which the standards were derived.

[4] Adult age change analyses were restricted to *S. fuscicollis*.

expand in both the anterior-posterior and medial-lateral dimensions. These changes in size and shape indicate a continual trend towards cortical bone loss similar to that identified for adult humans and other nonhuman primates. In contrast to similar studies involving human material, the adult loss of cortical bone in *S. fuscicollis* tibiae is more highly correlated with age along the medial-lateral dimension than the anterior-posterior.

The major adult changes in the size and shape of the ulnar cortex correspond to a significant decrease in the medial and lateral areas of cortex thickness over time. No significant change is documented for the anterior or posterior dimensions. However, a trend towards increasing thickness in these areas is suggested.

All of the significant correlations between cortex size and chronological age appear to follow a linear pattern. However, similar to the intracortical remodeling relationships, substantial variation within this pattern is known to exist.

Because of the extensive variation which exists within the age-related patterns of intracortical remodeling and cortex size and shape, prediction of chronological age for adult tamarins based upon these parameters is found at a low level of accuracy. Regression formulae derived from osteon counting data allow for accurate age assignment to within approximately six years. Only slightly better accuracy is attained from age-prediction formulae derived from cortex dimension measurements. Therefore, the need to investigate additional parameters for aging adult tamarins is warranted.

BIBLIOGRAPHY

BIBLIOGRAPHY

Adams, L. and S. G. Watkins
1967 Annuli in tooth cementum indicate age in California ground squirrels. Journal of Wildlife Management, 31:836-839.

Ahlqvist, J. and O. Damsten
1969 A modification of Kerley's method for the microscopic determination of age in human bone. Journal of Forensic Sciences, 14(2):205-212.

Allen, S. H.
1974 Modified techniques for aging red fox using canine teeth. Journal of Wildlife Management, 38:152-154.

Ammons, W. F., L. R. Schectman, and R. C. Page
1972 Host tissue response in chronic periodontal disease. I. The normal periodontium and clinical manifestations of dental and periodontal disease in the marmoset. Journal of Periodontal Research, 7:131-143.

Atkinson, P. J. and C. Woodhead
1973 The development of osteoporosis. Clinical Orthopaedics, 90:217-228.

Barnett, E. and B. E. C. Nordin
1960 The radiological diagnosis of osteoporosis: A new approach. Clinical Radiology, 11:166-174.

Bass, W. M.
1971 Human Osteology: A Laboratory and Field Manual of the Human Skeleton. (Second edition). Special Publications, Missouri Archaeological Society, Columbia.

Benirschke, K. and R. Richart
1960 Spontaneous acute toxoplasmosis in a marmoset monkey. American Journal of Tropical Medicine and Hygiene, 9:269-273.

Berkson, G.
1968 Weight and tooth development during the first year in *Macaca irus*. Laboratory Animal Care, 18:352-355.

Bermont, G. and D. G. Lindburg (eds.)
1975 Primate Utilization and Conservation. John Wiley and Sons, New York.

Bernstein, I. S., P. Balcaen, L. Dresdale, H. Gouzoules, M. Kavanaugh, T. Patterson and P. Neyman-Warner
1976 An appeal for the preservation of habitats in the interests of primate conservation. Primates, 17:413-415.

Bouvier, M. and D. H. Ubelaker
1977 A comparison of two methods for the microscopic determination of age at death. American Journal of Physical Anthropology, 46(3):391-394.

Bowden, D. M., C. Teets, J. Witkin, and D. M. Young
1979 Long bone calcification and morphology. *In* Aging in Nonhuman Primates, D. M. Bowden, ed., Van Nostrand Reinhold, New York, 335-347.

Bowen, W. H. and G. Koch
1970 Determination of age in monkeys (*Macaca irus*) on the basis of dental development, Laboratory Animals, 4:113-123.

Bramblett, C. A.
1969 Non-metric skeletal age changes in the Darajani baboon. American Journal of Physical Anthropology, 30:161-170.

Britton, S. W., H. Silvette and R. K. Kline
1939 Adrenal insufficiency in American monkeys. American Journal of Physiology, 123:705-711.

Brooks, S. T.
1955 Skeletal age at death: Reliability of cranial and pubic age indicators. American Journal of Physical Anthropology, 13(4):567-597.

Byrd, K. E.
1979 Sequences and asymmetries of dental development and eruption in the Ceboidea. Ph.D. Dissertation, University of Washington, Seattle.

Cartmill, M.
1974 Pads and claws in arboreal locomotion. *In* Primate Locomotion, F. Jenkins, ed., Academic Press, New York, 45-83.

Castro, R. and P. Soini
1977 Field studies on *Saguinus mystax* and other Callitrichids in Amazonian Peru. *In* The Biology and Conservation of the Callitrichidae, D. G. Kleiman, ed., Smithsonian Institution Press, Washington, D.C., 73-78.

Chaplin, R. E.
1971 The Study of Animal Bones from Archaeological Sites. Seminar Press, London.

Chase, J. E. and R. W. Cooper
1969 *Saguinus nigricollis*—Physical growth and dental eruption in a small population of captive born individuals. American Journal of Physical Anthropology, 30:111-116.

Chasen, S. H.
1978 Geometric Principles and Procedures for Computer Graphic Applications. Prentice Hall, New Jersey.

Clements, E. M. B. and S. Zuckerman
1953 The order of eruption of the permanent teeth in the Hominoidea. American Journal of Physical Anthropology, 11:313-332.

Cohen, B.
1960 Comparative studies in periodontal disease. Proceedings of the Royal Society of Medicine, 53:275.

Coimbra-Filho, A. F. and R. A. Mittermeier
1977 Tree-gouging, exudate-eating and the "short-tusked" condition in *Callithrix* and *Cebuella*. *In* The Biology and Conservation of the Callitrichidae, D. G. Kleiman, ed., Smithsonian Institution Press, Washington, D.C., 105-115.

Cooper, R. W.
1964 A description of a unique outdoor primate colony. Laboratory Animal Care, 14:474-482.

Cosgrove, G. E., G. Humason, and C. C. Lushbaugh
1970 *Trichospirura leptostoma*, a nematode of the pancreatic ducts of marmosets (*Saguinus* spp.). Journal of the American Veterinary Medical Association, 157(5):696-698.

Cosgrove, G. E., B. M. Nelson, and N. Gengozian
1968 Helminth parasites of the tamarin, *Saguinus fuscicollis*. Laboratory Animal Care, 18(6):654-656.

Currey, J. D.
1964 Some effects of aging in human haversion systems. Journal of Anatomy, 98:69-75.

Dawson, A. B.
1929 A histological study of the persisting cartilage plates in retarded or lapsed epiphyseal union in the albino rat. Anatomical Record, 43:109-129.

1934 Additional evidence on the failure of epiphyseal union in the skeleton of the rat. Anatomical Record, 60:83-86.

Dawson, G.
1976 Behavioral ecology of the Panamanian tamarin, *Saguinus oedipus* (Callitrichidae, Primates). Ph.D. Dissertation, Michigan State University.

Deinhardt, J. B.
1970a Use of marmosets in biomedical research. *In* Medical Primatology, E. I. Goldsmith and J. Moor-Jankowski, Karger, Basel, 918-925.

1970b Nutritional requirements of marmosets. *In* Feeding and Nutrition of Nonhuman Primates. R. S. Harris, ed., Academic Press, New York, 175-182.

Deinhardt, F., A. W. Holmes, R. B. Capps and H. Popper
1967a Studies on the transmission of human viral hepatitis to marmoset monkeys. Transmission of disease, serial passages, and description of liver lesion. Journal of Experimental Medicine, 126:673-688.

Deinhardt, F., A. W. Holmes, J. Devine, and J. Deinhardt
1967b Marmosets as laboratory animals. IV. The microbiology of laboratory kept marmosets. Laboratory Animal Care, 17(1):48-70.

Deinhardt, F., L. G. Wolfe, R. L. Northrop, B. Marczynska, J. Ogden, R. McDonald, L. Falk, G. Shramek, R. Smith, and J. Deinhardt
1972 Induction of neoplasms by viruses in marmoset monkeys. Journal of Medical Primatology, 1(1):29-50.

Deinhardt, F., L. G. Wolfe, G. H. Theilen, and S. P. Snyder
1970 ST-Feline fibrosarcoma virus: Inducation of tumors in marmoset monkeys. Science, 167:881.

Deming, J.
1957 Application of the Gompertz curve to the observed pattern of growth in length of 48 individual boys and girls during the adolescent cycle of growth. Human Biology, 29:83-122.

Dewey, J. R., M. H. Bartley, and G. J. Armelagos
1969 Rates of femoral cortical bone loss in two Nubian populations: Utilizing normalized and non-normalized data. Clinical Orthopaedics, 65:61-66.

Dunn, F. L.
1961 *Molineus vexillarius* sp. n. (Nematoda: Trichostrongylidae) from a Peruvian primate, *Tamarinus nigricollis* (Spix, 1823). Journal of Parasitology, 47:953-956.

Durham, N. M.
1974 Observations on the social groupings of the red-handed tamarin, *Saguinus midas* of the Guianas. American Journal of Physical Anthropology, 41:476.

Eckstein, F. M. P.
1948 Age changes in dentition in the rhesus monkey. British Medical Journal, 2:168.

Enlow, D. H.
1963 Principles of Bone Remodeling, Charles C. Thomas, Springfield, Illinois.

Epker, B. N., R. Hattner and H. M. Frost
1964 Radial rate of osteon closure: Its application in the study of bone formation in metabolic bone disease. Journal of Laboratory and Clinical Medicine, 64:643-653.

Epple, G.
1968 Comparative studies on vocalization in marmoset monkeys (Hapalidae). Folia Primatologica, 8:1-40.

1970a Maintenance, breeding and development of marmoset monkeys (Callitrichidae) in captivity. Folia Primatologica, 12: 56-76.

1970b Quantitative studies on scent marking in the marmoset (*Callithrix jacchus*). Folia Primatologica, 13:48-62.

1971 Discrimination of the odor of males and females by the marmoset *Saguinus fuscicollis* ssp. Proceedings of the Third International Congress of Primatology, Zurich, 3:166-171.

1974 Olfactory communication in South American primates. Annals of the New York Academy of Science, 237:261-278.

Ericksen, M. F.
1976 Cortical bone loss with age in three native American populations. American Journal of Physical Anthropology, 45:443-452.

1979 Aging changes in the medulary cavity of the proximal femur in American Blacks and Whites. American Journal of Physical Anthropology, 51:563-569.

Ford, S. M.
1980 Callitrichids as phyletic dwarfs, and the place of the Callitrichidae in Platyrrhini. Primates, 21(1):31-43.

Fritzgerald, A.
1935 Rearing marmosets in captivity. Journal of Mammalogy, 16:181-188.

Frost, H. M.
1963 Bone Remodeling Dynamics. Charles C. Thomas, Springfield, Illinois.

Garber, P. A.
1979 Locomotor behavior and feeding ecology of the Panamanian tamarin (*Saguinus oedipus geoffroyi*, Callitrichidae, Primates). Paper presented at the 48th Annual Meeting of the American Association of Physical Anthropologists, April, San Francisco.

Garn, S. M.
1970 The Earlier Gain and the Later Loss of Cortical Bone. Charles C. Thomas, Springfield, Illinois.

Garn, S. M., A. B. Lewis, and D. L. Polacheck
1959 Variability of tooth formation. Journal of Dental Research, 38:135-148.

Garn, S. M., C. G. Rohmann, B. Wagner, G. H. Davila, and W. Ascoli
1969 Population similarities in the onset and rate of adult endosteal bone loss. Clinical Orthopaedics, 65:51-60.

Garn, S. M. and H. Shaw
1977 Extending the Trotter model of bone gain and bone loss. Yearbook of Physical Anthropology, 1976, 45-56.

Gavan, J. A.
1967 Eruption of primate deciduous dentition: A comparative study. Journal of Dental Research, 46:984-988.

Gavan, J. A. and T. C. Hutchinson
1973 The problem of age estimation: A study using rhesus monkeys (*Macaca mulatta*). American Journal of Physical Anthropology, 38:69-82.

Gavan, J. A. and D. R. Swindler
1966 Growth rates and phylogeny in primates. American Journal of Physical Anthropology, 27:181-190.

Gengozian, N.
1969 Marmosets: Their potential in experimental medicine. Annals of the New York Academy of Science, 162:336-367.

Gengozian, N.
1971 Male and female cell populations in the chimeric marmoset. *In* Medical Primatology, Selected papers from the 2nd Conference on Experimental Medicine and Surgery in Primates, held in New York in 1969. Karger, Basel, 926-938.

Gengozian, N., J. S. Batson and T. A. Smith
1977 Breeding of tamarins (*Saguinus* spp.) in the laboratory. *In* The Biology and Conservation of the Callitrichidae. D. G. Kleiman, ed., Smithsonian Institution Press, Washington, D.C., 207-213.

Gilbert, F. F.
1966 Aging white-tailed deer by annuli in the cementum of the first incisor. Journal of Wildlife Management, 30:200-202.

Gisler, D. B., S. G. Wilson, and G. L. Hekhuis
1960 Correlation of skeletal growth, epiphyseal ossification with age of monkeys. Annals of the New York Academy of Sciences, 85:800-802.

Glassman, D. M.
1981 The functional anatomy of the postcranial skeleton of *Saguinus fuscicollis illigeri* and *Saguinus oedipus oedipus* (Callitrichidae, Primates). American Journal of Physical Anthropology, 54:225.

Glassman, D. M. and D. J. Schmidt
1980 Skeletal Age Changes in *Saguinus oedipus* and *S. fuscicollis* (Callitrichidae, Primates). Paper presented to the 49th Annual Meeting of the American Association of Physical Anthropologists, April, Niagara Falls, New York.

Glassman, D. M. and R. S. Webb
n.d. A method of recovering the palmar and plantar pads of small primate cadaver specimens for dermatoglyphic analysis (unpublished manuscript).

Glasstone, S.
1963 Regulative changes in tooth germs grown in tissue culture. Journal of Dental Research, 42(6):1364-1368.

1964 Cultivation of mouse tooth germs in a chemically defined protein-free medium. Archives of Oral Biology, 9:27-30.

Goss, C. M.
1976 Gray's Anatomy of the Human Body (29th edition). Lea and Febiger, Philadelphia.

Haigh, M. V. and A. Scott
1965 Some radiological and other factors for assessing age in the rhesus monkey using animals of known age. Laboratory Animal Care, 15:57-73.

Ham, A. W.
1957 Histology (Third edition). Lippincott, Philadelphia.

Hampton, J. K., Jr.
1964 Laboratory requirements and observations of *Oedipomidas oedipus*. American Journal of Physical Anthropology, 22: 239-244.

Hampton, J. K., Jr. and S. H. Hampton
1965 Marmosets (Hapalidae): Breeding seasons, twinning, and sex of offspring. Science, 150:915-917.

Hampton, J. K., Jr., S. H. Hampton, and B. T. Landwehr
1966 Observations on a successful breeding colony of the marmoset, *Oedipomidas oedipus*. Folia Primatologica, 4: 265-287.

Hampton, J. K., Jr., B. M. Levy, and P. M. Sweet
1969 Chorionic gonadotropin excretion during pregnancy in the marmoset. Endrocrinology, 85(1):171-174.

Hampton, S. H. and J. K. Hampton, Jr.
1967 Rearing marmosets from birth by artificial laboratory techniques. Laboratory Animal Care, 17(1):1-10.

Hancox, N. M.
1972 Biology of Bone. Cambridge University Press, Cambridge.

Harrison, B.
1971 Conservation of Nonhuman Primates in 1970, Vol. 5 of Primates in Medicine. S. Karger, Basel.

Hayama, S.
1965 Morphological studies of *Macaca fuscata*. II. The sequence of epiphyseal union by roentgenographic estimation. Primates, 6:249-269.

Hearn, J. P.
1975 Conservation of marmosets. Nature, (London), 257:358-359.

Heltne, P. G.
1957 Latin America: Call for conservation. Science, 158:717.

Heltne, P. G. and R. W. Thorington, Jr.
1975 Problems and potentials for primate biology and conservation in the New World. *In* Neotropical Primates: Field Studies and Conservation, R. W. Thorington and P. G. Heltne, eds., National Academy of Sciences, Washington, D.C., 110-124.

Hershkovitz, P.
1972 The recent mammals of the Neotropical region: a zoogeographic and ecological review. *In* Evolution, Mammals, and Southern Continents, A. Keast, F. Erk, and B. Glass, eds., Suny Press, Albany, New York, 311-431.

1977 Living New World Monkeys (Platyrrhini). The University of Chicago Press, Chicago.

Hurme, V. O.
1960 Estimation of monkey age by dental formula. Annals of the New York Academy of Sciences, 85(3):795-799.

Hurme, V. O. and G. van Wagenen
1953 Basic data on the emergence of deciduous teeth in the monkey (*Macaca mulatta*). Proceedings of the American Philosophical Society, 97:291-315.

1956 Emergence of permanent first molars in the monkey (*Macaca mulatta*): Association with other growth phenomena. Yale Journal of Biology and Medicine, 28:538-567.

1961 Basic data on the emergence of permanent teeth in the rhesus monkey (*Macaca mulatta*). Proceedings of the American Philosophical Society, 105:105-140.

Ikeda, J. and S. Hayama
1963 Observation on the growth and development of Japanese monkeys (*Macaca fuscata*). Primates, 4:90-91.

Izawa, K.
1976 Group sizes and compositions of monkeys in the Upper Amazon Basin. Primates, 17:367-399.

Jenkins, D. P.
1968 The degree of mineralization of the femoral cortex during aging and its relationship to the process, compact bone resorption. American Journal of Physical Anthropology, 29:135.

Jenss, R. M. and N. Bayley
1937 A mathematical model for studying the growth of a child. Human Biology, 9:556-563.

Johnston, F. E.
1962 Growth of the long bones of infants and young children at Indian Knoll. American Journal of Physical Anthropology, 20:249-254.

Johnston, G. W., S. Dreizen, and B. M. Levy
1970 Dental development in the cotton ear marmoset (*Callithrix jacchus*). American Journal of Physical Anthropology, 33: 41-48.

Jowsey, J.
1960 Age changes in human bone. Clinical Orthopaedics, 17: 210-218.

1964 Variations in bone mineralization with age and disease. *In* Bone Biodynamics, H. M. Frost, ed., Little, Brown, Boston, 461-479.

Kerley, E. R.
1965 Microscopic determination of age in human bone. American Journal of Physical Anthropology, 23:149-163.

1970 Estimation of skeletal age: After about age 30. *In* Personal Identification in Mass Disasters, T. D. Stewart, ed., Smithsonian Institution, Washington, D.C., 57-70.

Kerley, E. R. and D. H. Ubelaker
1978 Revisions in the microscopic method of estimating age at death in human cortical bone. American Journal of Physical Anthropology, 49(4):545-546.

Kerr, G. R., J. H. Wallace, C. F. Chesney, and H. A. Waisman
1972 Growth and development of the fetal rhesus monkey: II. Maturation and linear growth of the skull and appendicular skeleton. Growth, 36:59-76.

Kingston, W. R.
1977 The cost of developing and managing a marmoset colony. *In* The Biology and Conservation of the Callitrichidae, D. G. Kleiman, ed., Smithsonian Institution Press, Washington, D.C., 311-316.

Kinzey, W. G.
1973 Reduction of the cingulum in Ceboidea. *In* Craniofacial Biology of Primates, W. Montagna, ed., Karger, Basal, 101-127.

1974 Ceboid models for the evolution of hominoid dentition. Journal of Human Evolution, 3:193-203.

Kleiman, D. G.
1977 The Biology and Conservation of the Callitrichidae. Smithsonian Institution Press, Washington, D.C.

Kovacs, I.
1971 A systematic description of dental roots. *In* Dental Morphology and Evolution, A. A. Dahlberg, ed., University of Chicago Press, Chicago, 211-256.

Krogman, W. M.
1930 Studies in growth changes in the skull and face of anthropoids: The eruption of the teeth in anthropoids and Old World apes. American Journal of Anatomy, 46: 303-313.

Lacroix, P.
1951 The Organization of Bones. Translated by S. Gilder, Blakiston, Philadelphia.

Le Gros Clark, W. E.
1936 The problem of the claw in primates. Proceedings of the Zoological Society of London, 1-24.

Leutenegger, W.
1973 Maternal-fetal weight relationships in primates. Folia Primatologica, 20:280-293.

Levy, B. M.
1963 Induction of fibrosarcoma in the primate *Tamarinus nigricollis*. Nature, (London), 200:182.

Levy, B. M. and J. Artecona
1964 The marmoset as an experimental animal in biological research. I. Care and maintenance. Laboratory Animal Care, 14:20-27.

Levy, B. M., S. Dreizen, and S. Bernick
1972 The Marmoset Periodontium in Health and Disease. Vol. 1 of Monographs in Oral Science. Krager, Basel.

Levy, B. M., S. Dreizen, S. Bernick, and J. K. Hampton, Jr.
1970 Studies on the biology of the periodontium of marmosets. IX. Effects of parathyroid hormone on the alveolar bone of marmosets, pretreated with flouridated and nonflouridated drinking water. Journal of Dental Research, 49(4):816-821.

Levy, B. M., A. C. Taylor, S. H. Hampton, and G. W. Thoma
1969 Tumors of marmoset produced by Rous sarcoma virus. Cancer Research, 29:2237-2248.

Lewis, A. B. and S. M. Garn
1960 The relationship between tooth formation and other maturational factors. The Angle Orthodontist, 30:70-77.

Long, J. O. and R. W. Cooper
1968 Physical growth and dental eruption in captive-bred squirrel monkeys *Saimiri sciureus* (Leticia, Colombia). *In* The Squirrel Monkey, L. H. Rosenblum and R. W. Cooper, eds., Academic Press, New York, 183-205.

Low, W. A. and I. M. Cowan
1963 Age determination of deer by annular structure of dental cementum. Journal of Wildlife Management, 27:466-471.

Lusted, L., R. Miller and M. Malinow
1966 Radiographic study of the postnatal skeletal development in howler monkeys (*Aloutta caraya*). Primates, 7:263-270.

Mallinson, J. J. C.
1977 Maintenance of marmosets and tamarins at Jersey Zoological Park with special reference to the design of the new marmoset complex. *In* The Biology and Conservation of the Callitrichidae, D. G. Kleiman, ed., Smithsonian Institution Press, Washington, D.C., 323-330.

Marczynska, B., G. Treu-Sarnat, and F. Deinhardt
1970 Characteristics of long-term marmoset cell cultures spontaneously altered or transformed by Rous sarcoma virus. Journal of the National Cancer Institute, 44: 545-572.

Marks, S. A. and A. W. Ericksen
1966 Age determination in the black bear. Journal of Wildlife Management, 30:389-410.

McKern, T. W. and T. D. Stewart
1957 Skeletal age changes in young American males, analyzed from the standpoint of identification. Technical Report EP-45. Headquarters Quartermaster Research and Development Command, Natick, Massachusetts.

McLean, F. C. and M. R. Urist
1968 Bone: An Introduction to the Physiology of Skeletal Tissue. (Third edition). University of Chicago Press, Chicago.

Merchant, V. L. and D. H. Ubelaker
1977 Skeletal growth of the protohistoric Arikara. American Journal of Physical Anthropology, 46:61-72.

Mittermeier, R. A., R. C. Bailey, and A. F. Coimbra-Filho
1977 Conservation Status of the Callitrichidae in Brazilian Amazonia, Surinam, and French Guiana. *In* The Biology and Conservation of the Callitrichidae. D. G. Kleiman, ed., Smithsonian Institution Press, Washington, D.C., 137-146.

Morgan, D. B. and H. F. Newton-Jones
1969 Bone loss and senescence. Gerontologia, 15:140-154.

Moynihan, M.
1970 Some behavior patterns of platyrrhine monkeys. II. *Saguinus geoffroyi* and some other tamarins. Smithsonian Contributions to Zoology, 28:1-76.

1976 The New World Primates: Adaptive Radiation and the Evolution of Social Behavior, Languages, and Intelligence. Princeton University Press, New Jersey.

Napier, J. R. and P. H. Napier
1967 A Handbook of Living Primates: Morphology, Ecology and Behaviour of Nonhuman Primates. Academic Press, London.

Neyman, P. F.
1977 Aspects of the ecology and social organization of free-ranging cotton-top tamarins (*Saguinus oedipus*) and the conservation status of the species. *In* The Biology and Conservation of the Callitrichidae, D. G. Kleiman, ed., Smithsonian Institution Press, Washington, D.C., 39-72.

Nissen, H. W. and A. H. Riesen
1945 The deciduous dentition of chimpanzee. Growth, 9:265-274.

1964 The eruption of the permanent dentition of chimpanzee. American Journal of Physical Anthropology, 22:285-294.

Niswander, J. D. and C. Sujaku
1965 Permanent tooth eruption in children with major physical defect and disease. Journal of Dentistry for Children, 32:266-268.

Ockerse, T.
1959 The eruption sequence and eruption times of the teeth of the vervet monkey. Journal of the Dental Association of South Africa, 14:422.

Ortner, D. J.
1975 Aging effects on osteon remodeling. Calcified Tissue Research, 18:27-36.

Pankovich, A. M., D. J. Simmons and V. V. Kulkarni
1974 Zonal osteons in cortical bone. Clinical Orthopaedics, 100:356-363.

Paynter, K. J. and R. M. Grainger
1961 Influence of nutrition and genetics on morphology and caries susceptibility. Journal of the American Medical Association, 177:306-309.

1962 Relationships of morphology and size of teeth to caries. International Dental Journal, 12:147-160.

Porter, J. A., Jr. and M. D. Young
1967 The transfer of *Plasmodium falciparum* from man to the marmoset, *Saguinus geoffroyi*. Journal of Parasitology, 53(4):845-846.

Preslock, J. P., S. H. Hampton, and J. K. Hampton, Jr.
1973 Cyclic variation of serum progestins and immunerative estrogen in marmosets. Endocrinology, 92(4):1096-1101.

Przybeck, T. R.
1981 Age-related change in the bone of nonhuman primates. American Journal of Physical Anthropology, 54:265.

Rahlmann, D. F. and N. Pace
1969 Anthropoidimetric and roentgenographic growth changes in young pig-tailed monkeys (*Macaca nemestrina*). Proceedings of the Second International Congress of Primatology, Krager, Basel, 171-180.

Randall, F. E.
1943 The skeletal and dental development and variability of the gorilla. Human Biology, 15:236-254.

Rice, L. A.
1980 Influences of irregular dental cementum layers on aging deer incisors. Journal of Wildlife Management, 44:267-268.

Rosenberger, A. L.
1977 Xenothrix and ceboid phylogeny. Journal of Human Evolution, 6:461-481.

SAS Institute Inc.
1979 SAS User's Guide (1979 edition). SAS Institute, Raleigh.

Schultz, A. H.
1935 Eruption and decay of the permanent teeth in primates. American Journal of Physical Anthropology, 4:489-581.

Schultz, A. H.

1940 Growth and development of the chimpanzee. Carnegie Institute of Washington, Contributions to Embryology, 28:1-63.

1941 Growth and development of the orang-utan. Carnegie Institute of Washington, Contributions to Embryology, 29:57-110.

1942 Growth and development of the proboscis monkey. Bulletin of the Museum of Comparative Zoology, Harvard, 89:280-314.

1944 Age changes and variability in gibbons: A morphological study on a population sample of a man-like ape. American Journal of Physical Anthropology, 2:1-129.

1948 The number of young at birth and the number of nipples in primates. American Journal of Physical Anthropology, 6(1):1-23.

1956 Postembryonic age changes. Primatologia, 1:887-964.

Serra, O. D.

1952 A sequencia eruptiva dos dentes definitivos nos simios platyrrhina e sua interpretacao filogenetica. Anais da Faculdade de Farmacia e Odontologia da Universidade de Sae Paulo, 10:215-296.

Shigehara, N.

1980 Epiphyseal union, tooth eruption, and sexual maturation in the common tree shrew, with reference to its systematic problem. Primates, 21:1-19.

Silberberg, M. and R. Silberberg

1961 Aging changes in cartilage and bone. *In* Structural Aspects of Aging, G. H. Bourne, ed., Hafner, New York, 85-108.

Silberberg, R. and M. Silberberg

1950 Growth and articular changes in slowly and rapidly developing mice fed a high-fat diet. Growth, 14:213-230.

Singer, R.

1953 Estimation of age from cranial suture closure. Journal of Forensic Medicine, 1(1):52-59.

Singh, J. J. and D. L. Gunberg

1970 Estimation of age at death in human males from quantitative histology of bone fragments. American Journal of Physical Anthropology, 33:373-382.

Slutzky, G. D.
1981 Age determination of death from osteon counting by means of interactive computer graphics. Master's thesis, The University of Tennessee, Knoxville.

Smith, R. W., Jr., and R. R. Walker
1964 Femoral expansion in aging women: Implications for osteoporosis and fractures. Science, 145:156-157.

Stoneberg, R. P. and C. J. Jonkel
1966 Age determination of black bears by cementum layers. Journal of Wildlife Management, 30:411-414.

Stott, G. G., R. S. Sis and B. M. Levy
1980 Cemental annulation as an age criterion in the common marmoset (*Callithrix jacchus*). Journal of Medical Primatology, 9(5):274-285.

Suchey, J. M.
1977 Problems in the aging of females using the pubic symphysis. Paper presented at the 29th Annual Meeting of the American Academy of Forensic Sciences, February, San Diego, California.

Sundick, R. I.
1972 Human skeletal growth and dental development as observed in the Indian Knoll population. Ph.D. Dissertation, University of Toronto.

Swindler, D. R.
1976 Dentition of Living Primates. Academic Press, New York.

Tanner, J. M.
1962 Growth at Adolescence (Second edition). Blackwell Scientific Publications, Oxford.

1978 Foetus into Man: Physical Growth from Conception to Maturity. Harvard University Press, Cambridge.

Tappan, N. C. and A. Severson
1971 Sequence of eruption of permanent teeth and epiphyseal union in New World monkeys. Folia Primatologica, 15: 293-312.

Thompson, D. D.
1979 The core technique in the determination of age at death in skeletons. Paper presented to the 31st Annual Meeting of the American Academy of Forensic Sciences, February, Atlanta.

Thorington, R. W., Jr.
1968 Observations of the tamarin, *Saguinus midas*. Folia Primatologica, 9:95-98.

Thorington, R. W., Jr., and P. G. Heltne
1975 Introduction. *In* Neotropical Primates: Field Studies and Conservation. R. W. Thorington, Jr. and P. G. Heltne, eds., National Academy of Sciences, Washington, D.C., 1-3.

Thorington, R. W., Jr. and R. E. Vorek
1976 Observations on the geographic variation and skeletal development of *Aotus*. Laboratory Animal Science, 26: 1006-1021.

Thorndike, E. E.
1968 A microscopic study of the marmoset claw and nail. American Journal of Physical Anthropology, 28:247-262.

Todd, T. W.
1933 Human bodies and human beings. Sigma Xi Quarterly, 21: 123-140.

Tonna, E. A.
1977 Aging of skeletal-dental systems and supporting tissues. *In* Handbook of the Biology of Aging, C. E. Finch and L. Hayflick, eds., Van Nostrand Reinhold, New York, 470-495.

Tsalickis, M.
1972 Trapping, husbandry and transport conditions of South American primates destined for research. International Zoological Yearbook, 12:23-26.

Ubelaker, D. H.
1974 Reconstruction of demographic profiles from ossuary skeletal samples. Smithsonian Contributions to Anthropology, No. 18, Washington, D.C.

1978 Human Skeletal Remains: Excavation, Analysis, Interpretation. Aldine, Chicago.

Van Gerven, D. P.
1973 Thickness and area measurements as parameters of skeletal involution of the humerus, femur, and tibia. Journal of Gerontology, 28:40-45.

Van Gerven, D. P., G. J. Armelagos, and M. H. Bartley
1969 Roentgenographic and direct measurement of femoral cortical involution in a prehistoric Mississippian population. American Journal of Physical Anthropology, 31:23-28.

Voors, A. W. and D. Metselaar
1958 The reliability of dental age as a yard-stick to assess the unknown calendar age. Tropical and Geographical Medicine, 10:175-180.

Wagenen, G. van, and C. W. Asling
1958 Roentgenographic estimation of bone age in the rhesus monkey (*Macaca mulatta*). American Journal of Anatomy, 103:163-185.

Wagenen, G. van and H. R. Catchpole
1956 Physical growth of the rhesus monkey. (*Macaca mulatta*). American Journal of Physical Anthropology, 14:245-273.

Washburn, S. C.
1943 The sequence of epiphyseal union in Old World monkeys. American Journal of Anatomy, 72:339-360.

Watts, E. S.
1980 Patterns of postnatal growth in the long bones of rhesus monkeys. Paper presented at the 49th Annual Meeting of the American Association of Physical Anthropologists, April, Niagara Falls, New York.

Watts, E. S. and J. A. Gavan
1979 Postnatal growth of chimpanzees: The problem of the adolescent spurt. American Journal of Physical Anthropology, 50:490.

Willey, C. H.
1974 Aging black bears from first pre-molar tooth sections. Journal of Wildlife Management, 38:97-100.

Wintheiser, J. G., D. A. Clauser, and N. C. Tappan
1977 Sequence of eruption of permanent teeth and epiphyseal union in three species of African monkeys. Folia Primatologica, 27:178-197.

Wolfe, L. G., F. Deinhardt, J. D. Ogden, M. R. Adams and L. E. Fisher
1975 Reproduction of wild-caught and laboratory-born marmoset species used in biomedical research (*Saguinus* sp.; *Callithrix jacchus*). Laboratory Animal Science, 25(6): 802-813.

Wu, K., K. E. Schubeck, H. M. Frost and A. R. Villaneuva
1970 Haversian bone formation rates determined by a new method in a mastadon and in human mellitus and osteoporosis. Calcified Tissue Research, 6:204-219.

APPENDICES

APPENDIX A

SKELETAL AGING BY CEMENTAL ANNULATIONS

SKELETAL AGING BY CEMENTAL ANNULATIONS

A method of skeletal age determination has been proposed for various mammals based on the counting of cemental annulations. This method has been applied to both subadult and adult individuals. It is based on the systematic and continual deposition of cementum around the roots and below the crowns of the teeth. For a variety of mammals, it has been demonstrated that the rates of deposition vary over the year giving a banded appearance, most commonly an alternating dark/light configuration (Chaplin, 1971).

Factors which have been related to the formation of the annulations by altering the metabolic rate include rutting (Low and Cowan, 1963), hibernation (Stoneberg and Jonkel, 1966), and fluctuating endocrine rhythms (Stott et al., 1981). By using pairs of annuli to represent one year's growth, accurate age estimates have been made for the red fox (Allen, 1974), the squirrel (Adams and Watkins, 1967), the bear (Marks and Ericksen, 1966; Willey, 1974), and the deer (Gilbert, 1966).

Recently, Stott, Sis and Levy (1980) examined the use of cemental annulations for determining age in the common marmoset, *Callithrix jacchus*. This study represents the first attempt at using this method as an aging criterion for any nonhuman primate.

In their study, the teeth of ten marmosets of known age were sectioned, stained, and subjected to histological observation. Annulations were counted in pairs consisting of one dark and one light band. To correct for the age period prior to initial cementum deposition, a correction factor was added to the counts based on standards documented for the dental development in this species (Johnston et al., 1970; Levy et al., 1972).

Their results indicate strong agreement between the actual ages of the marmosets and the estimated ages based on annulation counts. In all cases, accurate assignment was made to within one-half year.

Although the potential for using cemental annulations as a parameter for estimating age in other nonhuman primates appears good, a number of wildlife biologists have pointed out certain limitations to this method. The major limitation involves the ability to identify the true annulation structure. Within the dental section, evaluation of the normal annulation pattern may be complicated by extraneous features such as false, split, and compound annuli (Rice, 1980). The mistaken inclusion of any of these features into the annulation count will lead to the overestimation of actual age. In addition, Adams and Watkins (1967) have demonstrated that for squirrels, the annuli become less distinct with advancing age and accurate age estimation could not be made for individuals older than four years. Since the oldest marmoset included in Stott's et al. (1980) study was approximately six years old, the potential for using annulations to accurately estimate age in older adults has not been demonstrated.

Although limitations in this method have been reported, it remains a potentially beneficial criterion for estimating age in nonhuman primates and warrants further investigation. At this time, Regina Pittman-Sharma at The University of Tennessee, Knoxville is investigating the pattern of cementum deposition in the tamarin species, *S. fuscicollis.*

APPENDIX B

TABLES OF DENTAL ERUPTION

Table 28. Dental Eruption by Age for *Saguinus fuscicollis*

Age In Days	Sex	Deciduous												Permanent															
		I_1	I^1	I_2	I^2	C_1	C^1	P_2	P^2	P_3	P^3	P_4	P^4	M_1	M^1	I_1	I^1	I_2	I^2	M_2	M^2	P_4	P^4	P_2	P^2	P_3	P^3	C_1	C^1
0001	F	2	2	2	2	2	2	1	1	1	1	1	1	1	1	1	1	1	1	1	1	1	1	1	1	1	1	1	1
0001	F	2	2	2	2	2	2	1	1	1	1	1	1	1	1	1	1	1	1	1	1	1	1	1	1	1	1	1	1
0001	M	2	2	2	2	2	2	1	1	1	1	1	1	1	1	1	1	1	1	1	1	1	1	1	1	1	1	1	1
0001	F	2	2	2	2	2	2	1	1	1	1	1	1	1	1	1	1	1	1	1	1	1	1	1	1	1	1	1	1
0001	M	2	2	2	2	2	2	1	1	1	1	1	1	1	1	1	1	1	1	1	1	1	1	1	1	1	1	1	1
0001	M	2	2	2	2	2	2	2	1	1	1	1	1	1	1	1	1	1	1	1	1	1	1	1	1	1	1	1	1
0001	F	2	2	2	2	2	2	2	1	1	1	1	1	1	1	1	1	1	1	1	1	1	1	1	1	1	1	1	1
0002	F	2	2	2	2	1	1	1	1	1	1	1	1	1	1	1	1	1	1	1	1	1	1	1	1	1	1	1	1
0002	M	2	2	2	2	2	2	1	1	1	1	1	1	1	1	1	1	1	1	1	1	1	1	1	1	1	1	1	1
0002	M	2	2	2	2	2	2	2	1	1	1	1	1	1	1	1	1	1	1	1	1	1	1	1	1	1	1	1	1
0003	M	2	2	2	2	2	2	1	1	1	1	1	1	1	1	1	1	1	1	1	1	1	1	1	1	1	1	1	1
0004	F	2	2	2	2	2	2	1	1	1	1	1	1	1	1	1	1	1	1	1	1	1	1	1	1	1	1	1	1
0005	M	2	2	2	2	2	2	1	1	1	1	1	1	1	1	1	1	1	1	1	1	1	1	1	1	1	1	1	1
0005	M	2	2	2	2	2	2	1	1	1	1	1	1	1	1	1	1	1	1	1	1	1	1	1	1	1	1	1	1
0007	F	2	2	2	2	2	2	1	1	1	1	1	1	1	1	1	1	1	1	1	1	1	1	1	1	1	1	1	1
0008	F	2	2	2	2	2	2	2	1	1	1	1	1	1	1	1	1	1	1	1	1	1	1	1	1	1	1	1	1
0008	M	2	2	2	2	2	2	2	1	1	1	1	1	1	1	1	1	1	1	1	1	1	1	1	1	1	1	1	1
0011	F	2	2	2	2	2	2	1	1	1	1	1	1	1	1	1	1	1	1	1	1	1	1	1	1	1	1	1	1
0011	F	2	2	2	2	2	2	2	1	1	1	1	1	1	1	1	1	1	1	1	1	1	1	1	1	1	1	1	1
0013	F	2	2	2	2	2	2	2	1	1	1	1	1	1	1	1	1	1	1	1	1	1	1	1	1	1	1	1	1
0013	F	2	2	2	2	2	2	2	1	1	1	1	1	1	1	1	1	1	1	1	1	1	1	1	1	1	1	1	1
0017	F	2	2	2	2	2	2	2	2	1	1	1	1	1	1	1	1	1	1	1	1	1	1	1	1	1	1	1	1
0034	F	2	2	2	2	2	2	2	2	2	2	1	1	1	1	1	1	1	1	1	1	1	1	1	1	1	1	1	1
0037	F	2	2	2	2	2	2	2	2	2	2	2	1	1	1	1	1	1	1	1	1	1	1	1	1	1	1	1	1
0039	F	2	2	2	2	2	2	2	2	2	2	2	2	1	1	1	1	1	1	1	1	1	1	1	1	1	1	1	1
0043	F	2	2	2	2	2	2	2	2	2	2	2	1	1	1	1	1	1	1	1	1	1	1	1	1	1	1	1	1
0046	F	2	2	2	2	2	2	2	2	2	2	2	2	1	1	1	1	1	1	1	1	1	1	1	1	1	1	1	1
0046	M	2	2	2	2	2	2	2	2	2	2	2	2	1	1	1	1	1	1	1	1	1	1	1	1	1	1	1	1
0050	M	2	2	2	2	2	2	2	2	2	2	2	2	1	1	1	1	1	1	1	1	1	1	1	1	1	1	1	1

Table 28 (continued)

Age In Days	Sex	Deciduous I_1	I^1	I_2	I^2	C_1	C^1	P_2	P^2	P_3	P^3	P_4	P^4	Permanent M_1	M^1	I_1	I^1	I_2	I^2	M_2	M^2	P_4	P^4	P_2	P^2	P_3	P^3	C_1	C^1
0051	M	2	2	2	2	2	2	2	2	2	2	1	1	1	1	1	1	1	1	1	1	1	1	1	1	1	1	1	1
0056	M	2	2	2	2	2	2	2	2	2	2	2	2	1	1	1	1	1	1	1	1	1	1	1	1	1	1	1	1
0064	M	2	2	2	2	2	2	2	2	2	2	2	2	1	1	1	1	1	1	1	1	1	1	1	1	1	1	1	1
0065	F	2	2	2	2	2	2	2	2	2	2	2	1	1	1	1	1	1	1	1	1	1	1	1	1	1	1	1	1
0082	F	2	2	2	2	2	2	2	2	2	2	2	2	1	1	1	1	1	1	1	1	1	1	1	1	1	1	1	1
0083	M	2	2	2	2	2	2	2	2	2	2	2	2	1	1	1	1	1	1	1	1	1	1	1	1	1	1	1	1
0096	M	2	2	2	2	2	2	2	2	2	2	2	2	1	1	1	1	1	1	1	1	1	1	1	1	1	1	1	1
0103	F	2	2	2	2	2	2	2	2	2	2	2	2	1	1	1	1	1	1	1	1	1	1	1	1	1	1	1	1
0105	F	2	2	2	2	2	2	2	2	2	2	2	2	1	1	1	1	1	1	1	1	1	1	1	1	1	1	1	1
0110	F	2	2	2	2	2	2	2	2	2	2	2	2	1	1	1	1	1	1	1	1	1	1	1	1	1	1	1	1
0113	F	2	2	2	2	2	2	2	2	2	2	2	2	2	1	1	1	1	1	1	1	1	1	1	1	1	1	1	1
0124	M	2	2	2	2	2	2	2	2	2	2	2	2	2	2	1	1	1	1	1	1	1	1	1	1	1	1	1	1
0131	F	2	2	2	2	2	2	2	2	2	2	2	2	1	1	1	1	1	1	1	1	1	1	1	1	1	1	1	1
0133	F	2	2	2	2	2	2	2	2	2	2	2	2	1	1	1	1	1	1	1	1	1	1	1	1	1	1	1	1
0134	F	2	2	2	2	2	2	2	2	2	2	2	2	2	1	1	1	1	1	1	1	1	1	1	1	1	1	1	1
0141	M	2	2	2	2	2	2	2	2	2	2	2	2	2	1	1	1	1	1	1	1	1	1	1	1	1	1	1	1
0142	M	2	2	2	2	2	2	2	2	2	2	2	2	2	1	1	1	1	1	1	1	1	1	1	1	1	1	1	1
0144	F	2	2	2	2	2	2	2	2	2	2	2	2	1	1	1	1	1	1	1	1	1	1	1	1	1	1	1	1
0146	F	-	-	2	2	2	2	2	2	2	2	2	2	2	2	2	2	1	1	1	1	1	1	1	1	1	1	1	1
0153	M	-	-	-	2	2	2	2	2	2	2	2	2	2	2	2	2	1	1	1	1	1	1	1	1	1	1	1	1
0155	M	2	2	2	2	2	2	2	2	2	2	2	2	1	1	1	1	1	1	1	1	1	1	1	1	1	1	1	1
0163	F	-	-	2	2	2	2	2	2	2	2	2	2	2	2	2	2	1	1	1	1	1	1	1	1	1	1	1	1
0206	F	-	-	-	-	2	2	2	2	2	2	-	-	2	2	2	2	2	2	2	2	2	2	1	1	1	1	1	1
0212	M	-	-	-	-	2	2	2	2	2	2	2	2	2	2	2	2	2	2	1	1	1	1	1	1	1	1	1	1
0219	M	-	-	-	-	2	2	-	2	2	-	-	-	2	2	2	2	2	2	2	2	2	2	1	1	1	1	1	1
0224	F	-	-	-	-	2	2	-	-	-	-	-	-	2	2	2	2	2	2	2	2	2	2	2	2	1	1	1	1
0234	M	-	-	-	-	2	2	2	2	2	2	-	2	2	2	2	2	2	2	2	2	1	1	1	1	1	1	1	1
0260	M	-	-	-	-	2	2	-	-	-	-	-	-	2	2	2	2	2	2	2	2	2	1	2	1	2	1	1	1
0267	M	-	-	-	-	2	2	2	2	2	2	2	2	2	2	2	2	2	2	2	1	1	1	1	1	1	1	1	1

Table 28 (continued)

Age In Days	Sex	Deciduous												Permanent															
		I_1	I^1	I_2	I^2	C_1	C^1	P_2	P^2	P_3	P^3	P_4	P^4	M_1	M^1	I_1	I^1	I_2	I^2	M_2	M^2	P_4	P^4	P_2	P^2	P_3	P^3	C_1	C^1
0273	F	-	-	-	-	2	2	-	-	-	-	-	-	2	2	2	2	2	2	2	2	2	2	2	2	2	2	1	1
0312	M	-	-	-	-	-	-	-	-	-	-	-	-	2	2	2	2	2	2	2	2	2	2	2	2	2	2	2	2
0333	F	-	-	-	-	-	-	-	-	-	-	-	-	2	2	2	2	2	2	2	2	2	2	2	2	2	2	2	2
0354	F	-	-	-	-	-	-	-	-	-	-	-	-	2	2	2	2	2	2	2	2	2	2	2	2	2	2	2	2

1 = Tooth not erupted. 2 = Tooth erupted. - Indicates replaced deciduous tooth.

Table 29. Dental Eruption by Age for *Saguinus oedipus*

Age In Days	Sex	Deciduous												Permanent															
		I_1	I^1	I_2	I^2	C_1	C^1	P_2	P^2	P_3	P^3	P_4	P^4	M_1	M^1	I_1	I^1	I_2	I^2	M_2	M^2	P_4	P^4	P_2	P^2	P^3	P_3	C_1	C^1
0000	F	1	1	1	1	1	1	1	1	1	1	1	1	1	1	1	1	1	1	1	1	1	1	1	1	1	1	1	1
0001	M	1	1	1	1	1	1	1	1	1	1	1	1	1	1	1	1	1	1	1	1	1	1	1	1	1	1	1	1
0001	M	1	1	1	1	1	1	1	1	1	1	1	1	1	1	1	1	1	1	1	1	1	1	1	1	1	1	1	1
0001	F	2	1	2	1	1	1	1	1	1	1	1	1	1	1	1	1	1	1	1	1	1	1	1	1	1	1	1	1
0001	M	2	2	2	1	1	1	1	1	1	1	1	1	1	1	1	1	1	1	1	1	1	1	1	1	1	1	1	1
0001	F	2	2	2	1	1	1	1	1	1	1	1	1	1	1	1	1	1	1	1	1	1	1	1	1	1	1	1	1
0001	F	2	2	2	2	1	1	1	1	1	1	1	1	1	1	1	1	1	1	1	1	1	1	1	1	1	1	1	1
0001	M	2	2	2	2	1	2	1	2	1	1	1	1	1	1	1	1	1	1	1	1	1	1	1	1	1	1	1	1
0004	M	2	2	2	2	1	1	1	1	1	1	1	1	1	1	1	1	1	1	1	1	1	1	1	1	1	1	1	1
0004	M	2	2	2	2	1	1	1	1	1	1	1	1	1	1	1	1	1	1	1	1	1	1	1	1	1	1	1	1
0005	?	2	2	2	2	1	1	1	1	1	1	1	1	1	1	1	1	1	1	1	1	1	1	1	1	1	1	1	1
0007	M	2	2	2	2	2	1	1	1	1	1	1	1	1	1	1	1	1	1	1	1	1	1	1	1	1	1	1	1
0008	M	2	2	2	2	2	2	1	1	1	1	1	1	1	1	1	1	1	1	1	1	1	1	1	1	1	1	1	1
0010	M	2	2	2	2	1	1	1	1	1	1	1	1	1	1	1	1	1	1	1	1	1	1	1	1	1	1	1	1
0011	M	2	2	2	2	1	1	1	1	1	1	1	1	1	1	1	1	1	1	1	1	1	1	1	1	1	1	1	1
0012	F	2	2	2	2	1	1	1	1	1	1	1	1	1	1	1	1	1	1	1	1	1	1	1	1	1	1	1	1
0012	M	2	2	2	2	2	1	1	1	1	1	1	1	1	1	1	1	1	1	1	1	1	1	1	1	1	1	1	1
0016	M	2	2	2	2	2	2	1	1	1	1	1	1	1	1	1	1	1	1	1	1	1	1	1	1	1	1	1	1
0095	F	2	2	2	2	2	2	2	2	2	2	2	2	1	1	1	1	1	1	1	1	1	1	1	1	1	1	1	1
0095	M	2	2	2	2	2	2	2	2	2	2	2	2	1	1	1	1	1	1	1	1	1	1	1	1	1	1	1	1
0098	M	-	2	-	2	2	2	2	2	2	2	2	2	1	1	1	1	1	1	1	1	1	1	1	1	1	1	1	1
0115	?	2	2	2	2	2	2	2	2	2	2	2	2	1	1	1	1	1	1	1	1	1	1	1	1	1	1	1	1
0115	M	2	2	2	2	2	2	2	2	2	2	2	2	2	2	1	1	1	1	1	1	1	1	1	1	1	1	1	1
0142	F	2	2	2	2	2	2	2	2	2	2	2	2	1	1	1	1	1	1	1	1	1	1	1	1	1	1	1	1
0218	M	-	-	-	2	2	2	2	2	2	2	2	2	2	2	2	2	2	1	1	1	1	1	1	1	1	1	1	1
0232	F	-	-	-	-	2	2	2	2	2	2	2	2	2	2	2	2	2	1	1	1	1	1	1	1	1	1	1	1
0297	M	-	-	-	-	2	2	-	-	-	-	-	-	2	2	2	2	2	2	2	2	2	2	2	2	2	1	1	1

1 = Tooth not erupted. 2 = Tooth erupted. - Indicates replaced deciduous tooth.

APPENDIX C

TABLES AND FIGURES OF LONG BONE GROWTH

Table 30. Long Bone Length Measurements for Growth Analysis of *Saguinus fuscicollis* (in millimeters)

Age[a]	Sex	Humerus	Radius	Ulna	Femur	Tibia	Fibula	Ilium
0000	M	15.2	14.4	16.2	15.3	16.3	16.1	06.2
0002	F	13.8	13.0	14.3	13.3	14.1	13.7	05.9
0002	M	12.7	12.3	13.5	12.3	13.4	12.8	05.5
0003	F	13.2	12.7	13.7	13.0	14.1	13.4	06.1
0003	F	15.3	15.1	16.8	15.7	17.2	16.9	06.5
0003	M	15.0	14.6	16.2	15.2	16.0	15.9	06.2
0003	M	15.5	15.3	16.8	15.6	17.1	16.5	06.7
0005	F	16.2	14.9	16.9	16.2	16.8	16.6	06.7
0008	F	16.9	16.7	18.6	17.5	18.7	17.9	07.6
0009	F	16.7	15.6	17.7	17.4	18.4	17.5	06.9
0015	F	14.9	14.8	16.4	15.5	16.4	15.5	06.4
0017	F	17.8	17.0	19.2	18.9	19.9	18.5	07.9
0032	M	19.6	18.4	21.3	21.1	21.7	20.4	08.6
0043	F	23.3	22.0	25.4	27.4	28.4	26.3	11.4
0059	F	24.7	23.5	26.5	36.7	31.0	29.0	12.2
0062	F	24.5	22.6	25.5	27.5	28.7	27.0	11.7
0064	F	21.6	20.0	22.9	23.2	23.5	22.9	08.9
0066	F	25.0	22.1	25.4	29.4	29.4	27.5	11.9
0072	M	28.3	25.9	29.0	33.2	34.2	32.2	13.8
0083	M	24.3	22.8	26.5	28.5	29.0	27.4	11.4
0095	M	30.2 D	25.9	29.6	--	34.1	31.9	14.4
0097	F	27.2	24.2	28.0	--	32.5	30.4	13.8
0099	M	25.0	21.9	24.9	--	29.5	27.2	11.6
0107	M	27.8	26.1	29.5	33.2	35.7	32.8	14.2
0108	F	27.9	24.3	28.0	32.3	32.5	29.8	13.2
0110	M	33.3 D	29.5	32.6	36.4	39.6	37.4	16.1
0114	M	31.9 D	28.0	32.6	--	38.4	35.9	15.5
0117	F	31.0 D	26.7	30.9	--	36.4	33.6	14.4
0119	F	33.5 D	29.2	33.6	38.0	40.2	37.7	17.2
0120	F	30.0 D	26.7	29.5	34.0	36.3	33.3	15.0
0122	F	39.5 D	34.5	39.9	44.6	46.5	43.0	20.3

Table 30 (continued)

Age[a]	Sex	Humerus	Radius	Ulna	Femur	Tibia	Fibula	Ilium
0130	F	32.4 D	28.5	32.2	37.3	39.2	36.3	16.7
0133	M	30.9	27.8	31.7	35.4	38.4	35.9	15.5
0135	M	37.7 D	32.9	37.8	43.5	44.2	41.5	18.0
0137	M	30.9 D	26.7	30.8	34.8	36.0	33.0	14.4
0138	F	30.1 D	26.2	30.3	33.8	35.6	33.2	14.0
0140	F	32.1 D	27.3	31.4	36.4	38.2	35.5	16.2
0156	?	36.9 D	32.4	37.5	42.0	45.3	42.6	19.5
0167	M	30.9 D	29.0	32.2	--	38.0	35.3	15.5
0171	F	33.1 D	27.6	31.7	37.1	38.0	35.2	16.9
0172	M	39.4 D	33.6	38.4	44.3	45.2	43.4	18.1
0175	M	35.4 D	31.9	37.1	41.4	43.3	41.6	19.8
0183	F	37.9 D	32.7	38.1	45.1	48.1	43.8	19.9
0201	M	38.9 D	34.5	39.9	44.7	47.1	44.1	22.1
0204	F	38.0 D	32.8	37.4	42.5	42.5	39.8	18.0
0216	F	35.3 D	31.2	34.7	--	44.5	41.7	19.0
0225	F	38.7 D	33.2	38.0	--	44.0	41.1	18.3
0245	M	37.9 D	34.0 D	38.3 P	--	45.5	42.9	20.1
0269	M	39.1 D	33.0	38.0	43.4	45.2	41.6	18.8
0296	F	36.2 D	31.5	36.7	42.8	43.3	40.1	18.9
0441	M	40.2 D	36.3	41.2	--	47.8	45.6	21.6
0481	F	52.3 D,P	47.4 D,P	54.6 D,P	63.5 D,P	66.1 D,P	62.2 D,P	27.2
0493	F	47.6 D,P	41.6 P	46.6 P	55.5 P	58.4 D	56.5 D	26.1
0574	M	46.1 D,P	42.9 D,P	49.5 D,P	58.2 D,P	61.5 D,P	58.2 D,P	26.2
0586	F	49.3 D,P	45.0 P	50.9 P	57.8 P	64.3 D,P	59.4 D	26.3
0638	F	49.6 D,P	46.7 D,P	52.9 D,P	--	--	--	26.5
0657	F	55.0 D,P	49.1 D,P	55.0 P	67.1 D,P	67.7 D,P	64.1 D,P	28.0
0676	M	54.7 D,P	51.3 D,P	57.8 D,P	66.5 D,P	69.6 D,P	66.4 D,P	28.0
0677	M	51.1 D,P	48.0 D,P	54.8 D,P	62.8 D,P	64.1 D,P	60.4 D,P	27.5

[a] Age in days.

D = Distal epiphysis included in measurement. P = Proximal epiphysis included in measurement.

Table 31. Long Bone Length Measurements for Growth Analysis of *Saguinus oedipus* (in millimeters)

Age[a]	Sex	Humerus	Radius	Ulna	Femur	Tibia	Fibula	Ilium
0000	M	14.0	12.9	14.2	14.5	15.2	14.6	06.7
0000	M	11.3	10.0	11.5	11.4	11.8	10.8	05.3
0002	F	14.5	13.5	15.2	15.3	16.2	15.7	06.9
0002	M	15.5	13.9	15.5	16.2	16.4	15.5	07.2
0003	M	15.7	14.3	16.0	16.7	17.2	16.7	07.5
0003	F	15.0	13.1	14.2	14.7	15.2	14.3	06.7
0004	M	15.2	14.2	15.4	16.1	16.8	16.8	07.1
0004	M	16.2	15.8	16.3	16.8	17.2	16.9	07.7
0004	F	16.1	13.7	15.1	15.8	16.3	15.7	07.2
0011	M	17.8	16.3	17.8	18.2	19.2	18.5	08.1
0017	M	17.4	15.0	17.0	18.5	18.3	17.1	08.0
0026	M	20.6	18.0	20.0	22.4	22.2	21.0	09.5
0057	M	24.8	20.5	23.6	--	27.6	25.7	12.0
0081	M	25.6	22.5	25.7	29.1	28.9	27.6	12.8
0137	M	38.1 D	31.6	36.5	43.8	44.3	42.4	19.5
0138	F	39.5 D	33.6	38.1	45.7	47.0	44.3	21.4
0208	M	42.1 D	35.9	41.9	50.8	50.9	48.3	22.5
0213	M	36.3 D	30.6	35.8	43.3	46.0	43.1	18.8
0218	M	36.1 D	30.1	34.5	41.8	41.5	40.0	18.0
0254	M	44.8 D	36.8	43.8 P	52.3	55.2	52.0	24.0
0268	F	41.6 D,P	33.3	39.1	47.2	46.4	44.1	22.1
0316	M	41.0 D	35.0	40.1	50.6	51.8	49.0	23.4
0316	F	41.5 D	35.4	41.4	49.8	50.8	48.7	23.2
0410	M	46.3 D,P	41.0 P	47.0 P	57.0 P	54.6	52.5	26.7
0455	F	41.9 D	37.8 P	43.2	52.7	54.0	51.8	24.7
0455	M	44.1 D	39.2 P	46.1 P	56.2	57.1	53.8	24.8
0463	F	42.3 D	36.9 P	41.8	53.3	51.8	49.2	23.4
0712	F	52.4 D,P	45.7 D,P	52.4 D,P	66.3 D,P	65.6 D,P	63.0 D,P	28.5
0722	M	48.3 D,P	41.4 P	48.0 P	62.4 D,P	63.7 D,P	58.1 D	26.3
0730	F	52.7 D,P	46.6 D,P	53.4 D,P	65.4 D,P	67.2 D,P	63.2 D,P	29.0
0732	M	48.4 D,P	43.0 D,P	50.6 D,P	63.6 D,P	65.2 D,P	61.5 D,P	27.3
0757	M	47.4 D,P	42.8 D,P	50.2 D,P	61.8 D,P	62.8 D,P	59.5 D,P	28.4
0768	F	47.5 D,P	44.1 D,P	50.8 D,P	62.6 D,P	61.9 D,P	58.6 D,P	29.8

[a] Age in days.

D = Distal epiphysis included in measurement. P = Proximal epiphysis included in measurement.

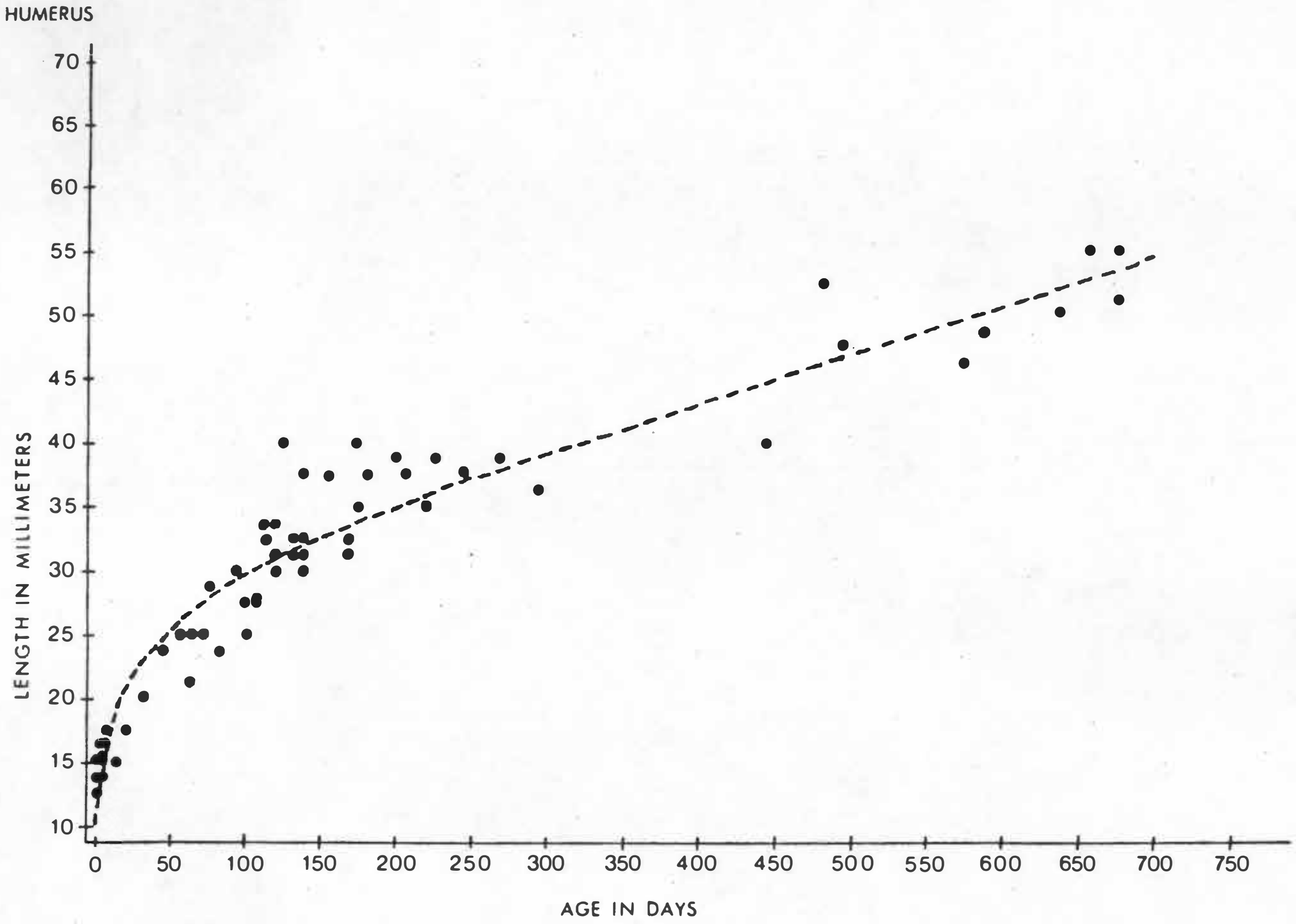

Figure 20. Bivariate plot illustrating the chronology of long bone growth for *Saguinus fuscicollis*—humerus.

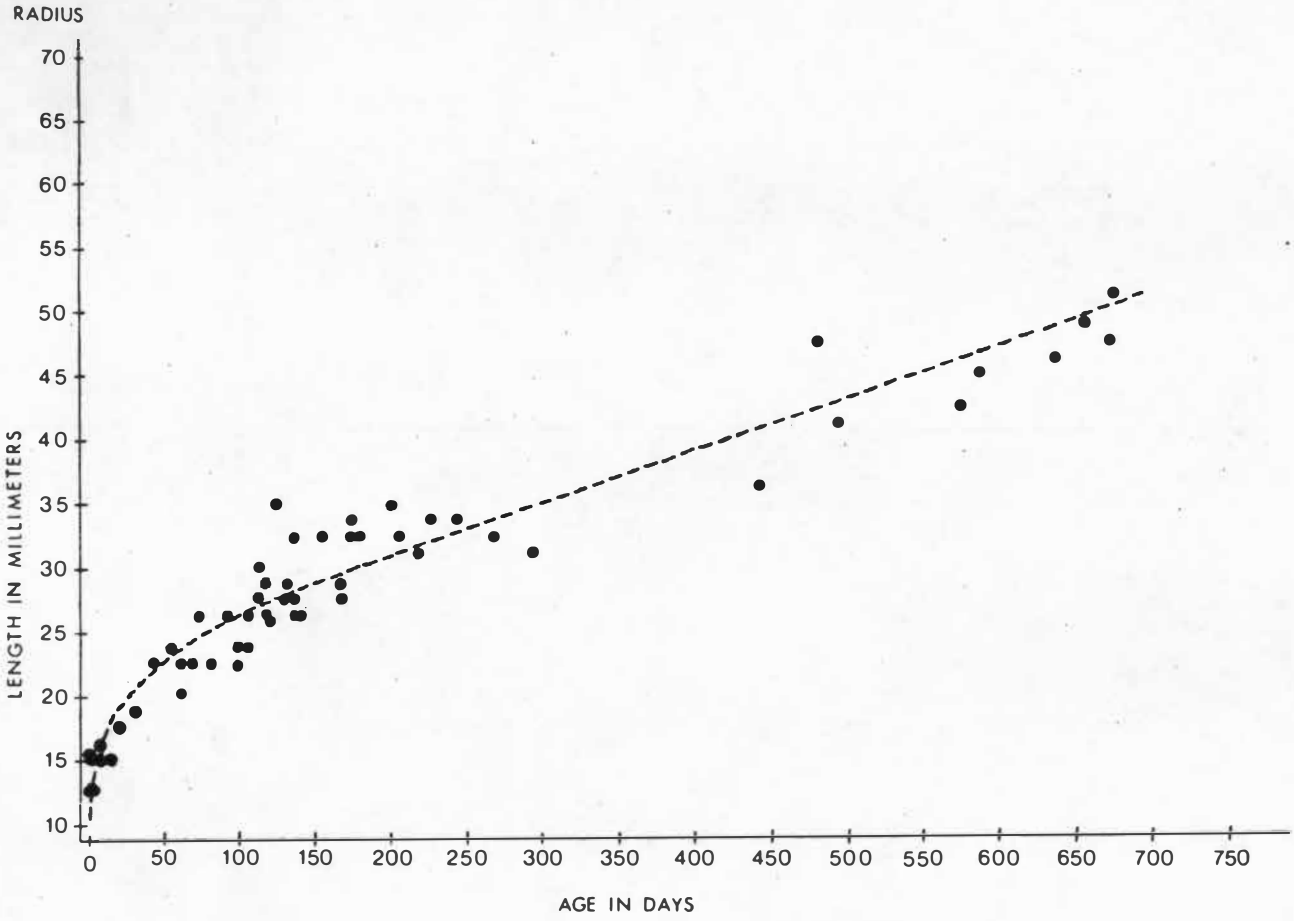

Figure 21. Bivariate plot illustrating the chronology of long bone growth for *Saguinus fuscicollis*—radius.

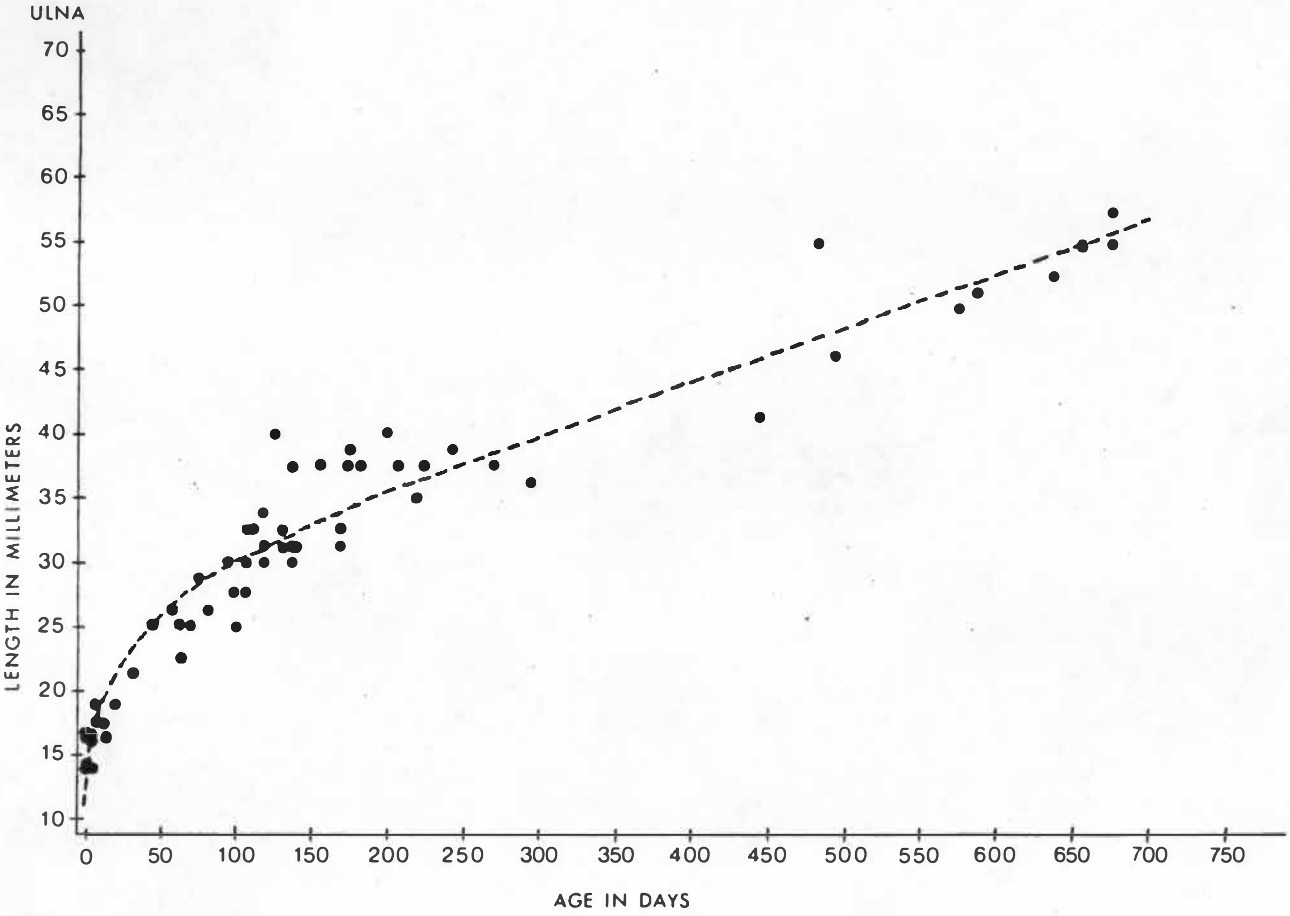

Figure 22. Bivariate plot illustrating the chronology of long bone growth for *Saguinus fuscicollis*—ulna.

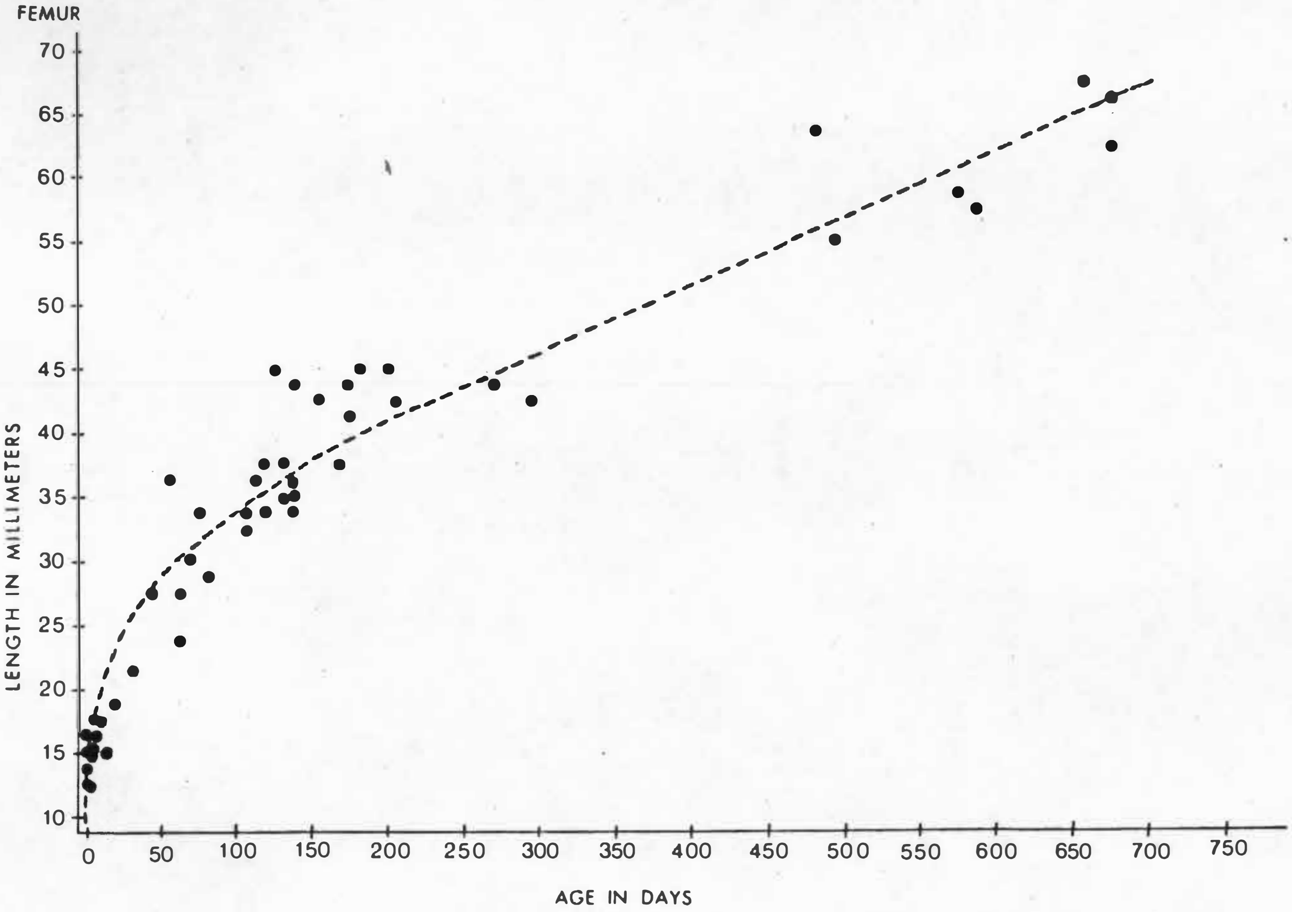

Figure 23. Bivariate plot illustrating the chronology of long bone growth for *Saguinus fuscicollis*—femur.

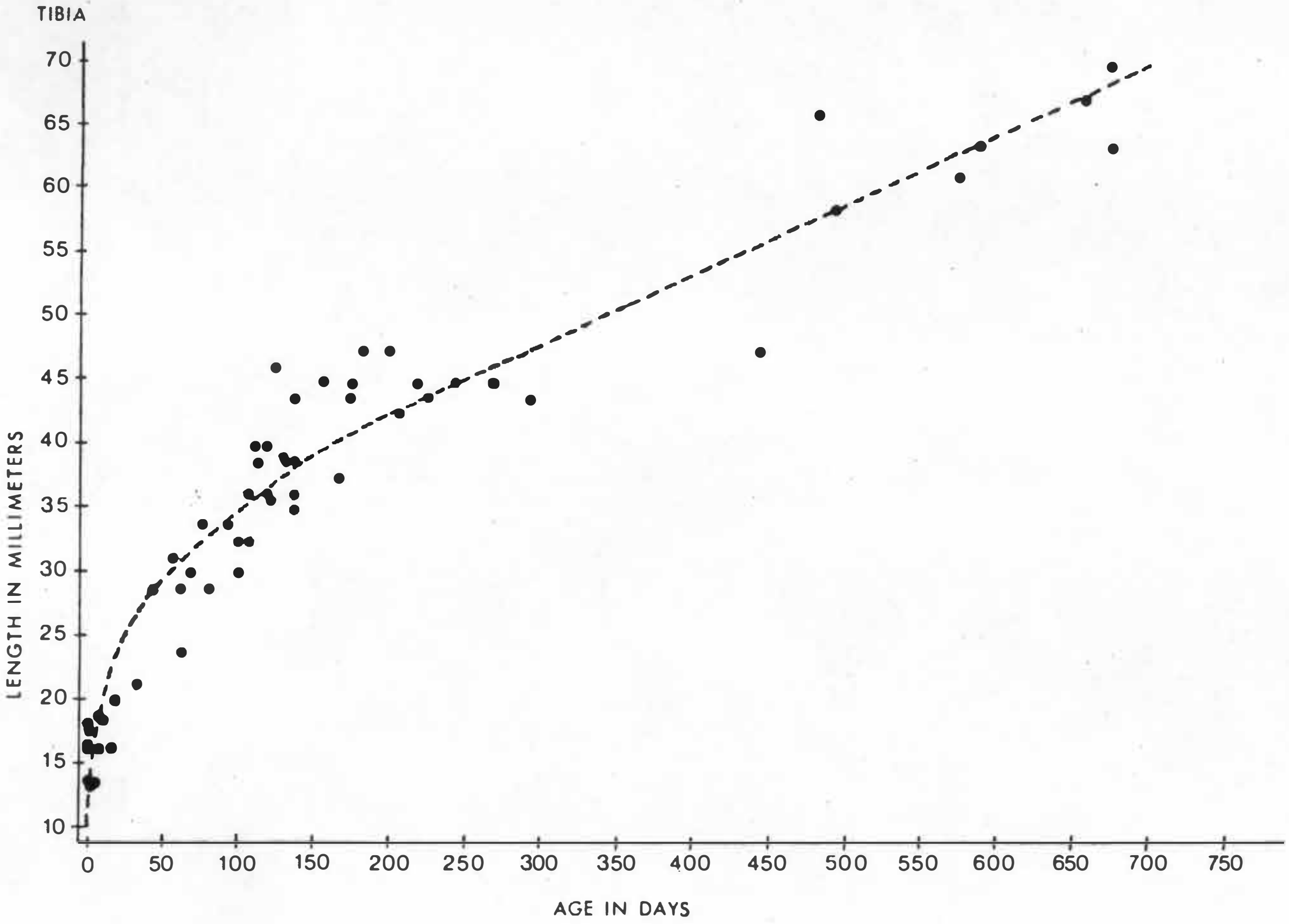

Figure 24. Bivariate plot illustrating the chronology of long bone growth for *Saguinus fuscicollis*—tibia.

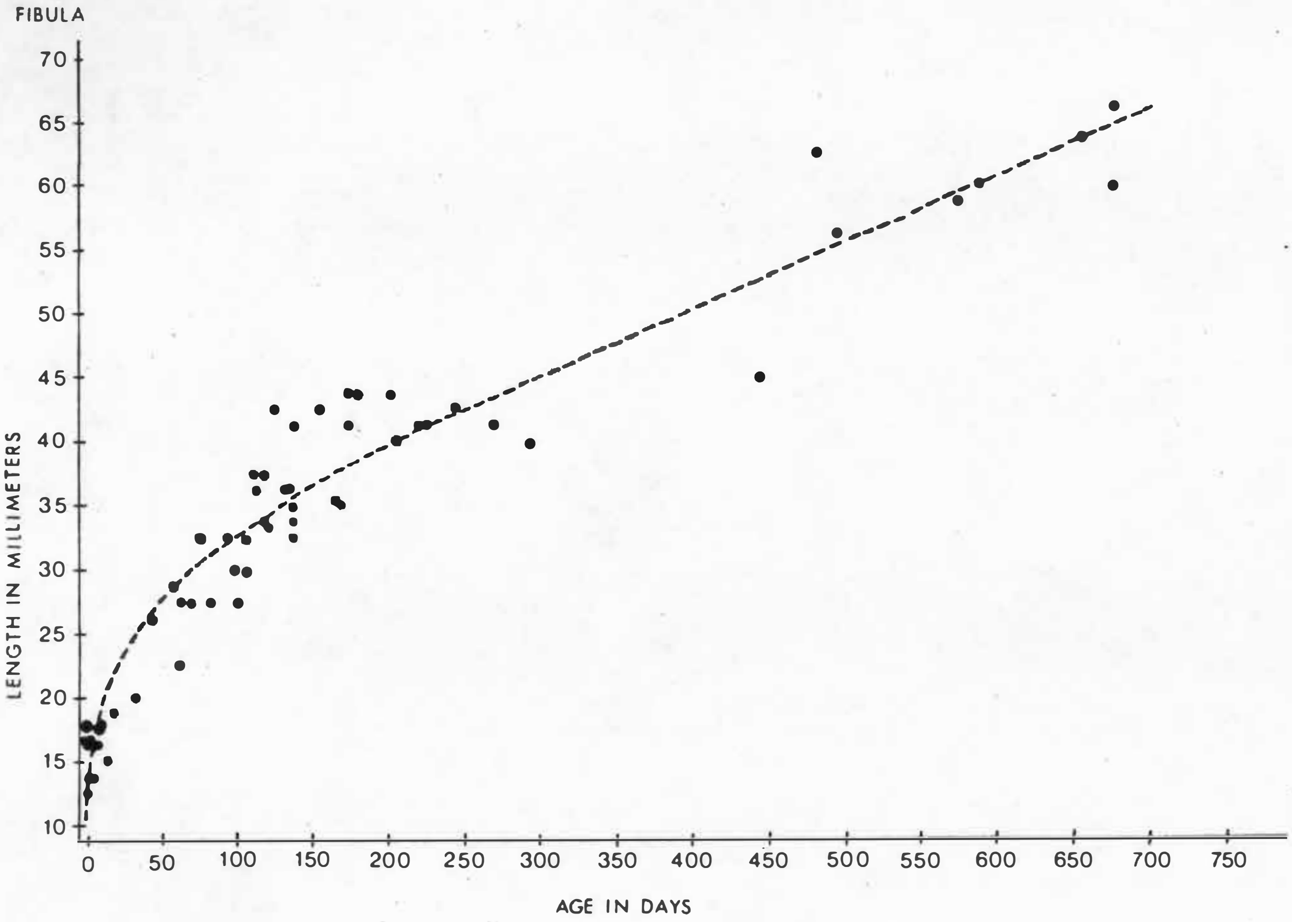

Figure 25. Bivariate plot illustrating the chronology of long bone growth for *Saguinus fuscicollis*—fibula.

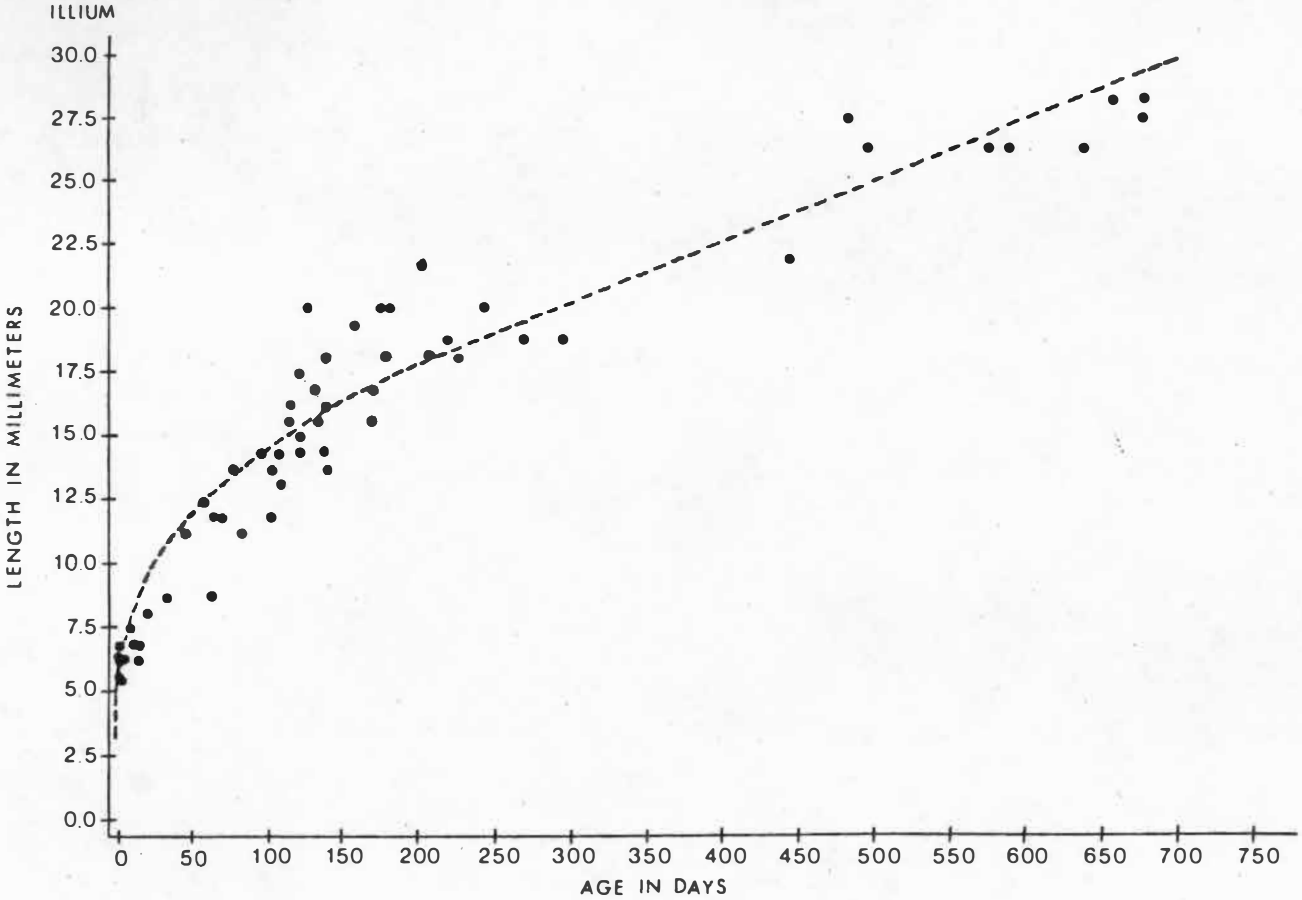

Figure 26. Bivariate plot illustrating the chronology of long bone growth for *Saguinus fuscicollis*—ilium.

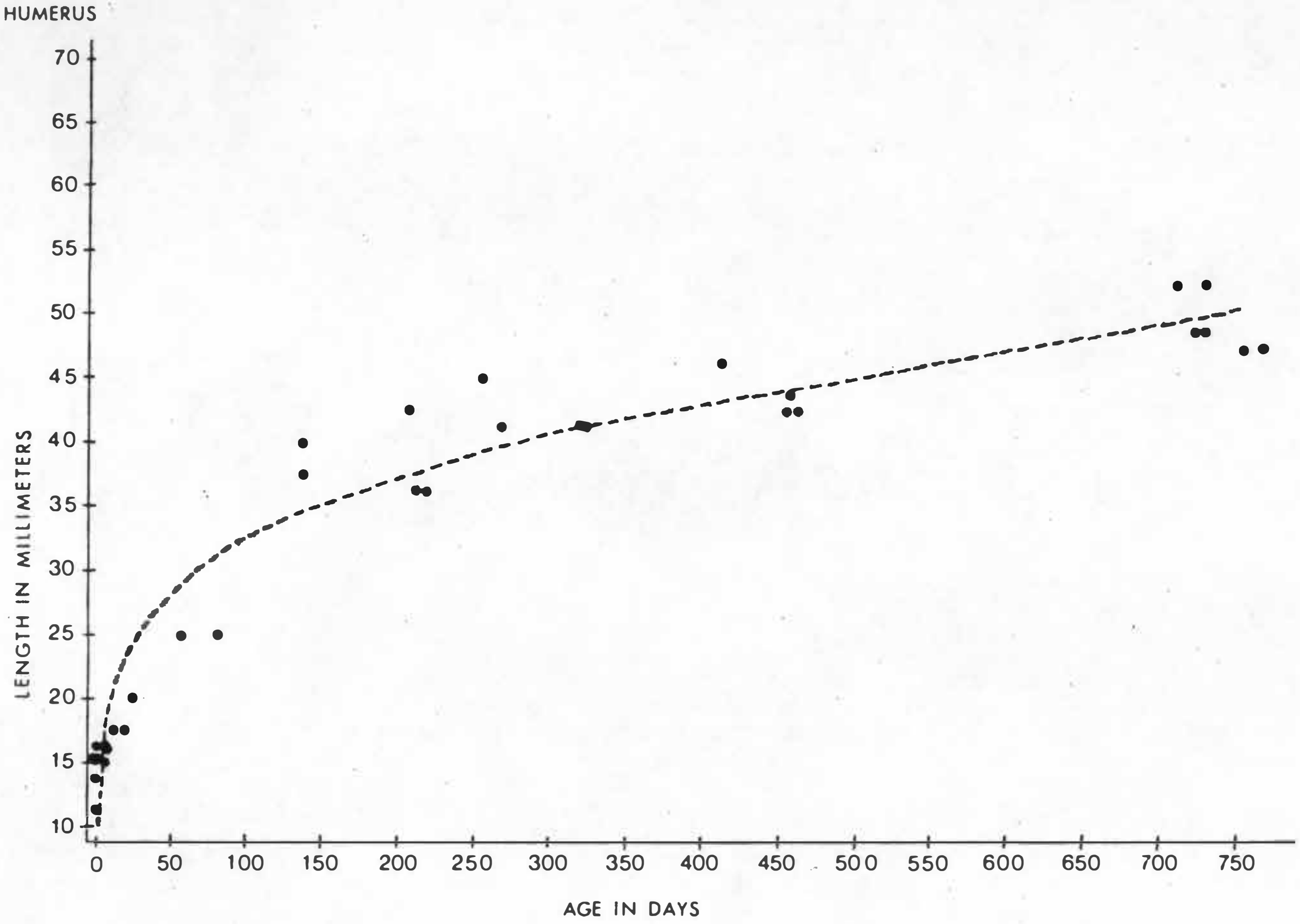

Figure 27. Bivariate plot illustrating the chronology of long bone growth in *Saguinus oedipus*—humerus.

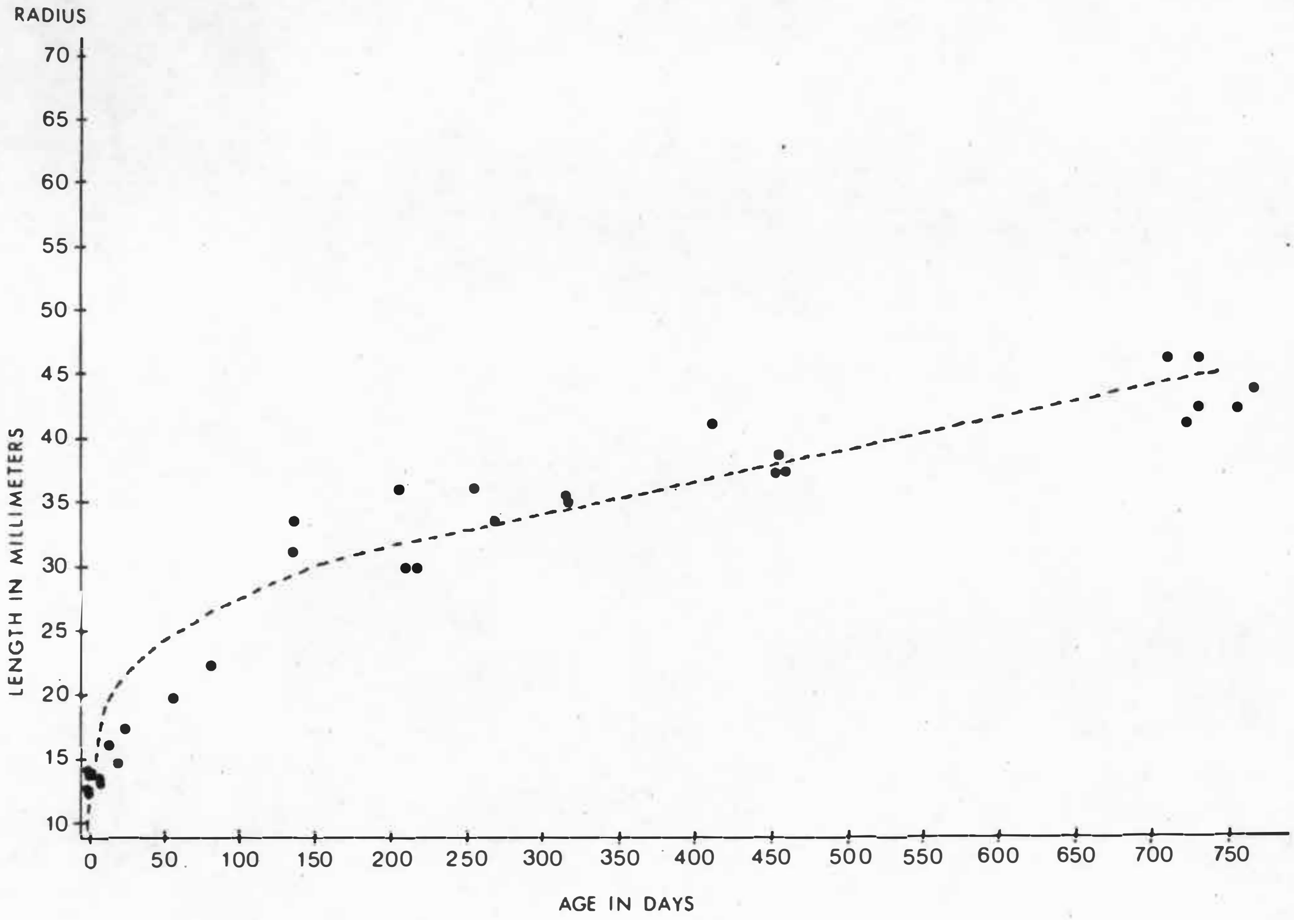

Figure 28. Bivariate plot illustrating the chronology of long bone growth in *Saguinus oedipus*—radius.

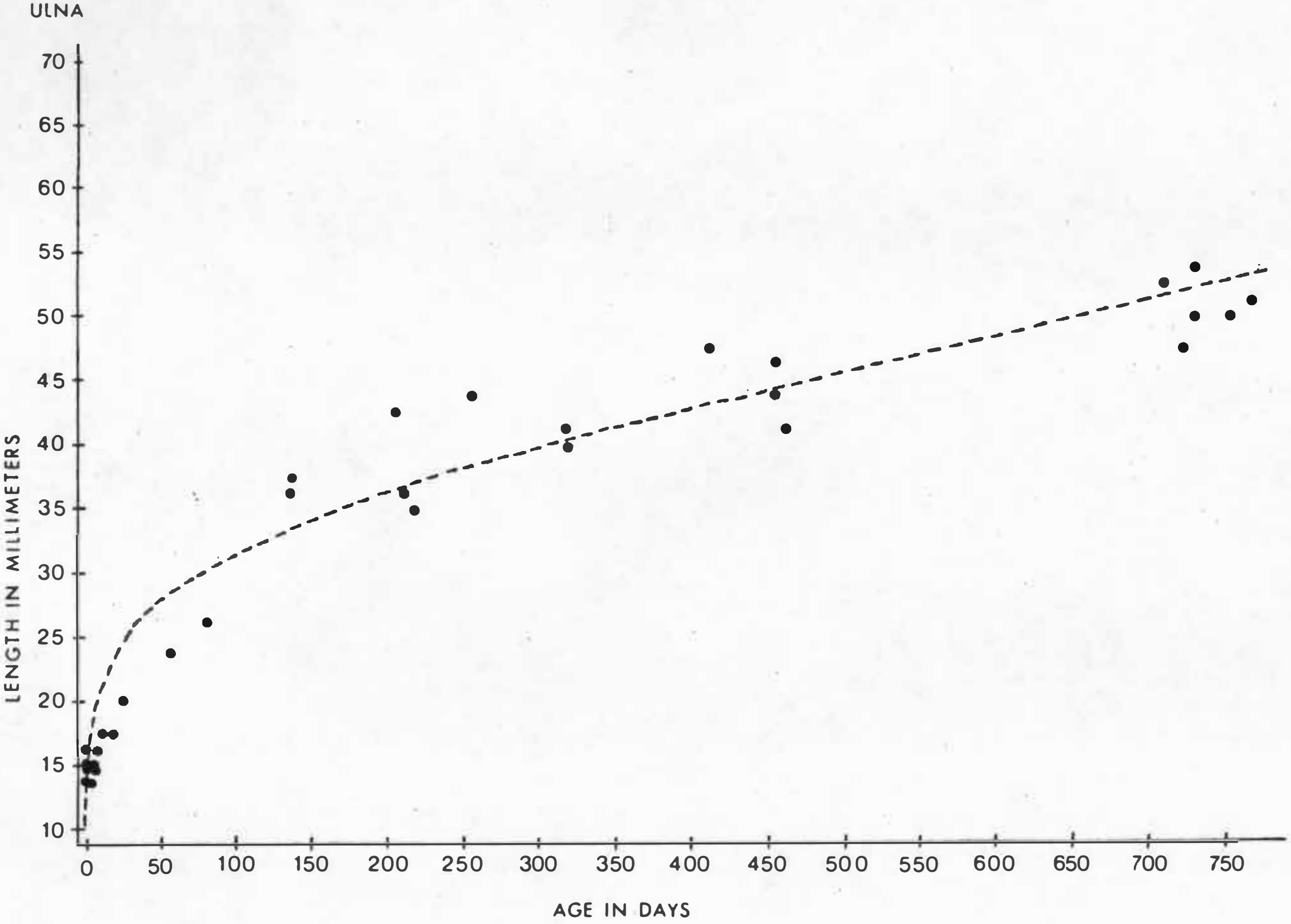

Figure 29. Bivariate plot illustrating the chronology of long bone growth in *Saguinus oedipus*—ulna.

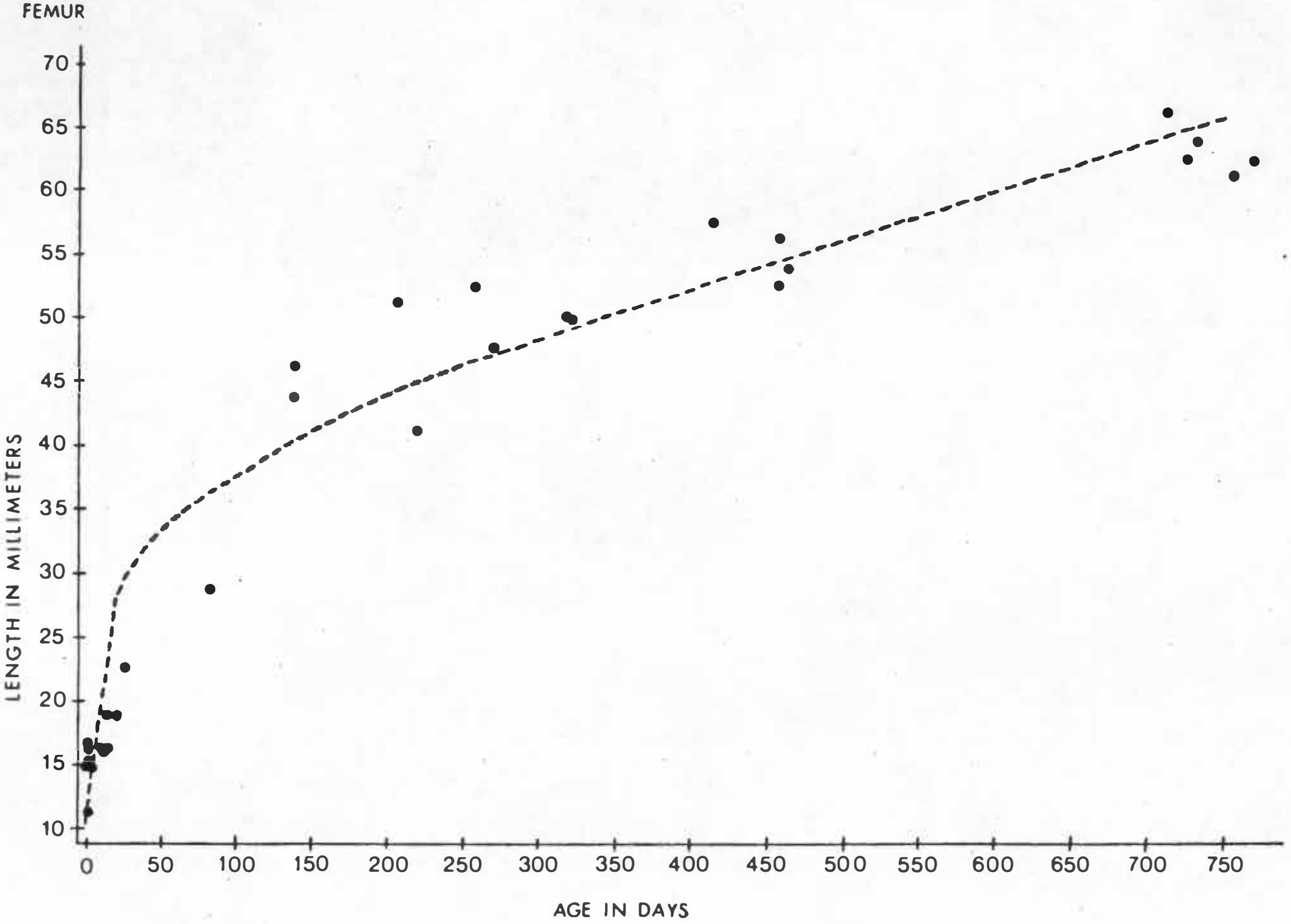

Figure 30. Bivariate plot illustrating the chronology of long bone growth in *Saguinus oedipus*—femur.

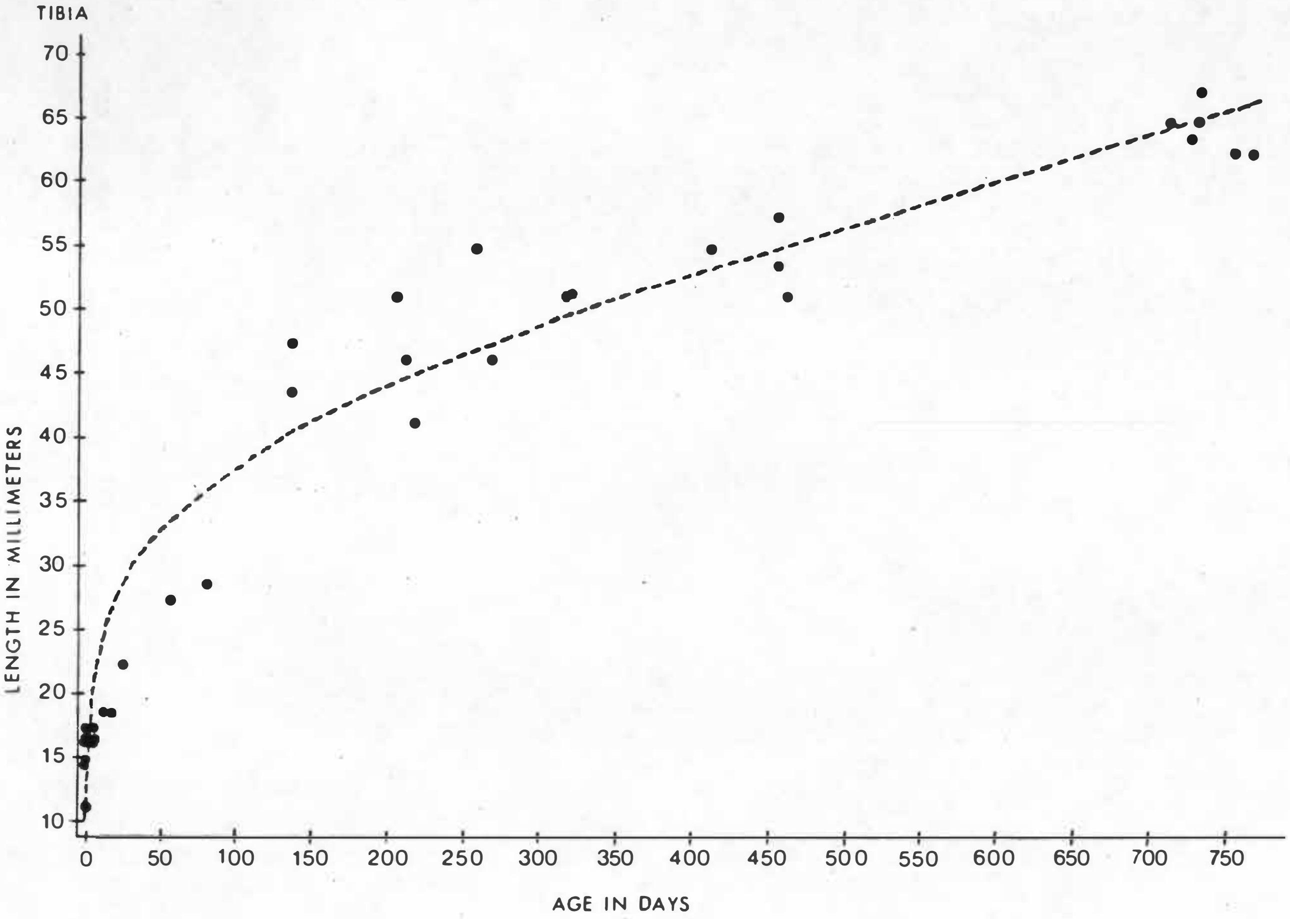

Figure 31. Bivariate plot illustrating the chronology of long bone growth in *Saguinus oedipus*—tibia.

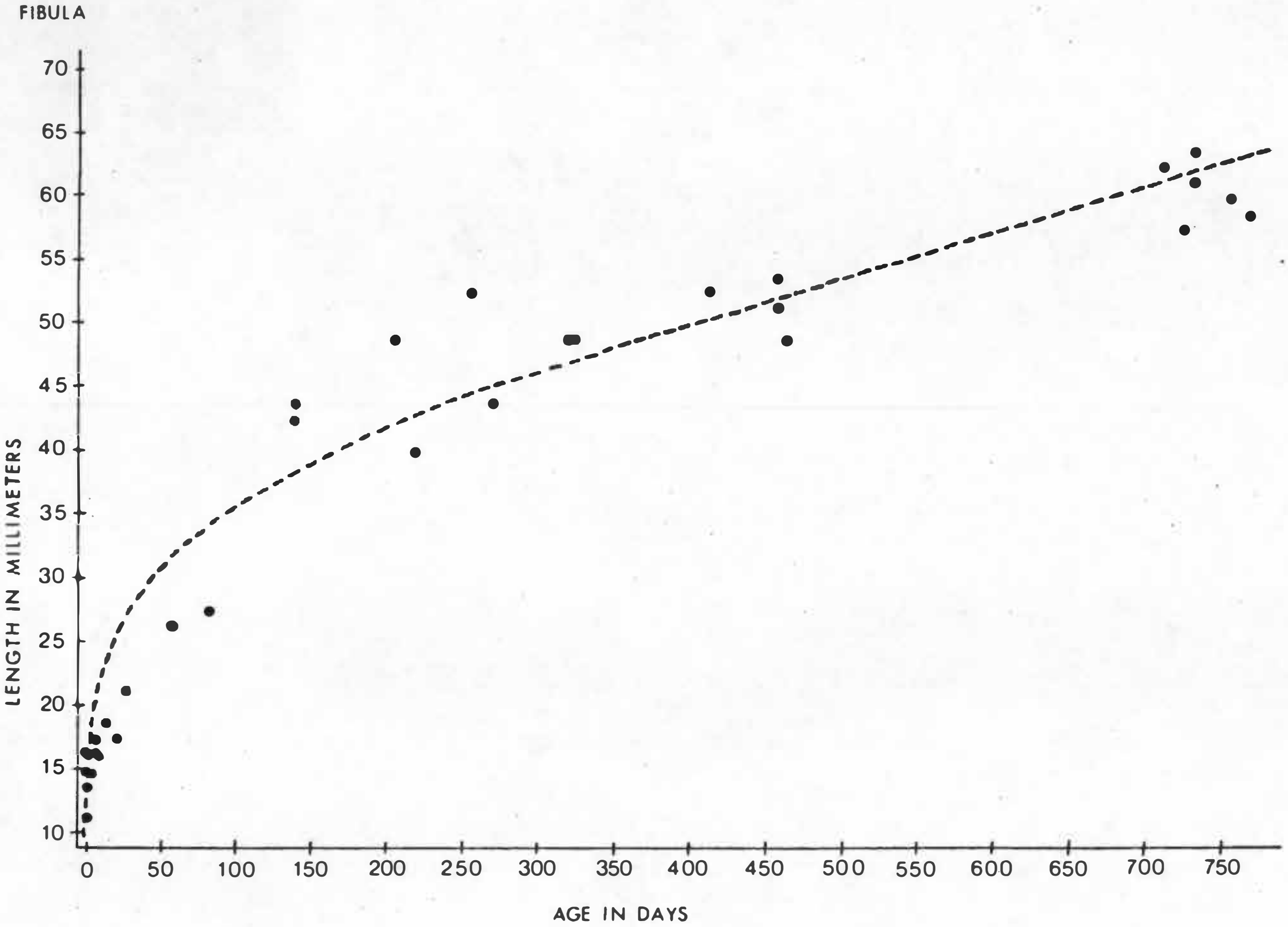

Figure 32. Bivariate plot illustrating the chronology of long bone growth in *Saguinus oedipus*—fibula.

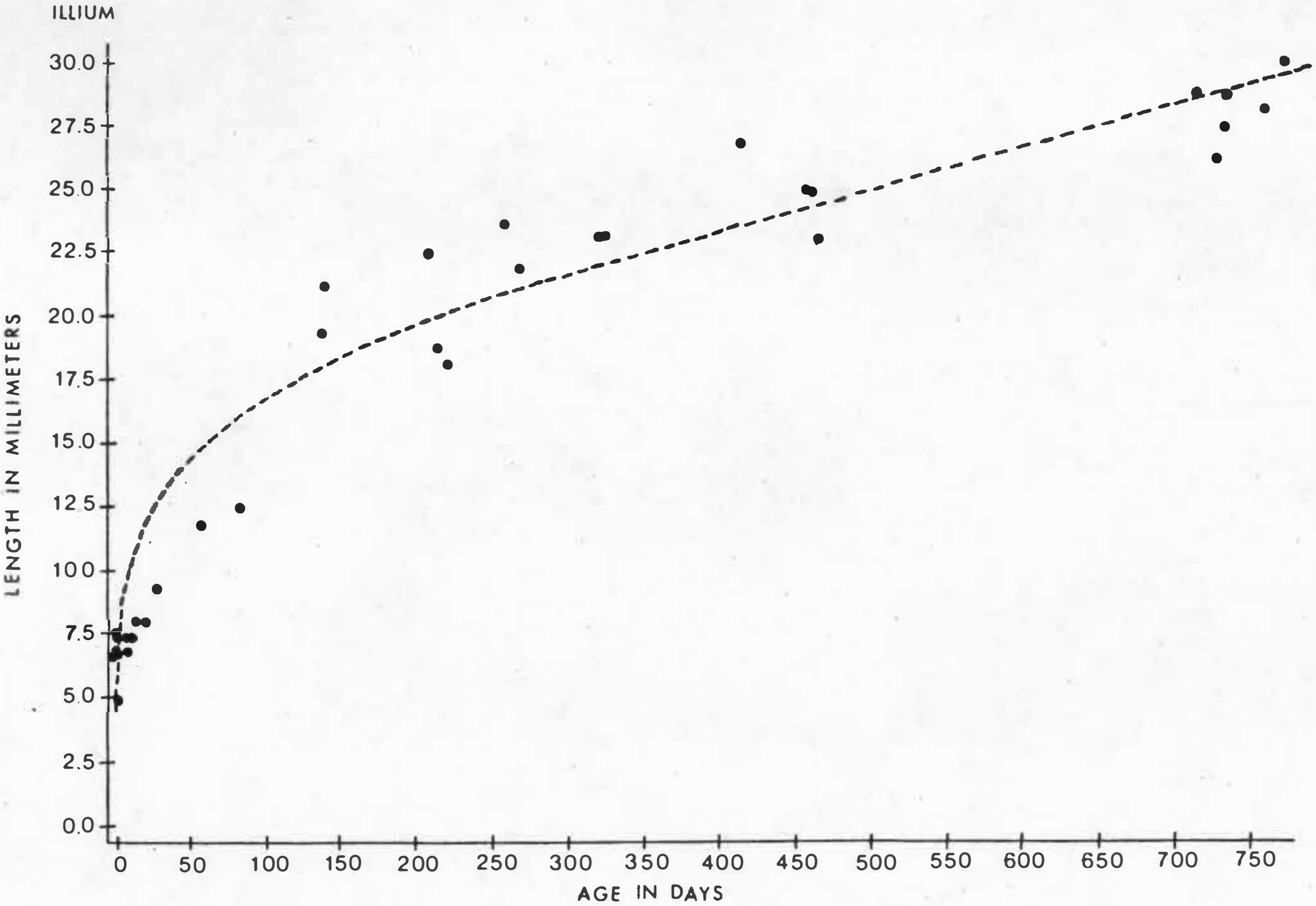

Figure 33. Bivariate plot illustrating the chronology of long bone growth in *Saguinus oedipus*—ilium.

APPENDIX D

TABLES OF EPIPHYSEAL UNION

Table 32. Epiphyseal Union by Age in Days for *Saguinus fuscicollis*

Age	Sex	Distal Humerus	Ischium-Pubic Ramus	Ischium-Pubis to Ili.	Ischium to Pubis	Medial Epicondyle	Coracoid Process	Lesser Trochanter	Proximal Ulna	Distal Radius	Greater Trochanter	Head of Femur	Proximal Radius	Distal Tibia	Distal Fibula	Distal Ulna	Proximal Tibia	Proximal Fibula	Proximal Humerus	Distal Femur	Ischial Epiphysis	Spheno-Occipital Syn.	Iliac Crest
0000	M	1	1	1	1	1	1	1	1	1	1	1	1	1	1	1	1	1	1	1	1	1	1
0002	F	1	1	1	1	1	1	1	1	1	1	1	1	1	1	1	1	1	1	1	1	1	1
0002	M	1	1	1	1	1	1	1	1	1	1	1	1	1	1	1	1	1	1	1	1	1	1
0003	F	1	1	1	1	1	1	1	1	1	1	1	1	1	1	1	1	1	1	1	1	1	1
0003	F	1	1	1	1	1	1	1	1	1	1	1	1	1	1	1	1	1	1	1	1	1	1
0003	M	1	1	1	1	1	1	1	1	1	1	1	1	1	1	1	1	1	1	1	1	1	1
0003	M	1	1	1	1	1	1	1	1	1	1	1	1	1	1	1	1	1	1	1	1	1	1
0005	F	1	1	1	1	1	1	1	1	1	1	1	1	1	1	1	1	1	1	1	1	1	1
0008	F	1	1	1	1	1	1	1	1	1	1	1	1	1	1	1	1	1	1	1	1	1	1
0009	F	1	1	1	1	1	1	1	1	1	1	1	1	1	1	1	1	1	1	1	1	1	1
0015	F	1	1	1	1	1	1	1	1	1	1	1	1	1	1	1	1	1	1	1	1	1	1
0017	F	1	1	1	1	1	1	1	1	1	1	1	1	1	1	1	1	1	1	1	1	1	1
0032	M	1	1	1	1	1	1	1	1	1	1	1	1	1	1	1	1	1	1	1	1	1	1
0043	F	1	1	1	1	1	1	1	1	1	1	1	1	1	1	1	1	1	1	1	1	1	1
0059	F	1	1	1	1	1	1	1	1	1	1	1	1	1	1	1	1	1	1	1	1	1	1
0062	F	1	1	1	1	1	1	1	1	1	1	1	1	1	1	1	1	1	1	1	1	1	1
0064	F	1	1	1	1	1	1	1	1	1	1	1	1	1	1	1	1	1	1	1	1	1	1
0066	F	1	1	1	1	1	1	1	1	1	1	1	1	1	1	1	1	1	1	1	1	1	1
0072	M	1	1	1	1	1	1	1	1	1	1	1	1	1	1	1	1	1	1	1	1	1	1
0083	M	1	1	1	1	1	1	1	1	1	1	1	1	1	1	1	1	1	1	1	1	1	1
0095	M	2	1	1	1	1	1	-	1	1	-	-	1	1	1	1	1	1	1	-	1	1	1

Table 32 (continued)

Age	Sex	Distal Humerus	Ischium-Pubic Ramus	Ischium-Pubis to Ili.	Ischium to Pubis	Medial Epicondyle	Coracoid Process	Lesser Trochanter	Proximal Ulna	Distal Radius	Greater Trochanter	Head of Femur	Proximal Radius	Distal Tibia	Distal Fibula	Distal Ulna	Proximal Tibia	Proximal Fibula	Proximal Humerus	Distal Femur	Ischial Epiphysis	Spheno-Occipital Syn.	Iliac Crest
0097	F	1	1	1	1	1	1	-	1	1	-	-	1	1	1	1	1	1	1	-	1	1	1
0099	M	1	1	1	1	1	1	-	1	1	-	-	1	1	1	1	1	1	1	-	1	1	1
0107	M	1	1	1	1		1	1	1	1	1	1	1	1	1	1	1	1	1	1	1	1	1
0108	F	1	1	1	1	1	1	1	1	1	1	1	1	1	1	1	1	1	1	1	1	1	1
0110	M	2	3	1	1	1	1	1	1	1	1	1	1	1	1	1	1	1	1	1	1	1	1
0114	M	3	3	1	1	1	1	-	1	1	-	-	1	1	1	1	1	1	1	-	1	1	1
0117	F	2	3	1	1	1	1	-	1	1	-	-	1	1	1	1	1	1	1	-	1	1	1
0119	F	2	1	1	1	1	1	1	1	1	1	1	1	1	1	1	1	1	1	1	1	-	1
0120	F	2	3	1	1	1	1	1	1	1	1	1	1	1	1	1	1	1	1	1	1	1	1
0122	F	3	2	2	2	2	1	1	1	1	1	1	1	1	1	1	1	1	1	1	1	1	1
0130	F	2	2	1	1	1	1	1	1	1	1	1	1	1	1	1	1	1	1	1	1	1	1
0132	F	2	2	1	1	1	1	1	1	1	1	1	1	1	1	1	1	1	1	1	1	1	1
0133	M	1	1	1	1	1	1	1	1	1	1	1	1	1	1	1	1	1	1	1	1	-	1
0135	M	2	2	1	1	1	1	1	1	1	1	1	1	1	1	1	1	1	1	1	1	1	1
0137	M	2	3	1	1	1	1	1	1	1	1	1	1	1	1	1	1	1	1	1	1	1	1
0138	F	3	1	1	1	2	1	-	1	1	-	-	1	1	1	1	1	1	1	-	1	1	1
0140	F	2	2	1	1	1	1	1	1	1	1	1	1	1	1	1	1	1	1	1	1	1	1
0156	?	3	3	3	3	2	3	1	1	1	1	1	1	1	1	1	1	1	1	1	1	1	1
0167	M	2	1	1	1	1	1	1	1	1	1	1	1	1	1	1	1	1	1	1	1	1	1
0171	F	2	3	1	1	1	1	1	1	1	1	1	1	1	1	1	1	1	1	1	1	1	1
0172	M	3	3	2	2	1	2	1	1	1	1	1	1	1	1	1	1	1	1	1	1	1	1
0175	M	3	3	2	2	2	2	2	1	1	1	1	1	1	1	1	1	1	1	1	1	-	1

Table 32 (continued)

Age	Sex	Distal Humerus	Ischium-Pubic Ramus	Ischium-Pubis to Ili.	Ischium to Pubis	Medial Epicondyle	Coracoid Process	Lesser Trochanter	Proximal Ulna	Distal Radius	Greater Trochanter	Head of Femur	Proximal Radius	Distal Tibia	Distal Fibula	Distal Ulna	Proximal Tibia	Proximal Fibula	Proximal Humerus	Distal Femur	Ischial Epiphysis	Spheno-Occipital Syn.	Iliac Crest
0183	F	3	3	3	2	1	2	1	1	1	1	1	1	1	1	1	1	1	1	1	1	1	1
0195	F	2	3	2	2	2	1	-	1	1	-	-	1	1	1	1	1	1	1	-	1	1	1
0201	M	2	3	2	2	2	2	1	1	1	1	1	1	1	1	1	1	1	1	1	1	-	1
0204	F	2	3	1	1	1	1	1	1	1	1	1	1	1	1	1	1	1	1	1	1	1	1
0216	F	2	3	1	1	1	2	-	1	1	-	-	1	1	1	1	1	1	1	-	1	1	1
0225	F	3	2	1	1	1	1	1	1	1	1	1	1	1	1	1	1	1	1	1	1	1	1
0245	M	3	3	2	2	1	2	1	2	2	1	-	1	1	1	1	1	1	1	-	1	1	1
0269	M	2	3	1	1	2	1	1	1	1	1	1	1	1	1	1	1	1	1	1	1	1	1
0296	F	3	-	3	2	2	2	1	1	1	1	1	1	1	1	1	1	1	1	1	1	1	1
0441	M	3	3	3	3	3	3	-	2	1	-	-	2	1	1	1	1	1	1	-	1	-	1
0481	F	3	3	3	3	3	3	3	3	2	3	3	3	3	3	2	2	2	2	2	1	1	1
0493	F	3	3	3	3	3	3	3	3	1	3	3	3	3	3	1	1	1	2	1	1	1	1
0574	M	3	3	3	3	3	3	3	3	2	3	3	3	3	3	2	2	2	2	2	1	1	1
0586	F	3	3	3	3	3	3	3	3	1	3	3	3	2	2	1	2	1	2	1	1	1	1
0596	F	3	-	3	3	3	3	3	3	2	3	3	3	3	3	2	2	2	-	-	2	1	1
0638	F	3	3	3	3	3	3	-	3	3	-	-	3	-	3	3	-	-	3	-	2	3	1
0657	F	3	3	3	3	3	3	3	3	2	3	3	3	3	3	1	2	2	2	2	1	1	1
0676	M	3	3	3	3	3	3	3	3	3	3	3	3	3	3	3	2	2	2	2	2	1	1
0677	M	3	3	3	3	3	3	3	3	3	3	3	3	3	3	3	2	2	2	2	2	1	1
0721	F	3	3	3	3	3	3	-	3	3	-	-	3	3	3	3	3	3	3	-	2	2	1
0771	F	3	3	3	3	3	3	3	3	3	3	3	3	3	3	3	3	2	2	2	2	1	1
0816	F	3	3	3	3	3	3	3	3	3	3	3	3	3	3	3	3	3	3	3	3	3	3
0841	M	3	3	3	3	3	3	3	3	3	3	3	3	3	3	3	3	3	3	-	2	3	1

Table 32 (continued)

Age	Sex	Distal Humerus	Ischium-Pubic Ramus	Ischium-Pubis to Ili.	Ischium to Pubis	Medial Epicondyle	Coracoid Process	Lesser Trochanter	Proximal Ulna	Distal Radius	Greater Trochanter	Head of Femur	Proximal Radius	Distal Tibia	Distal Fibula	Distal Ulna	Proximal Tibia	Proximal Fibula	Proximal Humerus	Distal Femur	Ischial Epiphysis	Spheno-Occipital Syn.	Iliac Crest
0907	M	3	3	3	3	3	3	3	3	3	3	3	3	3	3	3	3	3	-	-	2	-	1
0958	F	3	3	3	3	3	3	3	3	3	3	3	3	3	3	3	3	3	3	-	3	3	1
1167	F	3	3	3	3	3	3	3	3	3	3	3	3	3	3	3	3	3	3	3	3	3	1
1226	M	3	3	3	3	3	3	3	3	3	3	3	3	3	3	3	3	3	3	-	3	-	2
1450	F	3	3	3	3	3	3	3	3	3	3	3	3	3	3	3	3	3	3	3	2	-	2
1478	M	3	3	3	3	3	3	3	3	3	3	3	3	3	3	3	3	3	3	3	3	3	3
1501	F	3	3	3	3	3	3	3	3	3	3	3	3	3	3	3	3	3	3	3	3	3	3
1876	F	3	3	3	3	3	3	3	3	3	3	3	3	3	3	3	3	3	3	3	3	3	2
1893	F	3	3	3	3	3	3	3	3	3	3	3	3	3	3	3	3	3	3	3	3	3	2
1914	F	3	3	3	3	3	3	3	3	3	3	3	3	3	3	3	3	3	3	3	3	3	3
1950	F	3	3	3	3	3	3	3	3	3	3	3	3	3	3	3	3	3	3	3	3	3	3
1980	F	3	3	3	3	3	3	3	3	3	3	3	3	3	3	3	3	3	3	3	3	3	3
2038	F	3	3	3	3	3	3	3	3	3	3	3	3	3	3	3	3	3	3	3	3	3	3
2060	M	3	3	3	3	3	3	3	3	3	3	3	3	3	3	3	3	3	3	3	3	3	2
2074	M	3	3	3	3	3	3	3	3	3	3	3	3	3	3	3	3	3	3	3	3	3	3
2085	F	3	3	3	3	3	3	3	3	3	3	3	3	3	3	3	3	3	3	3	3	3	2
2178	F	3	3	3	3	3	3	3	3	3	3	3	3	3	3	3	3	3	3	3	3	3	2
2179	?	3	3	3	3	3	3	3	3	3	3	3	3	3	3	3	3	3	3	3	3	3	2
2267	M	3	3	3	3	3	3	3	3	3	3	3	3	3	3	3	3	3	3	3	3	3	2
2299	F	3	3	3	3	3	3	3	3	3	3	3	3	3	3	3	3	3	3	3	3	3	3
2391	F	3	3	3	3	3	3	3	3	3	3	3	3	3	3	3	3	3	3	3	3	3	3

1 = Epiphysis not united; 2 = Epiphysis uniting; 3 = Epiphysis united; - Indicates missing observation.

Table 33. Epiphyseal Union by Age in Days for *Saguinus oedipus*

Age	Sex	Distal Humerus	Coracoid Process	Ischium-Pubic Ramus	Ischium to Pubis	Ischium-Pubis to Ili.	Lesser Trochanter	Medial Epicondyle	Greater Trochanter	Proximal Radius	Proximal Ulna	Head of Femur	Distal Tibia	Distal Fibula	Distal Radius	Distal Femur	Proximal Humerus	Distal Ulna	Proximal Tibia	Proximal Fibula	Ischial Epiphysis	Speno-Occipital Syn.	Iliac Crest
0000	M	1	1	1	1	1	1	1	1	1	1	1	1	1	1	1	1	1	1	1	1	1	1
0000	M	1	1	1	1	1	1	1	1	1	1	1	1	1	1	1	1	1	1	1	1	1	1
0002	F	1	1	1	1	1	1	1	1	1	1	1	1	1	1	1	1	1	1	1	1	1	1
0002	M	1	1	1	1	1	1	1	1	1	1	1	1	1	1	1	1	1	1	1	1	1	1
0003	M	1	1	1	1	1	1	1	1	1	1	1	1	1	1	1	1	1	1	1	1	1	1
0003	F	1	1	1	1	1	1	1	1	1	1	1	1	1	1	1	1	1	1	1	1	1	1
0004	M	1	1	1	1	1	1	1	1	1	1	1	1	1	1	1	1	1	1	1	1	1	1
0004	M	1	1	1	1	1	1	1	1	1	1	1	1	1	1	1	1	1	1	1	1	1	1
0004	F	1	1	1	1	1	1	1	1	1	1	1	1	1	1	1	1	1	1	1	1	1	1
0011	M	1	1	1	1	1	1	1	1	1	1	1	1	1	1	1	1	1	1	1	1	1	1
0017	M	1	1	1	1	1	1	1	1	1	1	1	1	1	1	1	1	1	1	1	1	1	1
0026	M	1	1	1	1	1	1	1	1	1	1	1	1	1	1	1	1	1	1	1	1	1	1
0057	M	1	1	1	1	1	-	1	-	1	1	-	1	1	1	-	1	1	1	1	1	1	1
0081	M	1	1	1	1	1	1	1	1	1	1	1	1	1	1	1	1	1	1	1	1	-	1
0137	M	3	1	1	1	1	1	1	1	1	1	1	1	1	1	1	1	1	1	1	1	1	1
0138	F	3	2	1	1	1	1	1	1	1	1	1	1	1	1	1	1	1	1	1	1	1	1
0208	M	3	2	3	2	2	2	1	1	1	1	1	1	1	1	1	1	1	1	1	1	1	1
0213	M	3	2	2	2	2	1	1	1	1	1	1	1	1	1	1	1	1	1	1	1	1	1
0218	M	2	1	1	1	1	1	1	1	1	1	1	1	1	1	1	1	1	1	1	1	1	1
0254	M	3	2	3	3	2	1	2	1	1	1	1	1	1	1	1	1	1	1	1	1	1	1
0268	F	3	2	3	1	1	1	1	1	1	1	1	1	1	1	1	1	1	1	1	1	1	1

Table 33 (continued)

Age	Sex	Distal Humerus	Coracoid Process	Ischium-Pubic Ramus	Ischium to Pubis	Ischium-Pubis to Ili.	Lesser Trochanter	Medial Epicondyle	Greater Trochanter	Proximal Radius	Proximal Ulna	Head of Femur	Distal Tibia	Distal Fibula	Distal Radius	Distal Femur	Proximal Humerus	Distal Ulna	Proximal Tibia	Proximal Fibula	Ischial Epiphysis	Spheno-Occipital Syn.	Iliac Crest
0316	M	3	3	3	3	2	2	2	2	1	1	1	1	1	1	1	1	1	1	1	1	1	1
0316	F	3	2	3	3	2	1	2	1	1	1	1	1	1	1	1	1	1	1	1	1	1	1
0410	M	3	3	3	3	3	3	3	3	3	2	2	1	1	1	1	1	1	1	1	1	1	1
0455	F	3	2	3	3	3	2	2	2	2	1	2	2	1	1	1	1	1	1	1	1	1	1
0455	M	3	3	3	3	3	3	2	2	2	2	1	1	1	1	1	1	1	1	1	1	1	1
0463	F	3	2	3	3	2	2	2	2	2	1	1	1	1	1	1	1	1	1	1	1	1	1
0557	F	3	3	3	3	3	3	3	3	3	3	3	2	2	2	2	2	1	1	1	1	1	1
0673	M	3	3	3	3	3	3	3	3	3	3	3	3	3	3	3	3	3	3	3	2	-	1
0712	F	3	3	3	3	3	3	3	3	3	3	3	3	3	3	2	2	2	2	2	2	1	1
0722	M	3	3	3	3	3	3	3	3	3	3	3	3	3	1	2	2	1	2	1	1	2	1
0730	F	3	3	3	3	3	3	3	3	3	3	3	3	3	3	3	3	3	3	3	1	2	1
0732	M	3	3	3	3	3	-	3	-	3	3	-	3	3	3	-	2	3	2	2	1	1	1
0757	M	3	3	3	3	3	3	3	3	3	3	3	3	3	3	3	3	3	3	3	2	2	2
0768	F	3	3	3	3	3	3	3	3	3	3	3	3	3	3	3	3	3	3	3	2	2	2
1799	M	3	3	3	3	3	3	3	3	3	3	3	3	3	3	3	3	3	3	3	3	3	2

1 = Epiphysis not united. 2 = Epiphysis uniting. 3 = Epiphysis united.

- Indicates missing observations.

VITA

David Michael Glassman was born in St. Paul, Minnesota on November 16, 1953. He attended primary and secondary school in that city and graduated from Highland Park Senior High School in 1971. He entered Arizona State University the following fall and remained for one year. In the fall of 1973 he returned to St. Paul and continued his undergraduate work at the University of Minnesota, receiving his B.A. in Anthropology in March 1976.

David entered graduate school at The University of Tennessee, Knoxville in the Winter Quarter of 1977 and received his M.A. in Anthropology in March 1978. He began work toward his doctorate the following quarter.

David has been involved in field research in Minnesota and Mexico and was the laboratory supervisor of the marmoset skeletal collection housed at The University of Tennessee. He is a member of the American Association of Physical Anthropologists, the American Society of Primatologists, and the International Society of Primatologists. David was elected into the honor society Phi Kappa Phi in 1980 and the scientific research society Sigma Xi in 1981.

David is currently employed as an Instructor of Anthropology at the Virginia Polytechnic Institute and State University, Blacksburg. Here he is continuing his research on the skeletal anatomy of marmoset primates.